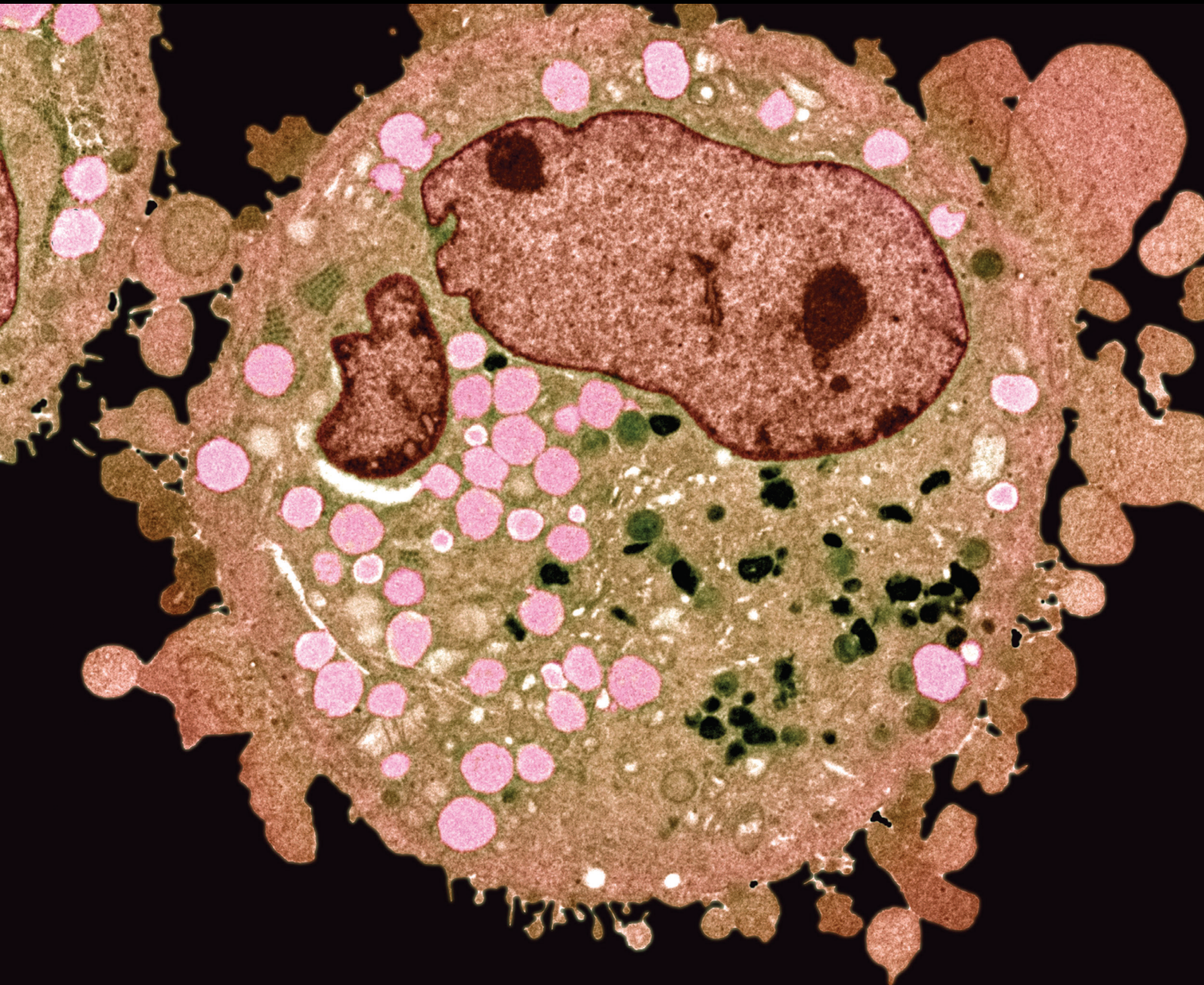


# Targeting Metabolism and Cell Signalling for Cancer Therapy

Lead Guest Editor: Victor H. Villar

Guest Editors: Juan Francisco Santibañez, Giovanny Rodriguez-Blanco,  
and Cesar Echeverria





---

# **Targeting Metabolism and Cell Signalling for Cancer Therapy**



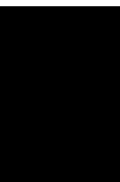
Analytical Cellular Pathology

---

## **Targeting Metabolism and Cell Signalling for Cancer Therapy**

Lead Guest Editor: Victor H. Villar

Guest Editors: Juan Francisco Santibañez,  
Giovanny Rodriguez-Blanco, and Cesar Echeverria




---

Copyright © 2021 Hindawi Limited. All rights reserved.

This is a special issue published in "Analytical Cellular Pathology." All articles are open access articles distributed under the Creative Commons Attribution License, which permits unrestricted use, distribution, and reproduction in any medium, provided the original work is properly cited.






# Chief Editor

Dimitrios Karamichos , USA

## Academic Editors

Salah M. Aly , Egypt  
Consuelo Amantini, Italy  
Elena Andreucci , Italy  
Nebojsa Arsenijevic, Serbia  
Fernando Augusto de Lima Marson ,  
Brazil  
Alan Betensley , USA  
Monica C. Botelho , Portugal  
Giuseppe Broggi , Italy  
Constantin Caruntu , Romania  
Alain Chapel , France  
Domenico D'Arca , Italy  
Attalla El-kott , Saudi Arabia  
Makoto Endo , Japan  
Leonardo Freire-de-Lima, Brazil  
Kevin Fuller, USA  
Ewelina Grywalska , Poland  
Luigina Guasti , Italy  
Simona Gurzu , Romania  
Atif Ali Hashmi, Pakistan  
Ekaterina Jordanova , The Netherlands  
Motohiro Kojima, Japan  
Maryou Lambros, United Kingdom  
Xiaoyan Liao, USA  
Yun Ping Lim , Taiwan  
Anant Madabhushi, USA  
Francesco A. Mauri, United Kingdom  
Tina B. McKay, USA  
Maria Beatrice Morelli , Italy  
Hung-Wei Pan, Taiwan  
Viswanathan Pragasam , India  
Alfredo Procino , Italy  
Liang Qiao, Australia  
Md. Atiar Rahman , Bangladesh  
Mahmood Rasool , Saudi Arabia  
Syed Ibrahim Rizvi , India  
José A. Sánchez-Alcázar , Spain  
Andrea Santarelli , Italy  
Fernando Schmitt , Portugal  
Enayatollah Seydi , Iran  
Dorota L. Stankowska , USA  
Sebastião Roberto Taboga , Brazil  
Lubna H. Tahtamouni , Jordan

Giovanni Tuccari , Italy  
Ulises Urzua , Chile  
Mukul Vij, India  
Vladislav Volarević , Serbia  
Sebastian Wachsmann-Hogiu, USA



## Contents

### **The Metabolic Features of Tumor-Associated Macrophages: Opportunities for Immunotherapy?**

Sonja S. Mojsilovic , Slavko Mojsilovic , Victor H. Villar , and Juan F. Santibanez 


Review Article (12 pages), Article ID 5523055, Volume 2021 (2021)

### **LINC00665 Facilitates the Malignant Processes of Osteosarcoma by Increasing the RAP1B Expression via Sponging miR-708 and miR-142-5p**

Limin Wang, Xinghua Song, Lijun Yu, Bing Liu, Jinfeng Ma , and Weihua Yang 

Research Article (9 pages), Article ID 5525711, Volume 2021 (2021)

### **GTSE1 Facilitates the Malignant Phenotype of Lung Cancer Cells via Activating AKT/mTOR Signaling**

Fan Zhang, Jingfei Meng, Hong Jiang, Xing Feng, Dongshan Wei, and Wen Meng 


Research Article (11 pages), Article ID 5589532, Volume 2021 (2021)

### **Comparison of the Fatty Acid Metabolism Pathway in Pan-Renal Cell Carcinoma: Evidence from Bioinformatics**

Ping Wu, Yingkun Xu , Jiayi Li, Xiaowei Li, Peizhi Zhang, Ningke Ruan, Cong Zhang, Panpan Sun, Qifei Wang , and Guangzhen Wu 


Research Article (25 pages), Article ID 8842105, Volume 2021 (2021)

### **p300-Catalyzed Lysine Crotonylation Promotes the Proliferation, Invasion, and Migration of HeLa Cells via Heterogeneous Nuclear Ribonucleoprotein A1**

Xuesong Han, Xudong Xiang, Hongying Yang, Hongping Zhang, Shuang Liang, Jie Wei, and Jing Yu 



Research Article (6 pages), Article ID 5632342, Volume 2020 (2020)

### **FKBP4 Accelerates Malignant Progression of Non-Small-Cell Lung Cancer by Activating the Akt/mTOR Signaling Pathway**

Wen Meng , Jingfei Meng, Hong Jiang, Xing Feng, Dongshan Wei, and Qingsong Ding

Research Article (11 pages), Article ID 6021602, Volume 2020 (2020)

### **PKM2 Promotes Breast Cancer Progression by Regulating Epithelial Mesenchymal Transition**

Hui Xiao, Longxiao Zhang, Yuan Chen, Chengjun Zhou, Xiao Wang, Dehai Wang , and Zhenzhong Liu 

Research Article (10 pages), Article ID 8396023, Volume 2020 (2020)



## Review Article

# The Metabolic Features of Tumor-Associated Macrophages: Opportunities for Immunotherapy?

Sonja S. Mojsilovic <sup>1</sup>, Slavko Mojsilovic <sup>2</sup>, Victor H. Villar <sup>3</sup> and Juan F. Santibanez <sup>4,5</sup>

<sup>1</sup>Laboratory for Immunochemistry, Institute for Medical Research, University of Belgrade, 11129 Belgrade, Serbia

<sup>2</sup>Laboratory of Experimental Hematology and Stem Cells, Institute for Medical Research, University of Belgrade, 11129 Belgrade, Serbia

<sup>3</sup>CRUK Beatson Institute, Glasgow G61 1BD, UK

<sup>4</sup>Molecular Oncology Group, Institute for Medical Research, University of Belgrade, 11129 Belgrade, Serbia

<sup>5</sup>Centro Integrativo de Biología y Química Aplicada (CIBQA), Universidad Bernardo O'Higgins, 8370993 Santiago, Chile

Correspondence should be addressed to Juan F. Santibanez; [jfsantibanez@imi.bg.ac.rs](mailto:jfsantibanez@imi.bg.ac.rs)

Received 12 February 2021; Revised 15 July 2021; Accepted 23 July 2021; Published 24 August 2021

Academic Editor: Elena Andreucci

Copyright © 2021 Sonja S. Mojsilovic et al. This is an open access article distributed under the Creative Commons Attribution License, which permits unrestricted use, distribution, and reproduction in any medium, provided the original work is properly cited.

Besides transformed cells, the tumors are composed of various cell types that contribute to undesirable tumor progression. Tumor-associated macrophages (TAMs) are the most abundant innate immune cells in the tumor microenvironment (TME). Within the TME, TAMs exhibit high plasticity and undergo specific functional metabolic alterations according to the availability of tumor tissue oxygen and nutrients, thus further contributing to tumorigenesis and cancer progression. Here, we review the main functional TAM metabolic patterns influenced by TME, including glycolysis, amino acid, and fatty acid metabolism. Moreover, this review discusses antitumor immunotherapies that affect TAM functionality by inducing cell repolarizing and metabolic profiles towards an antitumoral phenotype. Also, new macrophage-based cell therapeutic technologies recently developed using chimeric antigen receptor bioengineering are exposed, which may overcome all solid tumor physical barriers impeding the current adoptive cell therapies and contribute to developing novel cancer immunotherapies.

## 1. Introduction

Tumor-associated macrophages (TAMs) and their precursors represent a large proportion of infiltrating myeloid cells in the microenvironment of most solid human malignancies, and they play a crucial role in tumorigenesis [1–3]. TAMs can be derived from blood monocytes and tissue-resident macrophages (MΦs) [4] and comprise a highly dynamic and heterogeneous set of cells full of intermediate polarization phenotype. Indeed, a high degree of TAM heterogeneity is present between cancer patients and within different tumor areas of the same patient [5].

Within the tumor microenvironment (TME), O<sub>2</sub> levels vary dramatically depending on blood supply and hypoxic areas are often present within a tumor tissue [6]. TAMs infiltrate hypoxic regions, in part, being attracted by several chemotactic signals secreted by cancer cells due to low oxygen

pressure. Upon arrival, they suffer a reduction in motility and accumulate at ischemic tumor sites, which may explain the high TAM density in hypoxic and necrotic TME areas of some types of cancers [7, 8].

Furthermore, under different microenvironmental signals and perturbations, TAMs undergo different activation states, reflecting the capacity of these cells to acquire and move through an entire spectrum of phenotypic and metabolic functional patterns. The main MΦ phenotype extremes denominated as the proinflammatory M1 phenotype (or classical activation) that exhibits antitumoral functions and the anti-inflammatory M2 phenotype (or alternative activation) that possesses a protumoral phenotype [9]. Specific factors associated with inflammation, which include endotoxin, interferon- (IFN-)  $\gamma$ , and interleukin- (IL-) 1 $\alpha$ , induce M1, whereas M2, which comprises M2a, M2b, and M2c subtypes, is induced by specific stimuli, including IL-4, IL-10, IL-13,

transforming growth factor- (TGF-)  $\beta$ , and glucocorticoids [9–12]. Recently, an M2d subtype linked to TAMs has been proposed, induced by specific TME-associated anti-inflammatory signals, such as IL-6, Toll-like receptor (TLR) ligands, and adenosine A2 receptor (A2R) agonists. At the same time, they secrete elevated levels of IL-10, TGF- $\beta$ , and VEGF, which contribute to tumor growth, angiogenesis, and metastasis [9]. TAMs may secrete VEGF, anti-inflammatory cytokines TGF- $\beta$ , and IL-10, alongside immune checkpoint ligand expression, such as programmed death-ligand 1 (PD-L1). Moreover, TAMs exert T-cell immunosuppression by depleting essential amino acids via arginase-1 (ARG1) expression and recruit regulatory T-cells (Tregs) that further contribute to the inhibition of antitumor immune responses within the TME [13, 14].

In general, TAMs seem to display an M2-like polarization rather than an M1 phenotype preferentially. Nevertheless, at early tumor phases, TAMs are programmed by cancer signals into a more M1-like phenotype. Over the course of tumor progression to more advanced stages, with the establishment of inflammatory dysbalanced and immunosuppressive TME with prevalent necrotic/hypoxic areas, TAMs begin to display an anti-inflammatory M2-like phenotype [15, 16]. Furthermore, various subpopulations of TAMs have also been identified as TIE2-positive M $\Phi$ s [17], programmed cell death protein-1- (PD-1-) expressing TAMs [18], and C-C chemokine receptor type-2- (CCR2-) expressing TAMs [19]. In addition, it is essential to consider that, depending on nutrients, oxygen availability, and cell–matrix and cell–cell interactions in different sites of malignant tissue, TAMs can adapt their intracellular metabolism for the appropriate polarization [5, 20]. Moreover, TAM diversities require a rethinking and update of M1 and M2 nomenclature for a more accurate classification of their inflammatory phenotypes [21, 22]. Importantly, evidence supports a tumor-promoting role of TAMs and high frequencies of TAMs are generally associated with poor prognosis in most human cancers [23].

In this review, we analyzed the metabolic pathways of TAMs that allow them to adapt to oxygen and nutrient availability in the TME. This may contribute to the promotion of tumor growth and progression. Furthermore, because of the protumorigenic role of TAMs in cancer, we also present primary therapies targeting TAMs, including small drugs, combinations with immune-checkpoint inhibitors (ICI), and the current strategy of the chimeric antigen receptor (CAR) to engineer macrophages towards the adoption of antitumor functions.

## 2. Metabolic Activities in Tumor-Associated Macrophages

Solid tumors comprise complex protein and cellular components that generate a favorable ecosystem supporting transformed cell growth [24]. TAMs are recruited and infiltrate the tumor mass [25]. Moreover, TAMs contribute by promoting tumor initiation and progression, angiogenesis, and metastasis. Meanwhile, all these cancer events seem to be influenced by TAM subpopulations with relevant pheno-

types corresponding to specific tumor regions, exhibiting different cytokine and metabolic profiles regulated by TME [21, 26]. TAMs dynamically adjust their metabolism to survive hostile tumor conditions and display their anti-inflammatory potential to control the tumor's dysfunctional inflammation resulting from cancer cell transformation. In general, TAM literature data indicate that TAMs possess enhanced glycolysis, fatty acid oxidation (FAO), fatty acid synthesis (FAS), and altered glutamate metabolism [25] (Figure 1).

## 3. Glucose Metabolism in TAMs

TAMs are highly dependent on aerobic glycolysis to reach TME hypoxic regions, and ATP production by glycolysis sustains the necessary cytoskeletal reorganization for cell motility [8, 27, 28]. Once TAMs arrive at hypoxic tumor regions (less than 10 mmHg, <1% oxygen), hypoxia effects impair M $\Phi$  migration and TAMs accumulate at ischemic tumor sites [8]. Furthermore, the expression of regulated in development and DNA damage response 1 (REDD1), an inhibitor of the mechanistic target of rapamycin (mTOR), is upregulated in hypoxic TAMs and inhibits glycolysis [29], which may affect TAM motility in hypoxic tumor regions. Consistently, dichloroacetic acid, a glycolysis inhibitor, strongly reduces macrophage migration [30]. In addition, pyruvate kinase muscle 2 (PKM2) colocalizes with F-actin in macrophage filopodia and lamellipodia during cell migration [30].

Increased aerobic glycolytic activities of TAMs have been illustrated by comparing the metabolic reprogramming of bone marrow-derived macrophages; primary TAMs were derived from the mouse mammary tumor virus promoter-driven expression of the polyomavirus middle T antigen (MMTV-PyMT) tumor model and human monocytic THP-1 cell line stimulated with tumor extract solution from breast cancer patients. Critical glycolytic enzymes hexokinase 2 (HK2), downstream phosphofructokinase (PFKL), and enolase 1 (ENO1) were increased in all situations [31]. Similarly, conditioned media from human pancreatic ductal adenocarcinoma (PDAC) cell lines induce *in vitro* TAM-like cells with upregulated HK2, glucose-6-phosphate isomerase (GPI), aldolase A (ALDOA), triosephosphate isomerase 1 (TPI1), and phosphoglycerate kinase 1 (PGK1) transcript expression and increased L-lactate production by expression of lactate dehydrogenase A (LDHA) [32]. Additionally, non-medullary thyroid carcinoma-induced TAMs exhibit an elevated extracellular acidification rate (ECAR) and oxygen consumption rate (OCR) related to increased glucose metabolism via Akt/mTOR signaling [33]. More recently, de-Brito et al. [34] have demonstrated that TAMs show high glycolytic activity and secretion like the M1/M(LPS + IFN -  $\gamma$ ) phenotype. Obtained TAMs, by treating macrophages *in vitro* with a conditioned medium of human melanoma cells, exhibit increased glucose transporter 1 (GLUT-1) expression and elevated gene expression of HK2 alongside increased AKT/mTOR signaling. In line with Arts et al. [33], these TAMs also present high basal and maximal OCR and high mitochondrial ATP production, thus performing oxidative phosphorylation (OXPHOS) similarly to M2/M(IL-4).



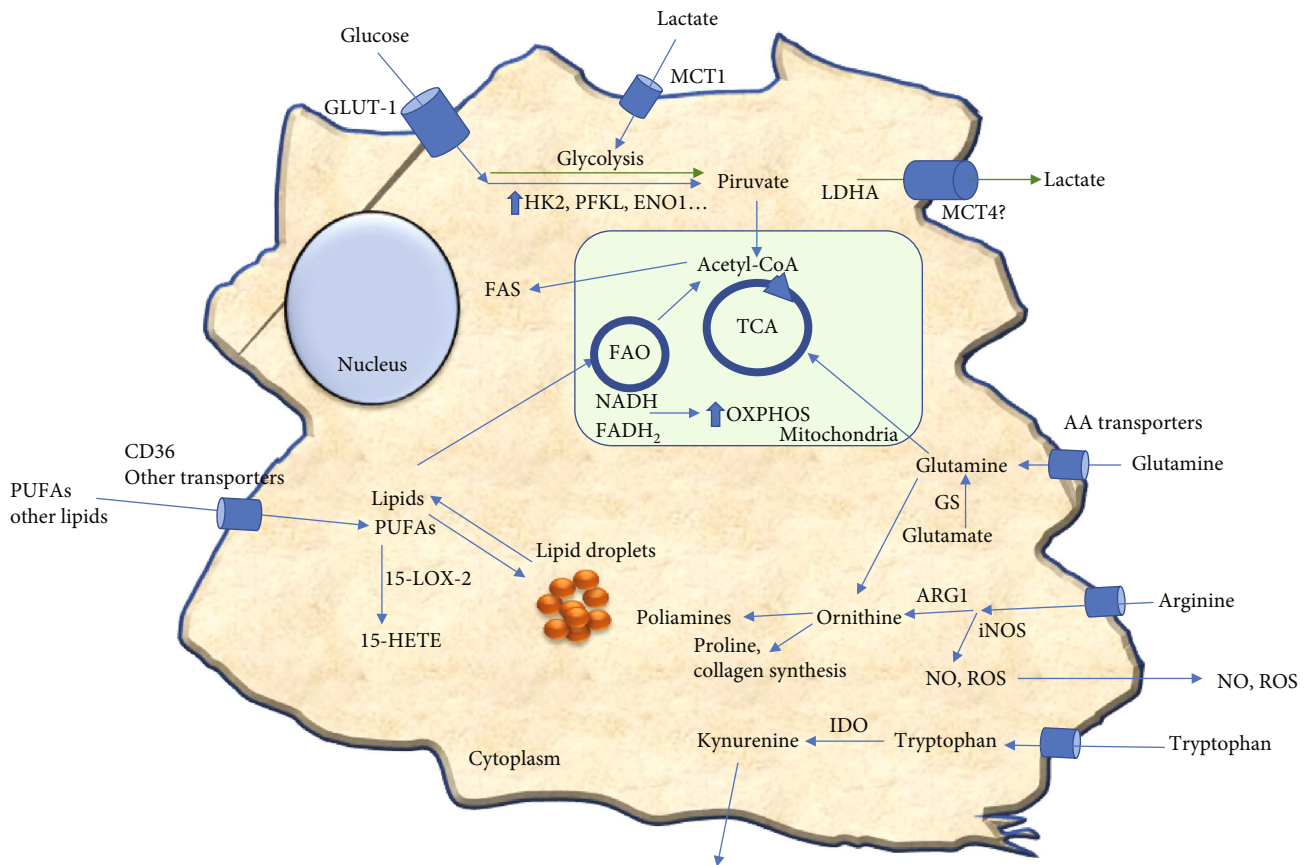


FIGURE 1: Metabolic features of tumor-associated macrophages (TAMs) may dynamically adjust their metabolism within the tumor microenvironment. Extracellular lactate can stimulate glycolysis by creating a pseudohypoxic milieu that may increase lactate production and secretion. Also, TAMs utilize glycolysis, TCA, and OXPHOS to increment the rate of bioenergetic production. TAMs exhibit increased glutamine, arginine, and tryptophan metabolism, increasing energy production, collagen synthesis, and immunosuppressive functions. Furthermore, depending on the TAM stage, lipid metabolism is also altered due to lipid uptake and storage may increase or lipids may be derived towards FAO and participate in TCA and OXPHOS. Moreover, active glycolysis may connect with F.A.S. by increasing acetyl-CoA production; for further details, see the text. TCA: tricarboxylic acid cycle; OXPHOS: oxidative phosphorylation; FAO: fatty acid oxidation; FAS: fatty acid synthesis; PUFAs: polyunsaturated fatty acids; 15-LOX-2: 15-lipoxygenase-2; 15-HETE: 15-hydroxyeicosatetraenoic acid; ARG1: arginase-1; iNOS: inducible nitric oxide synthetase; NO: nitric oxide; ROS: reactive oxygen species; IDO: indoleamine-2,3-dioxygenase; LDHA: lactate dehydrogenase A; MCT-1/4: monocarboxylate transporters-1/4; HK2: hexokinase-2; PFKL: phosphofruktokinase; ENO1: enolase-1.

Interestingly, the TAM maintenance phenotype depends on glycolysis and is independent of both OXPHOS and pentose phosphate pathways (PPP) [34].

Cancer cells metabolize glucose mainly via aerobic glycolysis, known as the “Warburg effect,” leading to high lactate concentrations in the TME [35]. For instance, thyroid cancer-derived lactate enhances the aerobic glycolysis of endogenous TAMs mediated by the AKT1/mTOR pathway and stabilizes their protumor phenotype [32]. CD163<sup>+</sup> TAMs correlate with LDHA2 expression in bladder cancer, head and neck cancer, and malignant skin cancer [8]. Meanwhile, MΦ uptake of cancer cell-derived lactate can be performed via monocarboxylate transporter-1 (MCT1) on the cell surface and be facilitated by a local low pH [36]. Afterwards, intracellular lactate can be metabolized to pyruvate again by LDH1, which competes with  $\alpha$ -ketoglutarate to negatively regulate prolyl hydroxylase, thus preventing hypoxia-inducible factor- (HIF-) 1 $\alpha$  ubiquitination and proteasomal

degradation and promoting a glycolytic pathway [37]. An elevated glucose consumption rate by TAMs is also potentially immunosuppressive since glucose-depleted TME reduces antitumor T-cell activities [14]. In addition, TAMs present a low PPP pathway activity and it seems to be nonessential for M2-like phenotype marker expression and TAM functions [34]. Furthermore, TAMs also present increased OCR and OXPHOS activities to produce high amounts of ATP [33, 34], which is in line with the M2 macrophage phenotype being related to an intact tricarboxylic acid cycle (TCA) and increased OXPHOS activity [9].

#### 4. Amino Acid Metabolism

Nutrients and metabolic waste products may alter the TAM phenotype and functions [38]. For instance, tumor-derived lactate potently induces ARG1 in TAMs via ERK1, 2/STAT3, and HIF-1 $\alpha$  stabilization. Additionally, this “*pseudo-hypoxic*”

HIF-1 $\alpha$  activation by tumor metabolites enhances proangiogenic TAM function that fosters tumor growth [39–41]. ARG1<sup>+</sup> TAMs may promote tumor growth as demonstrated by the fact that M $\Phi$ -overexpressing ARG1 enhances tumor cell proliferation, while ARG1-deficient M $\Phi$ s are associated with reduced tumor size in mice models [39, 42]. A potential mechanism has been proposed for ARG1 tumor-promoting functions. ARG-1 may promote cancer cells by enhancing polyamine production, stimulating M2 gene expression, and stabilizing TAMs' protumorigenic phenotype [43, 44]. Although TAMs seem to have a low NO production capacity, as is observed in murine mammary and human ovarian tumors, consistent with M2-like and protumor characteristics [44–46], simultaneous ARG1 and inducible nitric oxide synthase (iNOS) pathways have been observed in tumor-licensed TAMs [47]. ARG1 and iNOS coexpression at a low arginine concentration may favor reactive oxygen species (ROS) and reactive nitrogen species (RNS) production, thus further inhibiting intratumoral T-cell functions. This dissimilarity reinforces phenotype differences between TAMs and M2-polarized macrophages since, in ischemic tumor domains, TAMs may coexpress ARG1 and iNOS/NOS2, representing an intermediary M1/M2 stage [9].

TAM dependence on the glutamine-glutamate pathway is an essential metabolic characteristic. TAMs isolated from glioblastomas and glioblastoma cell-induced TAMs exhibit increased glutamate transport genes and cellular metabolism expression. qPCR analysis indicated an increased expression of glutamate receptor 2 (GRIA2), glutamate transporters GLT-1 (SLC1A2) and GLAST (SLC1A3), and glutamine synthetase (GS) and a decreased expression of cysteine glutamate antiporter, which may improve TAM resistance to glutamine starvation. Glutamate and glutamine can be used for energetic requirements in TAMs, while glutamine can also be released to the tumor extracellular milieu to fuel cancer cells [44, 48]. Additionally, thyroid cancer-induced TAMs show a reduced glutamate concentration due to a potential utilization by glutamine metabolism to replenish the TCA cycle [43]. In addition, targeting glutamine metabolism by JHU083, a prodrug that broadly inhibits glutamine-metabolizing enzymes, reprograms TAMs towards the M1-like phenotype and enhances antitumor immunity without affecting their total number within the tumor [49]. Moreover, targeting GS in M2 and TAMs can also shift macrophage polarization towards an M1-like phenotype. GS inhibition leads to HIF-1 $\alpha$  activation, promotes succinate accumulation and glucose-dependent metabolism, subverts T-cell immunosuppression, and prevents metastasis [50].

In addition, TAMs may strongly express IDO that contributes to creating an immunosuppressive microenvironment by tryptophan deprivation. In fact, the conditionate medium of IDO<sup>+</sup> TAMs suppressed T-cell response, while pretreatment of TAMs with an IDO inhibitor restored T-cell proliferation [51]. Besides the local tryptophan reduction, IDO also catabolizes tryptophan to kynurenine, which negatively influences T-cell proliferation and immune responses [52].

## 5. Fatty Acid Metabolism in TAMs

Tumor tissues may have aberrant activation of *de novo* lipogenesis due to an overexpression of fatty acid synthase (FASN), ATP citrate lyase (ACLY), and acetyl-CoA carboxylase (ACC), which is associated with unfavorable cancer outcomes. FAS inhibition suppresses transformed cell growth, while increased lipid synthesis promotes cancer cell proliferation by a continuous substrate supply for cellular membrane generation and bioenergy production [44, 53, 54].

Lipid metabolism may play a role in shaping the functional phenotype in TAMs in the TME. FAS is vastly increased at the transcriptome level in thyroid carcinoma-(TC-) induced TAMs. Moreover, TC-induced TAMs display increased glucose metabolism and increased intracellular levels of acetyl-CoA, which can be used for fatty acid synthesis. Furthermore, mTOR pathway activity and HIF-1 $\alpha$  expression are elevated in TAMs [33]. In addition, mTORC1 signaling is implicated in lipid, protein, and nucleotide syntheses. Thus, mTORC1 mediates metabolic reprogramming and differentiation in macrophages [38, 55].

Interestingly, TAMs isolated from ovarian carcinoma patients show a PPAR $\beta/\delta$ -dependent elevated transcriptome due to high polyunsaturated fatty acid (PUFA) levels in the TME. Specifically, linoleic acid and arachidonic acid are stored in highly stable lipid droplets in TAMs and may contribute to TAM polarization [56, 57]. In addition, TAMs derived from renal carcinoma produce elevated levels of eicosanoids via the activation of 15-lipoxygenase- (LOX-) 2 (15-LOX-2) and release substantial amounts of the arachidonic acid metabolite 15-hydroxyeicosatetraenoic acid (15-HETE) [58]. LOXs are nonheme iron-containing dioxygenases that catalyze the stereospecific peroxidation of PUFAs to the corresponding hydroperoxyl derivatives [59]. Beyond its role in regulating lipid homeostasis, 15-LOX-2 also contributes to an increased TAM expression of CCL2 chemokine and IL-10, leading to a local immune tolerance within the TME [58, 60].

Moreover, several studies have shown that cellular accumulation of lipids is crucial in regulating the function of TAMs. Macrophages accumulate lipids within the TME and support immunosuppression. Both *in vitro* cancer-stimulated macrophages and TAMs isolated from different tumor models exhibit an increased expression of ABHD5, a lipolytic factor of triglycerides, whereas monoacylglycerol lipase (MGLL) is downregulated. Meanwhile, M $\Phi$ s, derived from a transgenic mouse model with a specific overexpression of MGLL (Tg<sup>MGLL</sup>) in myeloid cells, were refractory to accumulated lipids in response to cancer cell stimuli. Furthermore, MGLL downregulation contributes to the suppression of tumor-associated CD8<sup>+</sup> T-cell function and tumor progression. In addition, myeloid MGLL overexpression potentiates M1-like TAM expansion to the detriment of M2-like TAMs. Thereby, the TAM phenotype requires a reduced MGLL expression to stabilize and display immunosuppressive and tumor promoter functions [61].

TAMs from both human and murine tumor tissues accumulate lipids that rely on elevated levels of CD36 expression and ensure substrates to FAO and OXPHOS for energy



production. Lipid accumulation in TAMs correlates with the upregulation of genes involved in fatty acid  $\beta$ -oxidation, such as CPT1A, an FAO rate-limiting enzyme, acyl-CoA dehydrogenase medium-chain (ACADM), hydroxyacyl-CoA dehydrogenase/3-ketoacyl-CoA thiolase/enoyl-CoA hydratase (a trifunctional protein), and hydroxyacyl-CoA dehydrogenase (HADH), without any modifications of gene expression involved in glucose metabolism. Conversely, reduced lipid uptake in CD36-KO M $\Phi$ s or FAO inhibition by etomoxir can prevent the generation of TAMs and reduce their protumor activities [62].

Interestingly, cell death-associated factors may regulate TAM generation and fatty acid metabolism. For example, TAM-like cells, generated from THP-1 M $\Phi$ s cocultured with MCF-7 tumor cells, depend on caspase-1-dependent peroxisome proliferator-activated receptor  $\gamma$  (PPAR  $\gamma$ ) cleavage. When truncated PPAR $\gamma$  translocates to mitochondria to interact and inhibit medium-chain acyl-CoA dehydrogenase (MCAD), it results in FAO inhibition and consequently induces lipid droplet accumulation and TAM differentiation [63]. On the other hand, receptor-interacting protein kinase 3 (RIPK3), a central factor in necroptosis, is downregulated in hepatocellular carcinoma- (HCC-) associated TAMs. RIPK3 reduction provokes an inhibition of caspase1-mediated cleavage of PPAR $\gamma$  that promotes FAO pathway activation and M2 polarization within the TME. Consistently, RIPK3 overexpression or FAO blockade prevents TAM-induced immunosuppression and impairs HCC tumorigenesis [64]. These data suggest a time-dependent relation of caspase-1 activation and RIPK3 downregulation to balance lipid storage and degradation according to TAM's energy needs in tumor tissues. Intriguingly, human TAMs, induced with a conditioned medium of human melanoma, demonstrate a low absorption of exogenous palmitate/BO-DIPY FLC16, reduced CD36 expression, and FAO activity similar to M1 M $\Phi$ .

Nevertheless, these determinations were done in environments with an atmospheric oxygen concentration, where glucose in culture media may be the primary fuel source and the TAM phenotype maintenance depends on the glycolytic pathway. Moreover, no determination of CD36 or lipid uptake was performed under hypoxic conditions [34]. In summary, lipid uptake, intracellular lipid accumulation, FAS, and FAO demonstrate TAMs' metabolic flexibility and adjustment to achieve a proinflammatory and protumorigenic program to sustain tumor development and malignancy.

## 6. TAMs and Immunotherapy Perspectives

The innate immune system cells that interplay with the adaptive immune system are essential in preventing the progression and acquisition of malignancy stages of transformed cells [65, 66], and a crucial subject in antitumor immunology is the struggle against of the immunosuppressive environment within the tumor stroma producing dysfunctional antitumor responses. TAMs exert protumoral functions that enhance tumor progression, tumor growth, and neoangiogenesis and facilitate the establishment of the immune-

suppressive microenvironment, making them attractive therapeutic targets for cancer therapy [26]. Therefore, targeting TAMs may provide novel treatment options to cancer types currently unresponsive to conventional chemotherapeutics and synergize with current immunotherapies [67].

*6.1. TAMs and Immune Checkpoint Inhibitors.* One of the main TAM mechanisms involved in cancer support and promotion is their potent capacity to create an immune-tolerant TME by preventing immune cytotoxic cell effector functions. TAMs may suppress antitumor immune responses; they can activate adverse regulatory pathways or checkpoints associated with immune homeostasis and can allow cancer cells to actively escape from immunosurveillance [26, 68]. Recent studies have indicated that TAMs express B7 family ligands PD-L1 (CD274) and PD-L2 as well as CD80 (B7-1) and CD86 (B7-2), which bind to inhibitory receptors PD-1 (CD279) and cytotoxic T-lymphocyte antigen 4 (CTLA-4 or CD152) and induce CD8<sup>+</sup> T-cell dysfunction [66]. PD-1 and CTLA-4 are expressed in activated immune effector cells as part of regulatory and safety mechanisms to control the resolution phase of immune response and inflammation [26]. Furthermore, TAMs also express B7 family checkpoint ligands with direct suppressive effects on tumor-infiltrating T-cells, such as the coinhibitory molecule B7-H4 and V domain immunoglobulin suppressor of T-cell activation (VISTA, B7-H5), which bind CD28H [69, 70]. B7-H4 binding to an unknown target-cell receptor inhibits T-cell proliferation, cell cycle progression, and cytokine production [71, 72]. In contrast, B7-H4 depletion, by using a B7-H4-specific morpholino antisense oligonucleotides (B7-H4 blocking oligos), switches TAMs to T-cell-stimulating functions alongside with tumor regression and tumor growth (Figure 2) [69]. TAMs may directly inhibit T-cell functions via these immune checkpoint ligands and reduce immune checkpoint therapy efficacy [73].

Although ICIs have shown great potential, due to their therapeutic success in several cancers, such as melanoma and lung cancers, and leukemias, the percentage of effectiveness still does not fulfill the expected outcomes in cancer immunotherapy [66, 74]. TAMs, the highest in abundance among tumor-infiltrating immune cells, exert multifaceted roles in promoting tumor progression, and it has been suggested that the selective targeting of TAM functions in combination with ICI therapies may synergize with current cancer immunotherapies [75].

For instance, targeting colony-stimulating factor (CSF) 1, a TAM recruitment factor, improves the therapeutic effect of checkpoint inhibitors. CSF1R inhibition by PLX3397 reduces TAMs' tumor infiltration and their immunosuppressive phenotypes, potentiates ICI effects against PD-1 and CTLA4, and impairs tumor expansion by approximately 50%. Moreover, this combinatory approach induces about a 15% regression in established pancreatic cancer tumors [76]. In line with these results, CCR2 antagonists increment anti-PD-1 antibody efficacy and reduce TAM accumulation within tumor tissues [77] (Figure 2). In addition, colon carcinoma CT26 murine syngeneic tumors that exhibit high immunogenicity and the mesenchymal-like phenotype are susceptible

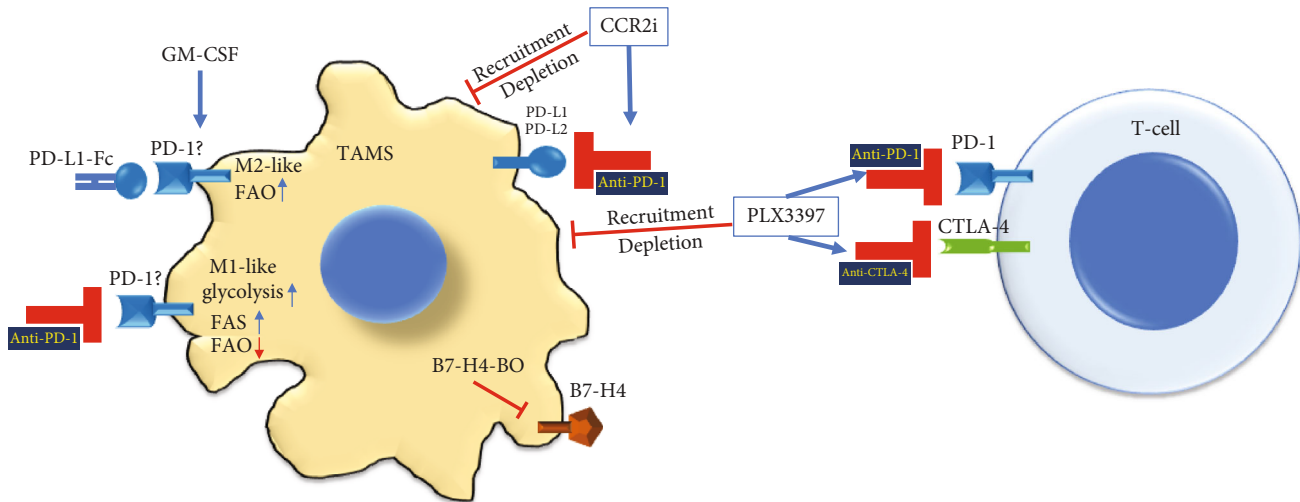


FIGURE 2: Examples of TAM combinatorial targeting with immune checkpoint inhibitors. TAM depletion and recruitment inhibition to the tumor microenvironment, by CCR2 inhibitor or PLX3397, potentiate immune checkpoint inhibition by anti-PD-1, anti-PD-L1/2, or anti-CTLA-4 and further stimulate T-cell functions. Similarly, inhibition of B7-H4 by specific morpholino antisense oligonucleotides (B7-H4-BO) contributes to T-cell stimulation, tumor regression, and tumor growth inhibition. In addition, under GM-CSF-induced macrophages, increased PD-1 expression, and manipulation either with PD-1 agonist (PD-L1-Fc) or with anti-PD-1 may favor the M2-like phenotype or M1-like phenotype, respectively, alongside metabolic reprogramming, which needed to be confirmed in TAMs. PD-1: programmed death protein-1; PD-L1: programmed death protein-ligand-1; CTLA-4: cytotoxic T-lymphocyte antigen 4; FAO: fatty acid oxidation; FAS: fatty acid synthesis; GM-CSF: granulocyte-macrophage colony-stimulating factor.

to immunotherapy with anti-PD-L1 mIgG2, an IgG subclass with the highest affinity for activating FcγR typically expressed by TAMs. Anti-PD-L1 mIgG2 antitumor therapy results in a significant inhibition of tumor growth and improved long-term mouse survival. This tumor inhibition was due to the anti-PD-L1 mIgG2 potential to directly target tumor-associated myeloid cells expressing FcγR [78].

Similarly, the antibody targeting macrophage receptor with the collagenous structure (MARCO), by crosslinking the inhibitory FcγRIIB on TAMs, synergistically increases anti-CTLA4 immunotherapy in melanoma and colon cancer mouse models. Interestingly, anti-MARCO treatment results in repolarization of the M2-like anti-inflammatory TAM population to M1-like proinflammatory TAMs that increase tumor immunogenicity [79]. Thus, it is believed that preventing or rescuing TAMs from immunosuppressive functions, either by depletion or phenotype repolarization, may significantly improve ICI immunotherapies by reversing immune dysfunction and restoring the cytotoxic antitumor function of T lymphocytes within the TME. Several ongoing clinical trials have considered combinatorial TAMs and immune checkpoints targeting and are reviewed elsewhere [26, 80].

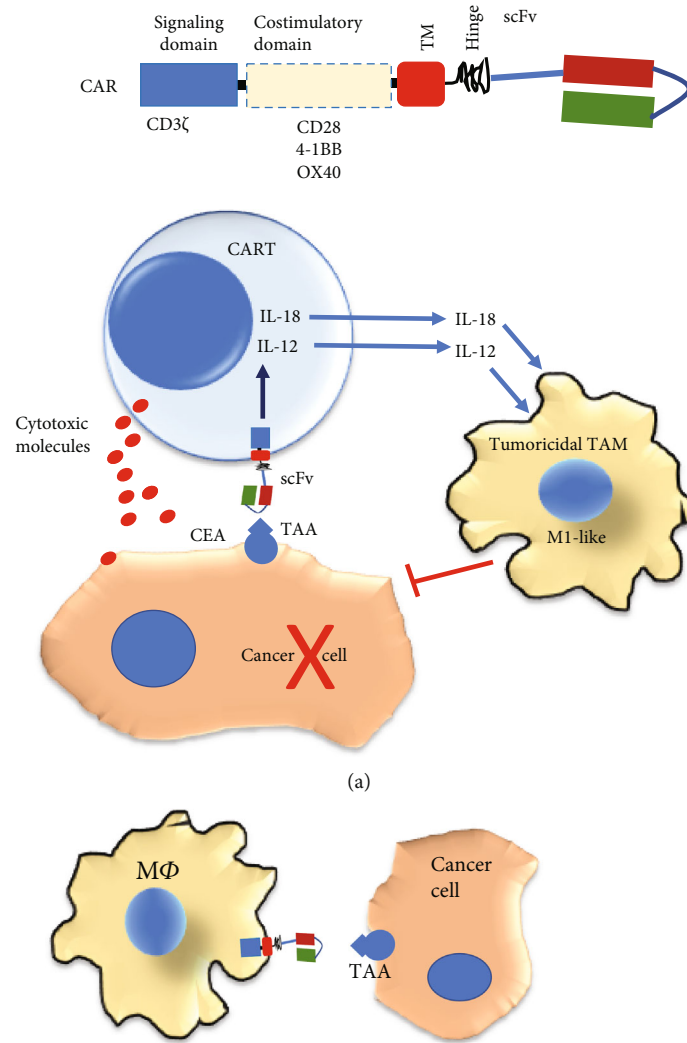
Notably, in chronic lymphocytic leukemia- (CLL-) derived monocytes, triggering the PD-1 checkpoint by using the bioactive recombinant PD-L1 protein hampers glycolysis (reduces glucose uptake, glucose transporters, and expression of glycolytic molecules) and shifts their metabolism toward OXPHOS, which may suggest the PD-1/PD-L1 axis as a novel immune metabolic player in myeloid cells [81, 82].

Although no data exist about ICI on TAM metabolism, some information can be taken from other models. Trophoblast-MΦ interaction during early pregnancy may illustrate

molecular pathways in the PD-1/PD-L1 axis-mediated regulation of myeloid cells. The treatment of normal monocytes with granulocyte-macrophage- (GM-) CSF significantly increases PD-1 mRNA expression. Afterwards, PD-L1 agonist (PD-L1 Fc) engages MΦs expressing PD-1 and triggers the polarization of GM-CSF-differentiated MΦs towards the M2 phenotype with increased FAO activity. The anti-PD-1 blocking antibody promotes macrophage polarization towards the M1 phenotype with enhanced glycolytic metabolism, reduced FAO, and increased fatty acid synthesis pathway. These events occur alongside increased PI3K/AKT/mTOR and MEK/ERK activity pathways. Thus, PD-1 signaling might modulate macrophage polarization via reprogramming their metabolism [83]. PD-1 expression has also been observed in other MΦ models, playing a suppressive role associated with M2 polarization and increasing with the stage of disease in colorectal cancer patients [18, 84].

Nevertheless, further investigations addressing the immune checkpoint regulation of TAM metabolism are required, as they would contribute to an understanding of the complex immune-metabolic network in the TME.

**6.2. TAMs and Adoptive Cell Therapy.** A new therapeutic technique has recently emerged, CAR T-cells, which provides new insight into adoptive cell therapy (ACT) for cancer. The CAR construct results from fusing a specific anti-tumor-associated antigen (TAA) antibody polypeptide chain with the TCR/CD3ζ signal-mediated activating machinery of the T-cell. Additionally, it may contain one or more domains derived from costimulatory T-cell receptors CD28, 4-1BB, or OX40 (Figure 3(a)). The TAA-CAR-specific construct is ectopically expressed in the immune effector cells to



Name	scFV/TAA	Cytoplasmic domains	Effects	Ref
CAR-P	$\alpha$ CD19, $\alpha$ CD22	CD3 $\zeta$	Phagocytosis	95
TK1 MOTO-CAR	$\alpha$ thymidine kinase 1	Toll/interleukin-1 receptor	Phagocytosis M1-like M $\Phi$	96
CAR-147	$\alpha$ HER2	CD147/EMMPRIN	MMP production. T-cell tumor infiltration	97
CAR-M	$\alpha$ mesothelin or $\alpha$ HER	CD3 $\zeta$	M1-like phenotype antitumor T cell activity	99

(b)

FIGURE 3: Adoptive cell therapy and macrophage. (a) Primary chimeric antigen receptor (CAR) features are exposed. scFv: single-chain antibody variable fragment; TM: transmembrane domain. The bottom figure indicates the treatment with the fourth-generation CAR T-cell strategy. After engagement to tumor-associated antigen (TAA), CAR T-cells are activated and may exert antitumor activities by releasing cytotoxic molecules. Furthermore, CAR activation promotes the expression and secretion of IL-12 or IL-18 that may induce TAM shift to tumoricidal functions. (b) TAMs engineered with CAR new strategies implicate the CAR-modified macrophages. The table indicates CAR-modified macrophages, specific targets, intracellular CAR domains, and the main functional activities promoted by CAR macrophage engineering.

recognize and potentially target cancer cells. When CAR T-cells bind to TAA at the cancer cell surface, they proliferate and kill tumor cells. Thus, CAR T-cells represent a significant advancement in cancer immunotherapy and a genetic engineering platform to develop CAR-based immunotherapies using other immune cells [85, 86]. Remarkably, fourth-generation CAR-T-cells (TRUCKs), engineered with anti-carcinoembryonic antigen (CEA, CD66) antibody single-chain peptide and modified to secrete inducible IL-12 (IL-12), upon engaging tumor cells, reprogram TAMs recruited into the tumors to be tumoricidal cells that cooperate with CAR-T-cells for tumor regression and cancer cell elimination (Figure 3(a)) [87, 88].

Similarly, CAR T-cells releasing inducible IL-18, upon CAR stimulation, change the TME immune cell landscape into an acute inflammatory feature, owing to an increased frequency of M1-like TAMs and the improved infiltration of activated dendritic cells and natural killer cells. As a result, an improvement of mice survival with advanced pancreatic and lung tumors has been observed, as has antigen-specific memory [89].

Although CAR T-cells have significant success in treating hematological malignancies, targeting solid tumors is challenging to implement for ACT due to impediments to trafficking and infiltrating tumor tissues [90]. Beyond functioning as professional antigen-presenting cells (APC) and actively participating in the immune response, MΦs possess a high capacity to migrate and infiltrate tumors in response to tumor-secreted chemokines [91, 92]. This tumor-infiltrating capacity makes MΦs strong candidates as vehicles for CAR therapy (Figure 3(b)). In this sense, the concept of CAR modification in MΦs has recently been introduced. Several CARs for CD19- or CD22-targeted phagocytosis were engineered for MΦ cell transfection and named CAR-Ps. The CAR-P molecules contain the extracellular single-chain antibody variable fragment (scFv) recognizing the B cell antigen CD19 or CD22 and the CD8 transmembrane domain as in the  $\alpha$ CD19/ $\alpha$ CD22 CAR-T, as well as cytoplasmic domains Megf10, the common  $\gamma$  subunit of Fc receptors (FcR $\gamma$ ), or CD3 $\zeta$ , and could promote phagocytosis. These CAR-Ps possess excellent specificity and a phagocytotic ability for both CD19- and CD22-coated beads and for Raji B cells *in vitro*. This study demonstrates that, beyond T-cell activation, the CAR strategy is transferrable to phagocytic cells and sufficient to promote specific engulfment and eliminate cancer cells. Tumor antigen-specific CARs make MΦs applicable in ACT to target solid tumors [93].

Another CAR-modified MΦ strategy considers a Toll-like receptor-chimeric antigen receptor expression. In this case, the chimeric protein is the result of the fusion of the Toll/interleukin-1 receptor (TIR) signaling domain for intracellular signal transduction and scFv for thymidine kinase 1 targeting (TK1 MOTO-CAR cells). The *in vitro* analysis indicates that TK1 MOTO-CAR cells exhibit an M1-skewed phenotype and phagocytic activity. Moreover, these CAR cells specifically induce cell death and form clusters around the TK1-positive non-small cell lung carcinoma NCI-H460 cell line [94, 95].

Furthermore, MΦs are modified with anti-hHER2 scFv and the transmembrane and intramembrane regions of the mouse CD147 molecule construct (CAR-147). CD147 (also named EMMPRIN) is a well-known extracellular matrix metalloproteinase (MMPs) inducer [96]. When cocultured with HER2-4T1 cells, the expression of MMP3, MMP9, MMP10, MMP11, MMP12, MMP13, and MMP14 in CAR-147 MΦ is significantly upregulated. Although CAR-147 MΦs did not inhibit cancer cell growth *in vitro*, they significantly inhibited tumor growth in the 4T1 breast cancer mouse model. Moreover, these MΦs promoted T-cell infiltration into the tumor concomitantly with the degradation of the dense collagen-based matrix that surrounds it. Furthermore, CAR-147-expressing human MΦ facilitated T-cell infiltration in a three-dimensional multicellular sphere model of human breast cancer [97].

Recently, the term CAR-M has been coined regarding human MΦ transduced with CARs encoding the CD3 $\zeta$  intracellular domain to target the tumor antigen mesothelin or HER2. CAR-M cells display tumor antigen-specific phagocytic activity while exhibiting a proinflammatory M1-like phenotype and promote antitumor T-cell activity [98]. Moreover, the investigational new drug application for anti-human HER2-CARM (CT-0508) was approved last year by the FDA to target recurrent or metastatic HER2-overexpressing solid tumors [99]. MΦs engineered with CAR molecules seem to preferentially exhibit a proinflammatory M1-like TAM phenotype. According to the metabolic adjustment of macrophages to TME signaling, oxygen, nutrient levels, and intratumor localization, it is plausible that the CAR modification of MΦs may influence glucose and nutrient flow to a more glycolytic and FAS metabolic M1-like profile.

## 7. Conclusions

Tumor metabolic activities are critical for tumor growth and progression. Cancer cells may create a dysfunctional microenvironment, producing a network of inflammatory factors, oxygen, nutrients, and metabolites that may alter the immune system response and make it protumorigenic. TAMs are one of the critical noncancer cell populations that infiltrate tumors. They actively interact with cancer cells and may promote tumor growth by regulating antitumor immune function. Moreover, TAMs dynamically adjust their metabolism according to different signals and interactions, depending on intratumor localization. Moreover, TAM-produced metabolites exert multiple biological effects in the whole TME. Thus, the success of tumor development and growth may depend on active TAM-TME metabolic crosstalk.

Due to the importance of TAMs in tumor progression, several therapeutic strategies have been investigated, from elimination to utilization as antitumor drug cargoes, including their shifting to proinflammatory and antitumoral phenotypes. All these therapies may also be combined with the current ICI immunotherapies. Furthermore, TAMs seem to be excellent candidates for adoptive cell therapy, especially as part of CAR technology. Moreover, an evaluation of



metabolic flux in TAMs and metabolism interventions might further improve tumor immunotherapy. Nonetheless, more investigations are needed to elucidate TAMs' metabolic adaptation to current immunotherapies. Therefore, the metabolic manipulation of TAMs may allow for the generation of more accurate oncotherapies and increment the life quality of cancer patients.

## Abbreviations

ACC:	Acetyl-CoA carboxylase
ACADM:	Acyl-CoA dehydrogenase medium chain
A2R:	Adenosine A2 receptor
ACT:	Adoptive cell therapy
ALDOA:	Aldolase A
APC:	Antigen-presenting cells
ARG1:	Arginase-1
ACLY:	ATP citrate lyase
CEA:	Carcinoembryonic antigen
CAR:	Chimeric antigen receptor
CCR2:	C-C chemokine receptor type-2
CLL:	Chronic lymphocytic leukemia
CSF:	Colony-stimulating factor
CTLA-4:	Cytotoxic T-lymphocyte antigen 4
ENO1:	Enolase 1
ECAR:	Extracellular acidification rate
FcR:	Fc receptors
FAO:	Fatty acid oxidation
FAS:	Fatty acid synthesis
FASN:	Fatty acid synthase
GM:	Granulocyte-macrophage
GPI:	Glucose-6-phosphate isomerase
GLUT-1:	Glucose transporter 1
GRIA2:	Glutamate receptor 2
SLC1A2:	Glutamate transporters GLT-1
GS:	Glutamine synthetase
HK2:	Hexokinase 2
15-HETE:	15-Hydroxyeicosatetraenoic acid
HADH:	Hydroxyacyl-CoA dehydrogenase
HCC:	Hepatocellular carcinoma
HIF:	Hypoxia-inducible factor
iNOS:	Inducible nitric oxide synthase
IFN:	Interferon
IL:	Interleukin
ICI:	Immune-checkpoint inhibitors
LDHA:	Lactate dehydrogenase A
15-LOX-2:	15-Lipoxygenase-2
MΦs:	Macrophages
MMP:	Matrix metalloproteinase
mTOR:	Mechanistic target of rapamycin
MCAD:	Medium-chain acyl-CoA dehydrogenase
MCT1:	Monocarboxylate transporter-1
MGLL:	Monoacylglycerol lipase
MMTV-PyMT:	Mouse mammary tumor virus promoter-driven expression of polyomavirus middle T antigen
OXPHOS:	Oxidative phosphorylation
OCR:	Oxygen consumption rate
PDAC:	Pancreatic ductal adenocarcinoma

PPP:	Pentose phosphate pathways
PPAR:	Peroxisome proliferator-activated receptor
PFKL:	Phosphofructokinase
PGK1:	Phosphoglycerate kinase 1
PUFAs:	Polyunsaturated fatty acids
PD-1:	Programmed cell death protein-1
PD-L1:	Programmed cell death-ligand 1
PKM2:	Pyruvate kinase muscle 2
RNS:	Reactive nitrogen species
ROS:	Reactive oxygen species
RIPK3:	Receptor-interacting protein kinase 3
REDD1:	Regulated in development and DNA damage response 1
scFv:	Single-chain antibody variable fragment
TGF-β:	Transforming growth factor-β
TCA:	Tricarboxylic acid cycle
TC:	Thyroid carcinoma
TPI1:	Triosephosphate isomerase
TLR:	Toll-like receptor
TAA:	Tumor-associated antigen
Tregs:	Regulatory T-cells
TRUCKs:	Fourth-generation CAR-T-cells
TAMs:	Tumor-associated macrophages
TME:	Tumor microenvironment
VISTA:	V domain immunoglobulin suppressor of T-cell activation.

## Data Availability

The material supporting the conclusion of this review has been included within the article.

## Conflicts of Interest

The authors declare no conflict of interest.

## Acknowledgments

We apologize to those colleagues whose work, although relevant to the issues dealt within this review, has not been included due to space limitations. This work was supported by the Ministry of Education, Science, and Technological Development of the Republic of Serbia. We also thank the support of the visiting professor program of UBO to JFS.

## References

- [1] Q. Guo, Z. Jin, Y. Yuan et al., "New mechanisms of tumor-associated macrophages on promoting tumor progression: recent research advances and potential targets for tumor immunotherapy," *Journal of Immunology Research*, vol. 2016, Article ID 9720912, 12 pages, 2016.
- [2] L. Cassetta, S. Fragkogianni, A. H. Sims et al., "Human tumor-associated macrophage and monocyte transcriptional landscapes reveal cancer-specific reprogramming, biomarkers, and therapeutic targets," *Cancer Cell*, vol. 35, no. 4, pp. 588–602.e10, 2019.
- [3] A. J. Gentles, A. M. Newman, C. L. Liu et al., "The prognostic landscape of genes and infiltrating immune cells across human cancers," *Nature Medicine*, vol. 21, no. 8, pp. 938–945, 2015.



- [4] T. Beltraminelli and M. De Palma, "Biology and therapeutic targeting of tumour-associated macrophages," *The Journal of Pathology*, vol. 250, no. 5, pp. 573–592, 2020.
- [5] I. Vitale, G. Manic, L. M. Coussens, G. Kroemer, and L. Galluzzi, "Macrophages and metabolism in the tumor microenvironment," *Cell Metabolism*, vol. 30, no. 1, pp. 36–50, 2019.
- [6] S. R. McKeown, "Defining normoxia, physoxia and hypoxia in tumours-implications for treatment response," *The British Journal of Radiology*, vol. 87, no. 1035, 2014.
- [7] T. Chanmee, P. Ontong, K. Konno, and N. Itano, "Tumor-associated macrophages as major players in the tumor microenvironment," *Cancers*, vol. 6, no. 3, pp. 1670–1690, 2014.
- [8] M. M. G. Kes, J. Van den Bossche, A. W. Griffioen, and E. J. M. Huijbers, "Oncometabolites lactate and succinate drive pro-angiogenic macrophage response in tumors," *Biochimica et Biophysica Acta (BBA) - Reviews on Cancer*, vol. 1874, no. 2, 2020.
- [9] A. Viola, F. Munari, R. Sánchez-Rodríguez, T. Scolaro, and A. Castegna, "The metabolic signature of macrophage responses," *Frontiers in Immunology*, vol. 10, 2019.
- [10] Y. Xing, S. Zhao, B. P. Zhou, and J. Mi, "Metabolic reprogramming of the tumour microenvironment," *The FEBS Journal*, vol. 282, no. 20, pp. 3892–3898, 2015.
- [11] S. K. Biswas, "Metabolic reprogramming of immune cells in cancer progression," *Immunity*, vol. 43, no. 3, pp. 435–449, 2015.
- [12] L. Cassetta and J. W. Pollard, "Targeting macrophages: therapeutic approaches in cancer," *Nature Reviews. Drug Discovery*, vol. 17, no. 12, pp. 887–904, 2018.
- [13] D. G. DeNardo and B. Ruffell, "Macrophages as regulators of tumour immunity and immunotherapy," *Nature Reviews. Immunology*, vol. 19, no. 6, pp. 369–382, 2019.
- [14] M. Lecoultre, V. Dutoit, and P. R. Walker, "Phagocytic function of tumor-associated macrophages as a key determinant of tumor progression control: a review," *Journal for Immunotherapy of Cancer*, vol. 8, no. 2, article e001408, 2020.
- [15] A. Mantovani, G. Germano, F. Marchesi, M. Locatelli, and S. K. Biswas, "Cancer-promoting tumor-associated macrophages: new vistas and open questions," *European Journal of Immunology*, vol. 41, no. 9, pp. 2522–2525, 2011.
- [16] F. Balkwill, A. Mantovani, A. Sica, and F. Balkwill, "Inflammation and cancer: back to Virchow?," *The Lancet*, vol. 357, no. 9255, pp. 539–545, 2001.
- [17] M. De Palma, C. Murdoch, M. A. Venneri, L. Naldini, and C. E. Lewis, "Tie2-expressing monocytes: regulation of tumor angiogenesis and therapeutic implications," *Trends in Immunology*, vol. 28, no. 12, pp. 519–524, 2007.
- [18] S. R. Gordon, R. L. Maute, B. W. Dulken et al., "PD-1 expression by tumour-associated macrophages inhibits phagocytosis and tumour immunity," *Nature*, vol. 545, no. 7655, pp. 495–499, 2017.
- [19] T. M. Nywening, B. A. Belt, D. R. Cullinan et al., "Targeting both tumour-associated CXCR2+ neutrophils and CCR2+ macrophages disrupts myeloid recruitment and improves chemotherapeutic responses in pancreatic ductal adenocarcinoma," *Gut*, vol. 67, no. 6, pp. 1112–1123, 2018.
- [20] R. T. Netea-Maier, J. W. A. Smit, and M. G. Netea, "Metabolic changes in tumor cells and tumor-associated macrophages: a mutual relationship," *Cancer Letters*, vol. 413, pp. 102–109, 2018.
- [21] F. Lopes-Coelho, S. Gouveia-Fernandes, and J. Serpa, "Metabolic cooperation between cancer and non-cancerous stromal cells is pivotal in cancer progression," *Tumour Biology*, vol. 40, no. 2, 2018.
- [22] A. Sica and V. Bronte, "Altered macrophage differentiation and immune dysfunction in tumor development," *The Journal of Clinical Investigation*, vol. 117, no. 5, pp. 1155–1166, 2007.
- [23] J. Kim, "Regulation of immune cell functions by metabolic reprogramming," *Journal of Immunology Research*, vol. 2018, Article ID 8605471, 12 pages, 2018.
- [24] S. Guo and C. X. Deng, "Effect of stromal cells in tumor microenvironment on metastasis initiation," *International Journal of Biological Sciences*, vol. 14, no. 14, pp. 2083–2093, 2018.
- [25] Y. Liu, R. Xu, H. Gu et al., "Metabolic reprogramming in macrophage responses," *Biomarker Research*, vol. 9, no. 1, 2021.
- [26] X. Li, R. Liu, X. Su et al., "Harnessing tumor-associated macrophages as aids for cancer immunotherapy," *Molecular Cancer*, vol. 18, no. 1, p. 177, 2019.
- [27] D. Pantaloni, C. Le Clainche, and M. F. Carlier, "Mechanism of actin-based motility," *Science*, vol. 292, no. 5521, pp. 1502–1506, 2001.
- [28] X. Zheng, S. Mansouri, A. Krager et al., "Metabolism in tumour-associated macrophages: aquid pro quowith the tumour microenvironment," *European Respiratory Review*, vol. 29, no. 157, 2020.
- [29] M. Wenes, M. Shang, M. di Matteo et al., "Macrophage metabolism controls tumor blood vessel morphogenesis and metastasis," *Cell Metabolism*, vol. 24, no. 5, pp. 701–715, 2016.
- [30] H. Semba, N. Takeda, T. Isagawa et al., "HIF-1 $\alpha$ -PDK1 axis-induced active glycolysis plays an essential role in macrophage migratory capacity," *Nature Communications*, vol. 7, no. 1, p. 11635, 2016.
- [31] D. Liu, C. Chang, N. Lu et al., "Comprehensive proteomics analysis reveals metabolic reprogramming of tumor-associated macrophages stimulated by the tumor microenvironment," *Journal of Proteome Research*, vol. 16, no. 1, pp. 288–297, 2017.
- [32] H. L. Penny, J. L. Sieow, G. Adriani et al., "Warburg metabolism in tumor-conditioned macrophages promotes metastasis in human pancreatic ductal adenocarcinoma," *Oncoimmunology*, vol. 5, no. 8, 2016.
- [33] R. J. Arts, T. S. Plantinga, S. Tuit et al., "Transcriptional and metabolic reprogramming induce an inflammatory phenotype in non-medullary thyroid carcinoma-induced macrophages," *Oncoimmunology*, vol. 5, no. 12, 2016.
- [34] N. M. de-Brito, J. Duncan-Moretti, H. C. Da-Costa et al., "Aerobic glycolysis is a metabolic requirement to maintain the M2-like polarization of tumor-associated macrophages," *Biochimica et Biophysica Acta (BBA) - Molecular Cell Research*, vol. 1867, no. 2, 2020.
- [35] N. Y. Spencer and R. C. Stanton, "The Warburg effect, lactate, and nearly a century of trying to cure cancer," *Seminars in Nephrology*, vol. 39, no. 4, pp. 380–393, 2019.
- [36] B. Li, Q. Yang, Z. Li et al., "Expression of monocarboxylate transporter 1 in immunosuppressive macrophages is associated with the poor prognosis in breast cancer," *Frontiers in Oncology*, vol. 10, 2020.
- [37] H. Lu, C. L. Dalgard, A. Mohyeldin, T. McFate, A. S. Tait, and A. Verma, "Reversible inactivation of HIF-1 prolyl hydroxylases allows cell metabolism to control basal HIF-1," *The*

- Journal of Biological Chemistry*, vol. 280, no. 51, pp. 41928–41939, 2005.
- [38] S. A. Hobson-Gutierrez and C. Carmona-Fontaine, “The metabolic axis of macrophage and immune cell polarization,” *Disease Models & Mechanisms*, vol. 11, no. 8, 2018.
- [39] O. R. Colegio, N. Q. Chu, A. L. Szabo et al., “Functional polarization of tumour-associated macrophages by tumour-derived lactic acid,” *Nature*, vol. 513, no. 7519, pp. 559–563, 2014.
- [40] L. Zhang and S. Li, “Lactic acid promotes macrophage polarization through MCT-HIF1 $\alpha$  signaling in gastric cancer,” *Experimental Cell Research*, vol. 388, no. 2, 2020.
- [41] X. Mu, W. Shi, Y. Xu et al., “Tumor-derived lactate induces M2 macrophage polarization via the activation of the ERK/STAT3 signaling pathway in breast cancer,” *Cell Cycle*, vol. 17, no. 4, pp. 428–438, 2018.
- [42] C. I. Chang, J. C. Liao, and L. Kuo, “Macrophage arginase promotes tumor cell growth and suppresses nitric oxide-mediated tumor cytotoxicity,” *Cancer Research*, vol. 61, no. 3, pp. 1100–1106, 2001.
- [43] J. van den Bossche, W. H. Lamers, E. S. Koehler et al., “Pivotal advance: arginase-1-independent polyamine production stimulates the expression of IL-4-induced alternatively activated macrophage markers while inhibiting LPS-induced expression of inflammatory genes,” *Journal of Leukocyte Biology*, vol. 91, no. 5, pp. 685–699, 2012.
- [44] K. Rabold, M. G. Netea, G. J. Adema, and R. T. Netea-Maier, “Cellular metabolism of tumor-associated macrophages – functional impact and consequences,” *FEBS Letters*, vol. 591, no. 19, pp. 3022–3041, 2017.
- [45] A. H. Klimp, H. Hollema, C. Kempinga, A. G. van der Zee, E. G. de Vries, and T. Daemen, “Expression of cyclooxygenase-2 and inducible nitric oxide synthase in human ovarian tumors and tumor-associated macrophages,” *Cancer research*, vol. 61, no. 19, pp. 7305–7309, 2001.
- [46] M. R. Dinapoli, C. L. Calderon, and D. M. Lopez, “The altered tumoricidal capacity of macrophages isolated from tumor-bearing mice is related to reduce expression of the inducible nitric oxide synthase gene,” *The Journal of Experimental Medicine*, vol. 183, no. 4, pp. 1323–1329, 1996.
- [47] A. Viola and V. Bronte, “Metabolic mechanisms of cancer-induced inhibition of immune responses,” *Seminars in Cancer Biology*, vol. 17, no. 4, pp. 309–316, 2007.
- [48] J. Choi, B. Stradmann-Bellinghausen, E. Yakubov, N. E. Savaskan, and A. Régnier-Vigouroux, “Glioblastoma cells induce differential glutamatergic gene expressions in human tumor-associated microglia/macrophages and monocyte-derived macrophages,” *Cancer Biology & Therapy*, vol. 16, no. 8, pp. 1205–1213, 2015.
- [49] M. H. Oh, I. H. Sun, L. Zhao et al., “Targeting glutamine metabolism enhances tumor-specific immunity by modulating suppressive myeloid cells,” *The Journal of Clinical Investigation*, vol. 130, no. 7, pp. 3865–3884, 2020.
- [50] E. M. Palmieri, A. Menga, R. Martín-Pérez et al., “Pharmacologic or genetic targeting of glutamine synthetase skews macrophages toward an M1-like phenotype and inhibits tumor metastasis,” *Cell Reports*, vol. 20, no. 7, pp. 1654–1666, 2017.
- [51] Q. Zhao, D. M. Kuang, Y. Wu et al., “Activated CD69+ T cells foster immune privilege by regulating IDO expression in tumor-associated macrophages,” *Journal of Immunology*, vol. 188, no. 3, pp. 1117–1124, 2012.
- [52] J. D. Mezrich, J. H. Fechner, X. Zhang, B. P. Johnson, W. J. Burlingham, and C. A. Bradfield, “An interaction between kynurenine and the aryl hydrocarbon receptor can generate regulatory T cells,” *Journal of Immunology*, vol. 185, no. 6, pp. 3190–3198, 2010.
- [53] F. Baenke, B. Peck, H. Miess, and A. Schulze, “Hooked on fat: the role of lipid synthesis in cancer metabolism and tumour development,” *Disease Models & Mechanisms*, vol. 6, no. 6, pp. 1353–1363, 2013.
- [54] H. N. Abramson, “The lipogenesis pathway as a cancer target,” *Journal of Medicinal Chemistry*, vol. 54, no. 16, pp. 5615–5638, 2011.
- [55] A. J. Covarrubias, H. I. Aksoylar, and T. Horng, “Control of macrophage metabolism and activation by mTOR and Akt signaling,” *Seminars in Immunology*, vol. 27, no. 4, pp. 286–296, 2015.
- [56] T. Schumann, T. Adhikary, A. Wortmann et al., “Deregulation of PPAR $\beta/\delta$  target genes in tumor-associated macrophages by fatty acid ligands in the ovarian cancer microenvironment,” *Oncotarget*, vol. 6, no. 15, pp. 13416–13433, 2015.
- [57] A. Puthenveetil and S. Dubey, “Metabolic reprogramming of tumor-associated macrophages,” *Annals of Translational Medicine*, vol. 8, no. 16, p. 1030, 2020.
- [58] I. Daurkin, E. Eruslanov, T. Stoffs et al., “Tumor-associated macrophages mediate immunosuppression in the renal cancer microenvironment by activating the 15-lipoxygenase-2 pathway,” *Cancer Research*, vol. 71, no. 20, pp. 6400–6409, 2011.
- [59] H. Kuhn, S. Banthiya, and K. van Leyen, “Mammalian lipoxygenases and their biological relevance,” *Biochimica et Biophysica Acta*, vol. 1851, no. 4, pp. 308–330, 2015.
- [60] R. G. Snodgrass and B. Brüne, “Regulation and functions of 15-lipoxygenases in human macrophages,” *Frontiers in Pharmacology*, vol. 10, 2019.
- [61] W. Xiang, R. Shi, X. Kang et al., “Monoacylglycerol lipase regulates cannabinoid receptor 2-dependent macrophage activation and cancer progression,” *Nature Communications*, vol. 9, no. 1, p. 2574, 2018.
- [62] P. Su, Q. Wang, E. Bi et al., “Enhanced lipid accumulation and metabolism are required for the differentiation and activation of tumor-associated macrophages,” *Cancer Research*, vol. 80, no. 7, pp. 1438–1450, 2020.
- [63] Z. Niu, Q. Shi, W. Zhang et al., “Caspase-1 cleaves PPAR $\gamma$  for potentiating the pro-tumor action of TAMs,” *Nature Communications*, vol. 8, no. 1, p. 766, 2017.
- [64] L. Wu, X. Zhang, L. Zheng et al., “RIPK3 orchestrates fatty acid metabolism in tumor-associated macrophages and hepatocarcinogenesis,” *Cancer Immunology Research*, vol. 8, no. 5, pp. 710–721, 2020.
- [65] S. Y. Zhang, X. Y. Song, Y. Li, L. L. Ye, Q. Zhou, and W. B. Yang, “Tumor-associated macrophages: a promising target for a cancer immunotherapeutic strategy,” *Pharmacological Research*, vol. 161, 2020.
- [66] A. J. Petty and Y. Yang, “Tumor-associated macrophages: implications in cancer immunotherapy,” *Immunotherapy*, vol. 9, no. 3, pp. 289–302, 2017.
- [67] X. Xiang, J. Wang, D. Lu, and X. Xu, “Targeting tumor-associated macrophages to synergize tumor immunotherapy,” *Sig Transduct Target Ther*, vol. 6, no. 1, p. 75, 2021.
- [68] C. Anfray, A. Umarmarino, F. T. Andón, and P. Allavena, “Current strategies to target tumor-associated-macrophages to improve antitumor immune responses,” *Cells*, vol. 9, 2020.

- [69] I. Kryczek, L. Zou, P. Rodriguez et al., “B7-H4 expression identifies a novel suppressive macrophage population in human ovarian carcinoma,” *The Journal of Experimental Medicine*, vol. 203, no. 4, pp. 871–881, 2006.
- [70] W. Xu, T. Hi u, S. Malarkannan, and L. Wang, “The structure, expression, and multifaceted role of immune-checkpoint protein VISTA as a critical regulator of anti-tumor immunity, autoimmunity, and inflammation,” *Cellular & Molecular Immunology*, vol. 15, no. 5, pp. 438–446, 2018.
- [71] D. V. Prasad, S. Richards, X. M. Mai, and C. Dong, “B7S1, a novel B7 family member that negatively regulates T cell activation,” *Immunity*, vol. 18, no. 6, pp. 863–873, 2003.
- [72] J. Li, Y. Lee, Y. Li et al., “Co-inhibitory molecule B7 superfamily member 1 expressed by tumor-infiltrating myeloid cells induces dysfunction of anti-tumor CD8<sup>+</sup> T cells,” *Immunity*, vol. 48, no. 4, pp. 773–786.e5, 2018.
- [73] L. Cassetta and T. Kitamura, “Targeting tumor-associated macrophages as a potential strategy to enhance the response to immune checkpoint inhibitors,” *Frontiers in Cell and Developmental Biology*, vol. 6, p. 38, 2018.
- [74] N. M. Ratnam, S. C. Frederico, J. A. Gonzalez, and M. R. Gilbert, “Clinical correlates for immune checkpoint therapy: significance for C.N.S. malignancies,” *Neuro-Oncology Advances*, vol. 3, no. 1, 2021.
- [75] A. Mantovani, F. Marchesi, A. Malesci, L. Laghi, and P. Allavena, “Tumour-associated macrophages as treatment targets in oncology,” *Nature Reviews. Clinical Oncology*, vol. 14, no. 7, pp. 399–416, 2017.
- [76] Y. Zhu, B. L. Knolhoff, M. A. Meyer et al., “CSF1/CSF1R blockade reprograms tumor-infiltrating macrophages and improves response to T-cell checkpoint immunotherapy in pancreatic cancer models,” *Cancer Research*, vol. 74, no. 18, pp. 5057–5069, 2014.
- [77] X. Wu, R. Singh, D. K. Hsu et al., “A Small Molecule CCR2 Antagonist Depletes Tumor Macrophages and Synergizes with Anti-PD-1 in a Murine Model of Cutaneous T-Cell Lymphoma (CTCL),” *Journal of Investigative Dermatology*, vol. 140, no. 7, pp. 1390–1400.e4, 2020.
- [78] H. S. Sow, H. Benonisson, C. Breukel et al., “FcγR interaction is not required for effective anti-PD-L1 immunotherapy but can add additional benefit depending on the tumor model,” *International Journal of Cancer*, vol. 144, no. 2, pp. 345–354, 2019.
- [79] A. M. Georgoudaki, K. E. Prokopec, V. F. Boura et al., “Reprogramming tumor-associated macrophages by antibody targeting inhibits cancer progression and metastasis,” *Cell Reports*, vol. 15, no. 9, pp. 2000–2011, 2016.
- [80] C. Ceci, M. G. Atzori, P. M. Lical, and G. Graziani, “Targeting tumor-associated macrophages to increase the efficacy of immune checkpoint inhibitors: a glimpse into novel therapeutic approaches for metastatic melanoma,” *Cancers*, vol. 12, no. 11, p. 3401, 2020.
- [81] M. Qorraj, H. Bruns, M. Böttcher et al., “The PD-1/PD-L1 axis contributes to immune metabolic dysfunctions of monocytes in chronic lymphocytic leukemia,” *Leukemia*, vol. 31, no. 2, pp. 470–478, 2017.
- [82] M. Qorraj, M. Böttcher, and D. Mougiakakos, “PD-L1/PD-1: new kid on the “immune metabolic” block,” *Oncotarget*, vol. 8, no. 43, pp. 73364–73365, 2017.
- [83] Y. Zhang, L. Ma, X. Hu, J. Ji, G. Mor, and A. Liao, “The role of the PD-1/PD-L1 axis in macrophage differentiation and function during pregnancy,” *Human Reproduction*, vol. 34, no. 1, pp. 25–36, 2019.
- [84] Z. N. Di Lu, X. Liu, S. Feng et al., “Beyond T cells: understanding the role of PD-1/PD-L1 in tumor-associated macrophages,” *Journal of Immunology Research*, vol. 2019, Article ID 1919082, 7 pages, 2019.
- [85] K. J. Caldwell, S. Gottschalk, and A. C. Talleur, “Allogeneic CAR cell therapy—more than a pipe dream,” *Frontiers in Immunology*, vol. 11, 2021.
- [86] Y. Chen, Z. Yu, X. Tan et al., “CAR-macrophage: A new immunotherapy candidate against solid tumors,” *Biomed Pharmacother*, vol. 139, Article ID 111605, 2021.
- [87] M. Chmielewski, C. Kopecky, A. A. Hombach, and H. Abken, “IL-12 release by engineered T cells expressing chimeric antigen receptors can effectively muster an antigen-independent macrophage response on tumor cells that have shut down tumor antigen expression,” *Cancer Research*, vol. 71, no. 17, pp. 5697–5706, 2011.
- [88] D. Li, X. Li, W. L. Zhou et al., “Genetically engineered T cells for cancer immunotherapy,” *Signal Transduction and Targeted Therapy*, vol. 4, no. 1, 2019.
- [89] M. Chmielewski and H. Abken, “CAR T cells releasing IL-18 convert to T-Bet<sup>high</sup> FoxO1<sup>low</sup> effectors that exhibit augmented activity against advanced solid tumors,” *Cell Reports*, vol. 21, no. 11, pp. 3205–3219, 2017.
- [90] J. M. Grimes, R. D. Carvajal, and P. Muranski, “Cellular therapy for the treatment of solid tumors,” *Transfusion and Apheresis Science*, vol. 60, no. 1, 2021.
- [91] Z. Ge and S. Ding, “The crosstalk between tumor-associated macrophages (TAMs) and tumor cells and the corresponding targeted therapy,” *Frontiers in Oncology*, vol. 10, 2020.
- [92] E. R. Unanue, “Antigen-presenting function of the macrophage,” *Annual Review of Immunology*, vol. 2, no. 1, pp. 395–428, 1984.
- [93] M. A. Morrissey, A. P. Williamson, A. M. Steinbach et al., “Chimeric antigen receptors that trigger phagocytosis,” *Elife*, vol. 7, 2018.
- [94] E. J. Velazquez, J. E. Lattin, T. D. Brindley et al., “Abstract 2563: Macrophage Toll-like receptor-chimeric antigen receptors (MOTO-CARs) as a novel adoptive cell therapy for the treatment of solid malignancies,” *Cancer Research*, vol. 78, 13, Supplement, 2018.
- [95] K. O’neill and Weber S, inventors, “Macrophage chimeric antigen receptor (moto-car) in immunotherapy,” 2017, WO2017025944A3.
- [96] D. Kumar, U. Vetrivel, S. Parameswaran, and K. K. Subramanian, “Structural insights on druggable hotspots in CD147: a bull’s eye view,” *Life Sciences*, vol. 224, pp. 76–87, 2019.
- [97] W. Zhang, L. Liu, H. Su et al., “Chimeric antigen receptor macrophage therapy for breast tumours mediated by targeting the tumour extracellular matrix,” *British Journal of Cancer*, vol. 121, no. 10, pp. 837–845, 2019.
- [98] M. Klichinsky, M. Ruella, O. Shestova et al., “Human chimeric antigen receptor macrophages for cancer immunotherapy,” *Nature Biotechnology*, vol. 38, no. 8, pp. 947–953, 2020.
- [99] N. Cheng, X. Bai, Y. Shu, O. Ahmad, and P. Shen, “Targeting tumor-associated macrophages as an antitumor strategy,” *Biochemical Pharmacology*, vol. 183, 2021.



## Research Article

# LINC00665 Facilitates the Malignant Processes of Osteosarcoma by Increasing the RAP1B Expression via Sponging miR-708 and miR-142-5p

Limin Wang,<sup>1</sup> Xinghua Song,<sup>1</sup> Lijun Yu,<sup>1</sup> Bing Liu,<sup>2</sup> Jinfeng Ma ,<sup>3</sup> and Weihua Yang <sup>4</sup>

<sup>1</sup>Department of Orthopedics, Dongying Traditional Chinese Medicine Hospital, Dongying, 257055 Shandong, China

<sup>2</sup>Department of Clinical Laboratory, Dongying Traditional Chinese Medicine Hospital, Dongying, 257055 Shandong, China

<sup>3</sup>Department of Orthopedics, Affiliated Hospital of Qingdao University, Qingdao 266003, China

<sup>4</sup>Department of Surgery, Dongying Traditional Chinese Medicine Hospital, Dongying, 257055 Shandong, China

Correspondence should be addressed to Jinfeng Ma; [lptmt47@163.com](mailto:lptmt47@163.com) and Weihua Yang; [weihuayang@protonmail.com](mailto:weihuayang@protonmail.com)

Received 7 February 2021; Revised 15 June 2021; Accepted 23 June 2021; Published 8 July 2021

Academic Editor: Victor H. Villar

Copyright © 2021 Limin Wang et al. This is an open access article distributed under the Creative Commons Attribution License, which permits unrestricted use, distribution, and reproduction in any medium, provided the original work is properly cited.

Osteosarcoma (OS) is a kind of fatal primary bone tumors in adolescents and young adults. Long noncoding RNAs (lncRNAs) are a group of noncoding RNAs which occupy a part of the latest hot topics. We aimed to investigate the roles of lncRNA LINC00665 in OS in this study. In this study, we found that LINC00665 was highly expressed in OS tissues and cell lines, and its high expression was associated with malignant feature and poor prognosis of OS. In OS cells, LINC00665 could facilitate the proliferation, migration, and invasion to play an oncogenic role. Mechanistically, LINC00665 served as a sponge for miR-708 and miR-142-5p and positively mediated the expression of their target RAP1B. Finally, we confirmed that LINC00665 exercised its biological functions by mediating RAP1B. In conclusion, LINC00665 is overexpressed in OS and facilitates the malignant processes of OS cells by increasing the RAP1B expression via sponging miR-708 and miR-142-5p.

## 1. Introduction

Osteosarcoma (OS) is one of the most frequently occurring primary bone tumors in adolescents and young adults [1, 2]. Although combination of multiple therapies prolonged the life expectancy of majority patients, the 5-year survival rate of OS is still low due to its high malignancy [3]. Many tumor-related molecules play key parts in the tumorigenesis of OS, making the pathogenesis of OS awfully complex [4]. Thus, it is urgently needed to find these molecules and uncover their roles in OS.

Long noncoding RNAs (lncRNAs) are a group of noncoding RNAs with over 200 nucleotides in length and have no protein-coding ability [5]. They are involved in a wide array of physiological and biological cellular processes including transcriptional regulation, epigenetic modification, and acting as microRNA (miRNA) sponges [6–8]. A large number of lncRNAs have been found to be abnormally

expressed in multiple tumors, exerting great impacts on carcinogenesis and cancer progression [9]. Regarding OS, lncRNAs have been identified as oncogenic or tumor suppressive genes to participate in the carcinogenesis or anti-tumor process [10]. For instance, lncRNA CEBPA-AS1 is found to be weakly expressed in OS and inhibit proliferation and migration and stimulate apoptosis of OS cells [11]. LncRNA RP11-361F15.2 is significantly increased in OS and promotes osteosarcoma tumorigenesis by inhibiting M2-Like polarization of tumor-associated macrophages of CPEB4 [12].

Long intergenic noncoding RNA 00665 (LINC00665), a newly identified lncRNA transcribed from chromosome 19q13.12, has been reported to function as an oncogene in several cancers such as prostate cancer [13], breast cancer [14], gastric cancer [15], non-small-cell lung cancer [16], and hepatocellular carcinoma [17]. To our knowledge, the expression and functions of LINC00665 in OS have not been investigated previously. Hence, in this study, we intended to

explore the expression, biological function, and possible mechanisms in OS.

## 2. Materials and Methods

**2.1. Tissue Samples.** Paired OS and the adjacent nontumorous normal tissues were obtained from 42 patients who underwent complete resection surgery at the Dongying Traditional Chinese Medicine Hospital. The adjacent normal tissues were at least 4 cm away from the tumor tissues, and all the tissues were histologically characterized by pathologists. None of these patients received radiotherapy or chemotherapy before surgery. The present study was approved by the ethics committee of Dongying Traditional Chinese Medicine Hospital and strictly followed the Declaration of Helsinki. Written informed consents were provided by all participants.

**2.2. Cell Culture and Transfection.** OS cell lines (MG63, U2OS, 143B and Saos-2) and normal osteoblast cell line (hFOB) were obtained from American Type Culture Collection (ATCC, USA). These cell lines were maintained in DMEM medium (Thermo Fisher Scientific, USA) with 10% FBS (Gibco, USA) in a humidified atmosphere of 5% CO<sub>2</sub> at 37°C. Cell lines used in this study had been authenticated by STR cell identification from May 2016 to April 2018. We confirm that all experiments were performed with mycoplasma-free cells. Cell transfection was carried out with Lipofectamine 3000 (Invitrogen, USA). The full-length LINC00665 was inserted into a pcDNA3.1 vector to realize the endogenous LINC00665 expression, and short-hairpin RNA (shRNA) targeting LINC00665 was constructed to knockdown LINC00665.

**2.3. Real-Time Quantification Polymerase Chain Reaction (qRT-PCR).** Total RNAs were extracted from tissues or cells using TRIzol Reagent (Invitrogen). Nuclear and cytoplasmic RNAs of OS cells were separated by a PARIS Kit (Invitrogen, USA). RNAs were then reversely transcribed by a Prime-Script RT Master Mix (Perfect Real Time) (TaKaRa, Japan). SYBR Green Realtime PCR Master Mix (Takara, Japan) and an ABI7500 system were utilized to accomplish qPCR reaction. Relative RNA expressions were calculated by the  $2^{-\Delta\Delta CT}$  method and normalized to GAPDH (for LINC00665) or U6 (for miRNAs). Sequences of primers used in this study were LINC00665, forward, 5'-GGTGCA AAGTGGGAAGTGTG-3', reverse, 5'-CGGTGGACGGA TGAGAAACG-3'; miR-708, forward, 5'-GGCGCGCAA GGAGCTTACAATC-3', reverse, 5'-GTGCAGGGTCC GAGGTAT-3'; miR-142-5p, forward, 5'-AGCTCGCGCAT AAAGTAGAAAG-3', reverse, 5'-TATGGTTGTTCTCGTC TCTGTGTC-3'; GAPDH, forward, 5'-ACCACAGTCCA TGCCATCAC-3', reverse, 5'-TCCACCCTGTTGCTGTA-3'; U6, forward, 5'-GCTTCGGCAGCACATATACTAAAA T-3', reverse, 5'-CGCTTACGAATTTGCGTGTGCAT-3'.

**2.4. Cell Proliferation Assays.** The proliferation of OS cells was investigated by the cell counting kit-8 (CCK8) assay and 5-ethynyl-2'-deoxyuridine (EdU) assay. For the CCK8

assay, cells were seeded into a 96-well plates and transfected with plasmids or oligonucleotides. CCK-8 reagent (Dojindo, Japan) was added into each well after cells were grown for 24, 48, and 72 hours. After incubation, optical density at 450 nm was detected using a microplate reader. For the EdU assay, cells were seeded in a 96-well plate and transfected for 48 h. Cell-light™ EdU ApolloR567 in Vitro Imaging Kit (Ribobio, China) was applied to fluorescently label cells those were synthesizing DNA. Images were taken with a fluorescent microscope to calculate the EdU-positive cells.

**2.5. Cell Migration and Invasion Assays.** Cell migration capability was assessed by the wound-healing assay. Transfected cells were inoculated in 6-well plates for 24 hours and scratched with a pipette tip (0 h). Cells were then cultured in FBS-free DMEM medium for another 24 hours (24 h). Cell migration was observed under the microscope.

Cell invasion potential was evaluated by the transwell assay using transwell chambers (Corning, USA). Cells transfected for 48 h were harvested and seeded in the matrigel coated upper chamber with FBS-free DMEM medium. The lower chamber was added with DMEM medium supplemented with 10% FBS. Cells that pierced through the membrane were fixed and dyed to count numbers.

**2.6. Fluorescence In Situ Hybridization (FISH) Assay.** The FISH assay was performed using a Fluorescent In Situ Hybridization Kit (RiboBio). Fluorescence-conjugated probes for LINC00665, miR-708, and miR-142-5p were designed and synthesized by RiboBio. These probes were used to fluorescently locate LINC00665, miR-708, and miR-142-5p, and DAPI served to show nucleus.

**2.7. RNA Immunoprecipitation (RIP) Assay.** The RIP assay was conducted using a Magna RIP RNA-binding protein immunoprecipitation kit (Millipore, USA). Cells were lysed with lysis buffer and incubated with magnetic beads coated with Ago2 antibody or IgG antibody. The RNA level in the immunoprecipitate complex was analyzed by qRT-PCR.

**2.8. Luciferase Reporter Assay.** The wild-type (wt) miRNAs target sites in LINC00665 or RAP1B 3'UTR, and the mutant-type (mut) binding sites were synthesized and cloned into the downstream of a pmirGLO vector (Promega, USA). Cells were cotransfected with pmirGLO luciferase plasmid and miRNA mimics. A Dual-Luciferase Reporter Assay System (Promega, USA) was used to detect the luciferase activity.

**2.9. Western Blot Assay.** Total proteins were isolated by RIPA buffer containing protease inhibitor. Proteins were separated on the 10% sodium dodecyl sulfate-polyacrylamide gradient gel and then transferred onto PVDF membranes (Millipore). The blocked membranes were incubated with primary antibodies (Anti-RAP1B, ab182606, Abcam, USA) at 4°C overnight and secondary antibody at room temperature for 1 h. Signals were visualized using ECL Substrates (Millipore), and GAPDH was used as an internal control.

**2.10. Statistical Analysis.** Statistical analyses were implemented with SPSS 19.0 software (IBM, USA). All data from



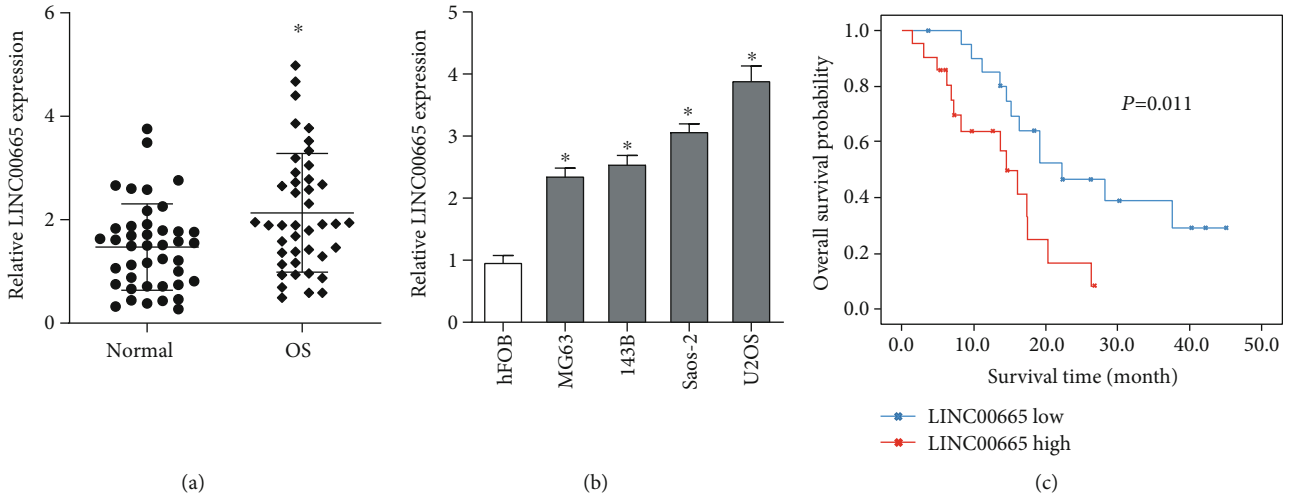


FIGURE 1: LINC00665 is upregulated in OS. (a) Expressions of LINC00665 in paired OS and nontumorous normal tissues were detected by qRT-PCR. (b) Expressions of LINC00665 in OS cell lines and normal osteoblast cell line were detected by qRT-PCR. (c) Overall survival of OS patients was analyzed by the Kaplan-Meier method. \* $P < 0.05$ .

TABLE 1: Association between clinical features of OS patients and LINC00665 expression in OS tissues.

Features	Cases	LINC00665 low	LINC00665 high	<i>P</i> value
Sex				
Male	22	10	12	
Female	20	11	9	0.537
Age(years)				
<20	25	11	14	
≥20	17	10	7	0.346
Tumor size (cm)				
<5 cm	25	16	9	
≥5 cm	17	5	12	0.028
Clinical stage				
I/IIA	23	17	6	
IB/III	19	4	15	0.001
Distant metastasis				
No	24	15	9	
Yes	18	6	12	0.061
Anatomic location				
Femur/tibia	28	13	15	
Elsewhere	14	8	6	0.513

at least three independent experiments were presented in terms of the mean  $\pm$  standard deviation (SD). Differences between two or more groups were evaluated by Student's *t*-test or one-way analysis of variance (ANOVA), respectively.  $P < 0.05$  was considered to be statistically significant.

### 3. Results

**3.1. LINC00665 Is Upregulated in OS.** First, qRT-PCR was utilized to determine the LINC00665 expression in OS tissues and cell lines. We observed that the expression of LINC00665 was increased in OS tissues (Figure 1(a)) and cell lines (Figure 1(b)). After evaluating the correlation between the

LINC00665 expression and clinicopathological characteristics, we noticed that patients with larger tumor size and later clinical stages presented higher LINC00665 level (Table 1). We also exhibited that high LINC00665 expression implied poor overall survival of OS patients (Figure 1(c)).

**3.2. LINC00665 Facilitates the Malignant Progressions of OS Cells.** To uncover the function of LINC00665 in OS, LINC00665 was endogenously overexpressed in MG63 cells and knocked down in U2OS cells (Figure 2(a)). Then, data of CCK8 assays and EdU assays showed that the overexpression of LINC00665 promoted the proliferation ability of MG63 cells, and knockdown of LINC00665 restrained the

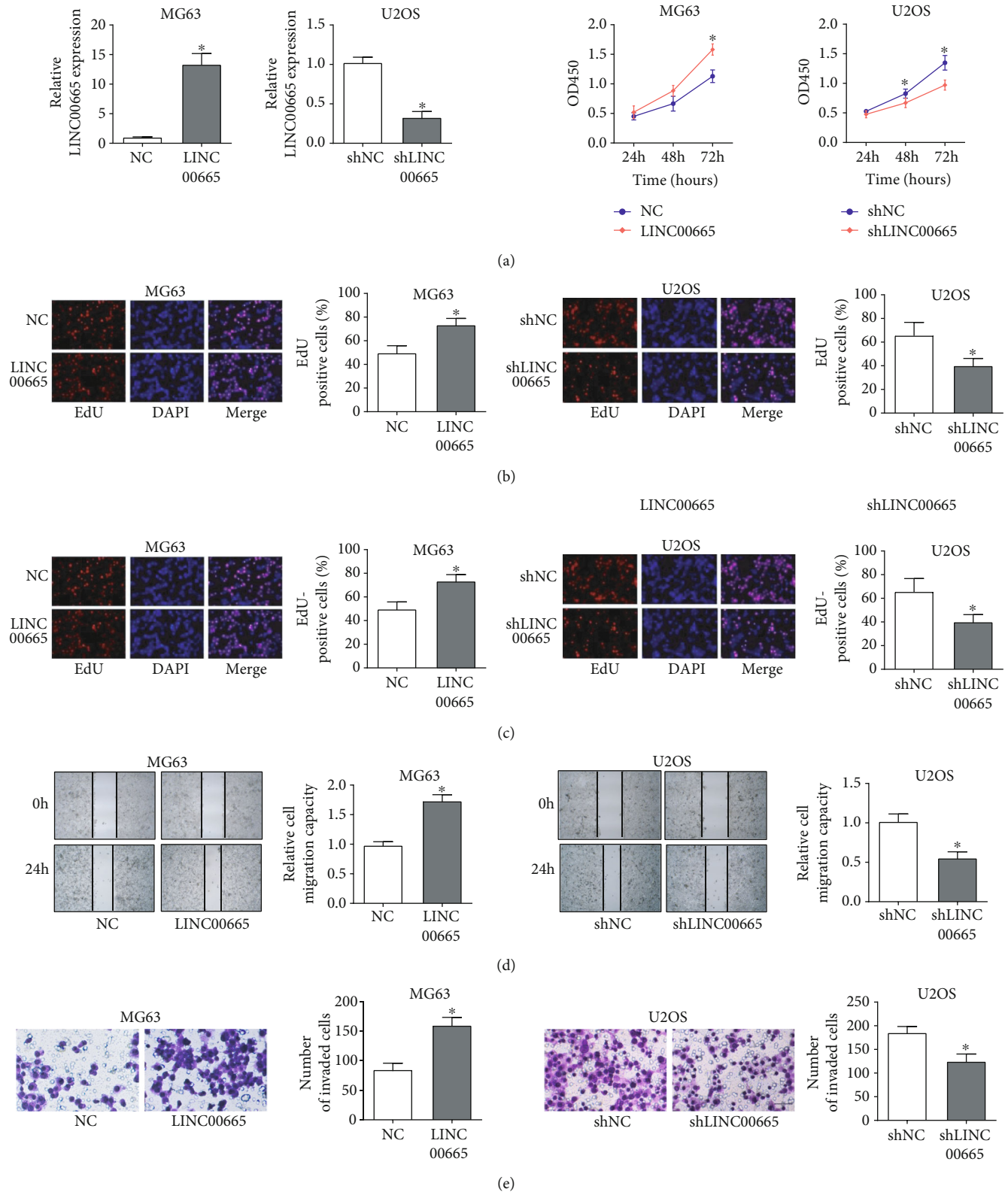


FIGURE 2: LINC00665 facilitates the malignant progressions of OS cells. (a) Overexpression or knockdown efficiency of LINC00665 in OS cells was determined by RT-qPCR analysis. (b, c) The impact of the LINC00665 overexpression or knockdown on OS cells proliferation was examined by CCK-8 assays (b) and EdU assays (c). (d, e) The effects of LINC00665 overexpression or knockdown on OS cells migration and invasion were assessed by wound-healing assays ((d), magnification, 40 $\times$ ) and transwell assay ((e), magnification, 100 $\times$ ). \* $P < 0.05$ .

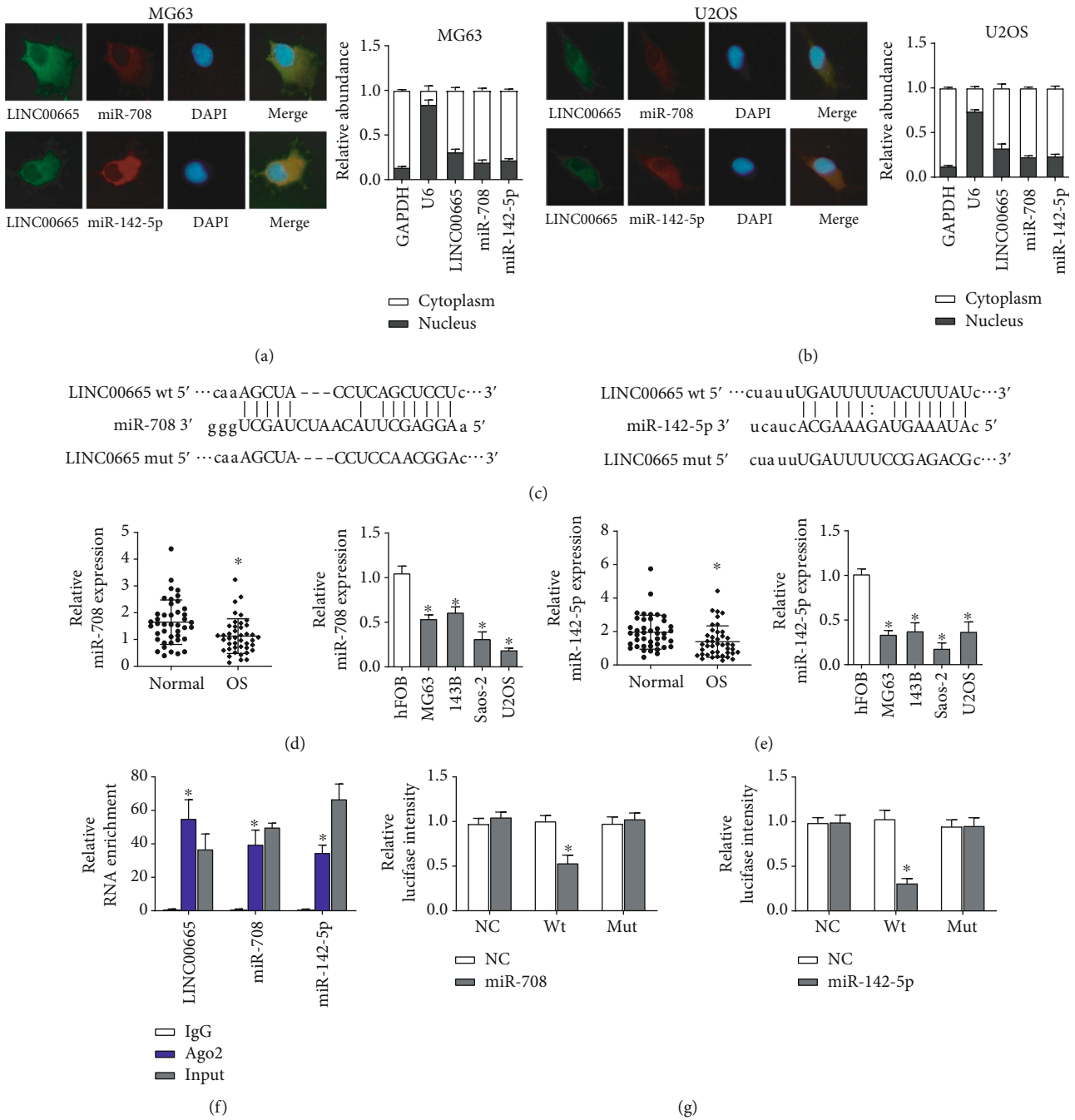


FIGURE 3: LINC00665 operates as a miRNA sponge for miR-708 and miR-142-5p. (a, b) FISH assays and qRT-PCR assays determined the subcellular localization of LINC00665, miR-708, and miR-142-5p in OS cells. (c) Predicted binding sequences of miR-708 or miR-142-5p with LINC00665. (d, e) Expressions of miR-708 and miR-142-5p in OS tissues and cell lines detected by qRT-PCR. (f) RIP assays identified the enrichment of LINC00665, miR-708, and miR-142-5p in Ago2 conjugates. (g) Predicted binding sequences of miR-708 or miR-142-5p with LINC00665 were validated by luciferase reporter assays. \**P* < 0.05.

proliferation capacity of U2OS cells (Figures 2(b) and 2(c)). Moreover, the wound-healing assay and transwell assay exhibited that the overexpression of LINC00665 was raised while silence of LINC00665 depressed migration and invasion capacity of OS cells (Figures 2(d) and 2(e)). Here, we concluded that LINC00665 facilitated the malignant progressions of OS cells.

**3.3. LINC00665 Operates as a miRNA Sponge for miR-708 and miR-142-5p.** To explore the molecular roles of LINC00665 in OS, we performed FISH assays and qRT-PCR assay to study the subcellular localization of LINC00665. We found that LINC00665 mainly existed in the cytoplasm of MG63 and U2OS cells (Figures 3(a) and 3(b)). LINC00665 was reported to mainly locate in cytoplasm and functioned as

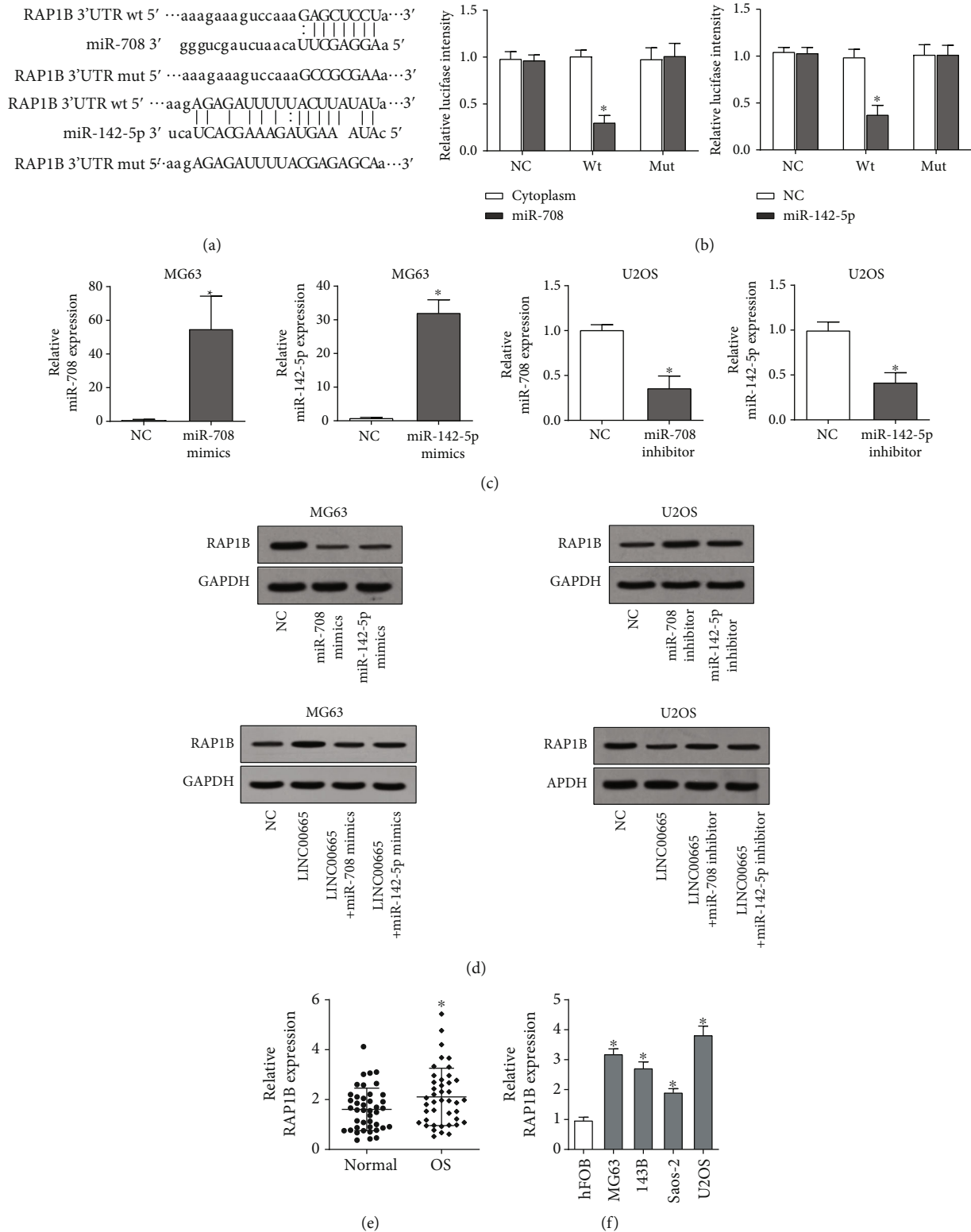


FIGURE 4: LINC00665 upregulates the RAP1B expression via miR-708 and miR-142-5p. (a) Predicted binding sequences of miR-708 or miR-142-5p with 3'UTR of RAP1B mRNA. (b) Predicted binding sequences of miR-708 or miR-142-5p with 3'UTR of RAP1B mRNA were validated by luciferase reporter assays. (c) The efficiency of the overexpression and knockdown of miR-708 and miR-142-5p in OS cells detected by qRT-PCR. (d) Western blot assays indicated the impact of miR-708 and miR-142-5p on the protein level of RAP1B, as well as the impact of LINC00665 together with miR-708 or miR-142-5p on the protein level of RAP1B. (e) Expressions of RAP1B mRNA in paired OS and nontumorous normal tissues were detected by qRT-PCR. (f) Expressions of RAP1B mRNA in OS cell lines and normal osteoblast cell line were detected by qRT-PCR.

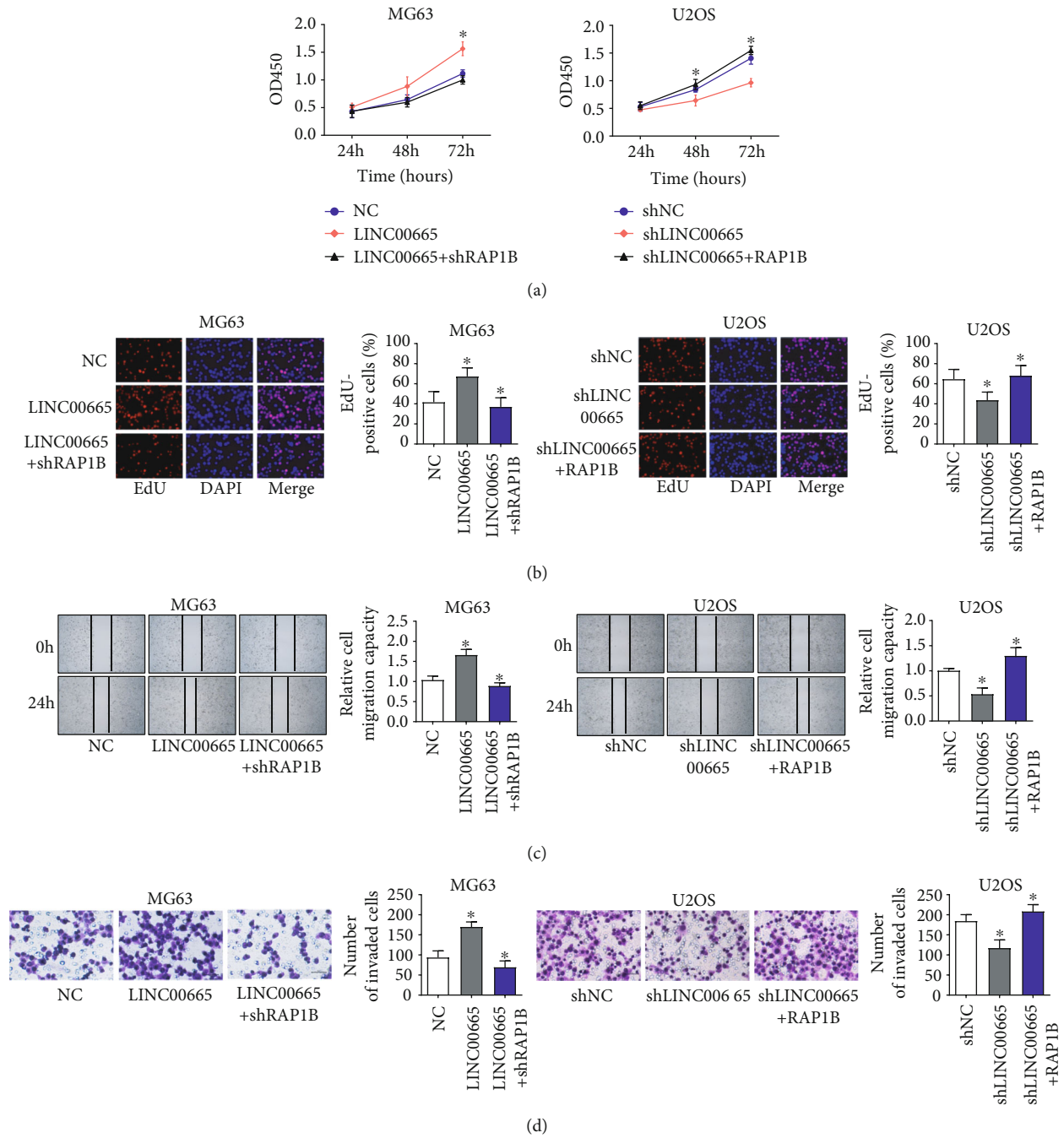


FIGURE 5: LINC00665 exercises its biological functions by mediating RAP1B. (a, b) CCK8 (a) and EdU assays (b) showed the regulation of LINC00665 and RAP1B on proliferation of OS cells. (c) Wound-healing assays showed the influence of LINC00665 and RAP1B on migration of OS cells; magnification, 40 $\times$ . (d) Transwell assays displayed the influence of LINC00665 and RAP1B on invasion of OS cells, magnification, 100 $\times$ . \* $P < 0.05$ .

miRNA sponges in lung adenocarcinoma and breast cancer cells [18, 19]. So, we predicted the miRNAs that might bind to LINC00665 via the starBase database and found that miR-708 and miR-142-5p were potential candidates (Figure 3(c)). We also presented that miR-708 and miR-142-5p showed similar subcellular localization with LINC00665 (Figures 3(a) and 3(b)) and decreased expression in OS tissues and cell lines (Figures 3(d) and 3(e)). Subse-

quently, we carried out RIP assays, and the results revealed that LINC00665, miR-708, and miR-142-5p were significant enriched in Ago2 conjugates (Figure 3(f)) which indicated that these genes may possess a common acting basis. More important, the specific binding sites were validated by luciferase reporter assays (Figure 3(g)). These data all together suggested that LINC00665 operated as a miRNA sponge for miR-708 and miR-142-5p.



**3.4. LINC00665 Upregulates the RAP1B Expression via miR-708 and miR-142-5p.** Next, we attempted to discover the possible target genes of miR-708 and miR-142-5p. Through starBase and microRNA.org databases, we identified RAP1B as a common target of miR-708 and miR-142-5p (Figure 4(a)). We then used luciferase reporter assays verified the specific binding of miR-708 and miR-142-5p in the 3' UTR of RAP1B mRNA (Figure 4(b)). We then overexpressed and knocked down miR-708 and miR-142-5p in OS cells (Figure 4(c)) and discovered that both miR-708 and miR-142-5p could decrease the protein level of RAP1B (Figure 4(d)). What is more, we demonstrated that LINC00665 upregulated the RAP1B expression which could be attenuated by miR-708 or miR-142-5p (Figure 4(e)). Collectively, the above data suggested that LINC00665 upregulated the RAP1B expression via miR-708 and miR-142-5p. Moreover, we found that the RAP1B expression was also increased in OS tissues (Figure 4(f)) and cell lines (Figure 4(g)), which indicated that it may play carcinogenic effects.

**3.5. LINC00665 Exercises Its Biological Functions by Mediating RAP1B.** Finally, we investigated the roles of RAP1B in the regulation of OS cellular progressions by LINC00665. We discovered that the RAP1B overexpression could absorb the accelerating effects of LINC00665 on proliferation, migration, and invasion (Figures 5(a)–5(d)). Accordingly, silence of RAP1B could abate the inhibitory effects of LINC00665 on proliferation, migration, and invasion (Figures 5(a)–5(d)). On the whole, these results uncovered that LINC00665 exercises its biological functions by mediating RAP1B.

#### 4. Discussion

Accumulating evidence has suggested that many lncRNAs play vital roles in multiple cellular processes during tumorigenesis, whereas only few of them have been well characterized [9]. LINC00665 is a newly identified lncRNA which has been studied in several cancers but not in OS. Consistent with the conclusions of previous studies in other cancers, our present study uncovered that LINC00665 is also an oncogene in OS.

In this study, we displayed that LINC00665 was highly expressed in OS tissues and cell lines. The high LINC00665 expression was closely associated with aggressive clinicopathological characteristics and poor prognosis of OS. Therefore, as in other cancers [13–16], LINC00665 might also be a promising biomarker in OS. Functionally, we further discovered that LINC00665 facilitated OS cells proliferation, migration, and invasion with loss- and gain-of-function assays. These data means that LINC00665 also plays oncogenic roles in OS.

In addition, we showed a new regulation pathway of LINC00665 in OS. LINC00665 mainly exists in cytoplasm of OS cells that operates as a miRNA sponge for miR-708 and miR-142-5p. Then, LINC00665 upregulates the expression of RAP1B which is a target of both miR-708 and miR-142-5p in a competing endogenous RNA (ceRNA) manner. MiR-708 and miR-142-5p have been confirmed to be onco-

genes in OS [20, 21]. RAP1B is a member of the RAS oncogene family and participated in multiple cellular processes including cell growth, adhesion, and differentiation [22]. Increasing evidences reveal that the deregulated activation of RAP1B is involved in a spectrum of malignancies [23]. Here, we demonstrated that RAP1B is essential for LINC00665 that exercises its biological functions of promoting proliferation, migration, and invasion.

#### 5. Conclusions

In summary, we report that LINC00665 is overexpressed in OS and associated with malignant feature and poor prognosis of OS. LINC00665 facilitates the proliferation, migration, and invasion of OS cells by increasing the RAP1B expression via sponging miR-708 and miR-142-5p.

#### Data Availability

All the data is available with the handwritten notebook documented in our lab.

#### Conflicts of Interest

The authors declare that there are no conflicts of interest regarding the publication of this paper.

#### Acknowledgments

This study was supported by the Scientific Research Foundation for Advanced Talents (Grant No. 20190911).

#### References

- [1] M. A. Anwar, C. El-Baba, M. H. Elnaggar et al., “Novel therapeutic strategies for spinal osteosarcomas,” *Seminars in Cancer Biology*, vol. 64, pp. 83–92, 2020.
- [2] K. Scotlandi, C. M. Hattinger, E. Pellegrini, M. Gambarotti, and M. Serra, “Genomics and therapeutic vulnerabilities of primary bone tumors,” *Cell*, vol. 9, no. 4, p. 968, 2020.
- [3] V. Carina, V. Costa, M. Sartori et al., “Adjuvant biophysical therapies in osteosarcoma,” *Cancers (Basel)*, vol. 11, no. 3, p. 348, 2019.
- [4] Y. H. Lin, B. E. Jewell, J. Gingold et al., “Osteosarcoma: molecular pathogenesis and iPSC modeling,” *Trends in Molecular Medicine*, vol. 23, no. 8, pp. 737–755, 2017.
- [5] I. Tsagakis, K. Douka, I. Birds, and J. L. Aspden, “Long non-coding RNAs in development and disease: conservation to mechanisms,” *The Journal of Pathology*, vol. 250, no. 5, pp. 480–495, 2020.
- [6] R. Gong and Y. Jiang, “Non-coding RNAs in pancreatic ductal adenocarcinoma,” *Frontiers in Oncology*, vol. 10, p. 309, 2020.
- [7] W. Lou, B. Ding, and P. Fu, “Pseudogene-derived lncRNAs and their miRNA sponging mechanism in human cancer,” *Frontiers in Cell and Development Biology*, vol. 8, p. 85, 2020.
- [8] X. Xia, Y. Ruan, B. Li et al., “The long non-coding RNA lnc-DMP1 regulates DMP 1 expression through H3K27Ac modification,” *Frontiers in Genetics*, vol. 11, p. 233, 2020.
- [9] R. Choudhari, M. J. Sedano, A. L. Harrison et al., “Long non-coding RNAs in cancer: from discovery to therapeutic targets,” *Advances in Clinical Chemistry*, vol. 95, pp. 105–147, 2020.

- [10] C. Wang, J. Jing, and L. Cheng, "Emerging roles of non-coding RNAs in the pathogenesis, diagnosis and prognosis of osteosarcoma," *Investigational New Drugs*, vol. 36, no. 6, pp. 1116–1132, 2018.
- [11] P. Xia, R. Gu, W. Zhang, and Y. F. Sun, "lncRNA CEBPA-AS1 overexpression inhibits proliferation and migration and stimulates apoptosis of OS cells via notch signaling," *Mol Ther Nucleic Acids*, vol. 19, pp. 1470–1481, 2020.
- [12] D. Yang, K. Liu, L. Fan et al., "LncRNA RP11-361F15.2 promotes osteosarcoma tumorigenesis by inhibiting M2-like polarization of tumor-associated macrophages of CPEB4," *Cancer Letters*, vol. 473, pp. 33–49, 2020.
- [13] W. Chen, Z. Yu, W. Huang, Y. Yang, F. Wang, and H. Huang, "LncRNA LINC00665 promotes prostate cancer progression via miR-1224-5p/SND1 axis," *Oncotargets and Therapy*, vol. 13, pp. 2527–2535, 2020.
- [14] J. L. Zhou, L. Zou, and T. Zhu, "Long non-coding RNA LINC00665 promotes metastasis of breast cancer cells by triggering EMT," *European Review for Medical and Pharmacological Sciences*, vol. 24, no. 6, pp. 3097–3104, 2020.
- [15] B. Yang, Q. Bai, H. Chen, K. Su, and C. Gao, "LINC00665 induces gastric cancer progression through activating Wnt signaling pathway," *Journal of Cellular Biochemistry*, vol. 121, no. 3, pp. 2268–2276, 2020.
- [16] X. Liu, X. Lu, F. Zhen et al., "LINC00665 induces acquired resistance to gefitinib through recruiting EZH2 and activating PI3K/AKT pathway in NSCLC," *Mol Ther Nucleic Acids*, vol. 16, pp. 155–161, 2019.
- [17] Y. Shan and P. Li, "Long intergenic non-protein coding RNA 665 regulates viability, apoptosis, and autophagy via the MiR-186-5p/MAP4K3 Axis in hepatocellular carcinoma," *Yonsei Medical Journal*, vol. 60, no. 9, pp. 842–853, 2019.
- [18] Z. Cong, Y. Diao, Y. Xu et al., "Long non-coding RNA linc00665 promotes lung adenocarcinoma progression and functions as ceRNA to regulate AKR1B10-ERK signaling by sponging miR-98," *Cell Death & Disease*, vol. 10, no. 2, p. 84, 2019.
- [19] W. Ji, Y. L. Diao, Y. R. Qiu, J. Ge, X. C. Cao, and Y. Yu, "LINC00665 promotes breast cancer progression through regulation of the miR-379-5p/LIN28B axis," *Cell Death & Disease*, vol. 11, no. 1, p. 16, 2020.
- [20] H. Liu, R. Chen, F. Kang, H. Lai, and Y. Wang, "KCNQ1OT1 promotes ovarian cancer progression via modulating MIR-142-5p/CAPN10 axis," *Molecular Genetics & Genomic Medicine*, vol. 8, no. 2, article e1077, 2020.
- [21] C. Sui, D. Liu, Y. Hu, and L. Zhang, "MicroRNA-708-5p affects proliferation and invasion of osteosarcoma cells by targeting URGCP," *Experimental and Therapeutic Medicine*, vol. 17, pp. 2235–2241, 2019.
- [22] L. Stefanini and W. Bergmeier, "RAP GTPases and platelet integrin signaling," *Platelets*, vol. 30, no. 1, pp. 41–47, 2019.
- [23] L. Zhang, M. Cui, L. Song, M. Zhang, and J. Zhang, "Function, significance, and regulation of Rap1b in malignancy," *Critical Reviews in Eukaryotic Gene Expression*, vol. 29, no. 2, pp. 151–160, 2019.

## Research Article

# GTSE1 Facilitates the Malignant Phenotype of Lung Cancer Cells via Activating AKT/mTOR Signaling

Fan Zhang,<sup>1</sup> Jingfei Meng,<sup>2</sup> Hong Jiang,<sup>1</sup> Xing Feng,<sup>1</sup> Dongshan Wei,<sup>1</sup> and Wen Meng<sup>1</sup> 

<sup>1</sup>Department of Cardiothoracic Surgery, Affiliated Hangzhou First People's Hospital, Zhejiang University School of Medicine, 310006, China

<sup>2</sup>The Second Affiliated Hospital of Xi'an Jiaotong University, Xi'an 710061, China

Correspondence should be addressed to Wen Meng; mengwentaian@163.com

Received 1 February 2021; Revised 17 April 2021; Accepted 19 April 2021; Published 3 May 2021

Academic Editor: Victor H. Villar

Copyright © 2021 Fan Zhang et al. This is an open access article distributed under the Creative Commons Attribution License, which permits unrestricted use, distribution, and reproduction in any medium, provided the original work is properly cited.

The expression of G2 and S phase-expressed-1 (GTSE1) was upregulated in human cancer. However, its expression and roles in lung cancer have not been identified yet. In our study, we reported that GTSE1 expression was statistically higher in lung tissues than in the adjacent noncancerous tissues which might be a consequence of hypomethylation of the GTSE1 promoter. The upregulated expression of GTSE1 mRNA predicted the poorer survival of the lung patients. Ectopic expression of GTSE1 in lung cancer cells significantly increased while knockdown of GTSE1 decreased cell proliferation, cell migration, and cell invasion in H460 and A549 cells. Furthermore, knockdown of GTSE1 regulated the cell cycle and promoted cell apoptosis in H460 and A549 cells. Finally, we presented that GTSE1 was able to activate AKT/mTOR signaling in H460 and A549 cells. In conclusion, these results indicated that the overexpressed GTSE1 was involved in the progress of lung cancer by promoting proliferation migration and invasion and inhibiting apoptosis of lung cancer cells via activating AKT/mTOR signaling.

## 1. Introduction

Lung cancer is one of the most common and deadly cancers worldwide [1, 2]. Lung cancer is primarily initiated from a combination of factors including smoking, genetic factors, asbestos, radon gas, and air pollution [3, 4]. The current treatment methods for lung cancer include laser ablation of malignant lesion, surgery, chemotherapy, photodynamic therapy, and radiation therapy [5]. Thus, identification of new targets for lung cancer is of great importance for prognosis prediction and therapy.

G2 and S phase-expressed-1 (GTSE1) is found in chromosome 22q13.2-q13.3 and expressed during the cell cycle S and G2 phases [6, 7]. Its common molecular function is to bind to the tumor suppressor protein p53 and impede the cancer suppressor ability of p53 in cancers [8]. Some studies further reported that upregulation of GTSE1 was frequently found in several types of human cancers [9, 10]. Upregulation of GTSE1 promoted cell proliferation and cell

migration and invasion in the progress of hepatocellular carcinoma [11]. In gastric cancer cells, GTSE1 expression inhibited apoptotic signaling and conferred resistance to cisplatin [12]. The overexpression of GTSE1 suppressed cisplatin sensitivity via p53 apoptotic signaling in gastric cancer [12]. It has been confirmed that the expression of GTSE1 was increased in lung cancer, and its high expression has a close relationship to the histological types [13]. However, the prognosis and roles of GTSE1 have not yet been investigated in the development of lung cancer.

In this study, we demonstrated that GTSE1 was upregulated and correlated with worse outcome in lung cancer. Ectopic expression of GTSE1 promoted whereas knockdown of GTSE1 inhibited the proliferation, migration, and invasion of lung cancer cells A549 and H460. Deletion of GTSE1 regulated the cell cycle and triggered apoptosis in A549 and H460 cell lines. We think that GTSE1 may exert the above biological functions by activating the AKT/mTOR signaling pathway in lung cancer.

## 2. Materials and Methods

**2.1. Tissue Specimens.** Lung cancer tissues and adjacent non-cancerous tissues from patients with lung cancer were collected from Affiliated Hangzhou First People's Hospital, Zhejiang University School of Medicine. This study was approved by the ethics committee of Affiliated Hangzhou First People's Hospital, Zhejiang University School of Medicine. Written informed consent was obtained from all the participants.

**2.2. Data Mining and Analysis.** The online cancer microarray database, Oncomine (<http://www.oncomine.org>), and TCGA database were used to assess the GTSE1 transcription level in lung cancer compared with that in normal controls by Student's *t*-test.

**2.3. Survival Analysis.** Kaplan-Meier survival curves with a hazard ratio (HR), logrank *p* value (*p*), and 95% confidence interval (CI) were analyzed and plotted using the Kaplan-Meier plotter (<http://kmplot.com>) platform and Xen platform, which has integrated the gene expression data, relapse-free, and TCGA (The Cancer Genome Atlas), EGA (European Genome-phenome Archive), and overall survival information from GEO (Gene Expression Omnibus).

**2.4. Cell Culture and Transfection.** The lung cell lines (H146, H82, H460, A549, and H460) and human normal lung epithelial cell line (Beas-2b) were cultured in RPMI 1600 added with 10% fetal bovine serum (FBS) in a humidified incubator with 5% CO<sub>2</sub> at 37°C.

**2.5. Lentivirus Infection.** The lentiviruses used to overexpress GTSE1 and control empty vector were from GeneChem (Shanghai, China), and lenti-shRNA for GTSE1 knockdown and scramble shRNA were synthesized by GenePharma (Shanghai, China). Lentivirus productions were described previously [14].

**2.6. Cell Proliferation Assay.** Cell proliferation was assessed using the CCK8 counting kit (Promega). The cells were uniformly seeded in a 96-well plate at a density of  $1 \times 10^4$ , and the OD value of the cells at 450 nm wavelength was measured at the same time for 5 consecutive days to evaluate cell viability.

**2.7. Colony Formation Assay.** Cell number was counted, and cells were seeded in a six-well plate with 300 cells per well. After culturing for 2 weeks, cell colonies were fixed using methanol, dyed with 5% crystal violet, and counted.

**2.8. Wound Healing Assay.** The cells were seeded in 6-well plates until 90% confluence. The confluent monolayers were scratched with a 200  $\mu$ l pipette tip to generate the wound. The debris and floating cells were removed by PBS washing. The cells were cultured for 24 hours and 48 hours for wound healing. The photographic images were taken at 0 hour, 24 hours, and 48 hours.

**2.9. Transwell Invasion Assays.** The invasive activity of the cells was detected using the transwell migration assay. Briefly,

the cell culture medium containing 10% FBS was added into the lower chamber. After transduction, the cells were seeded onto the upper chamber of the transwell. The invasive cells at the lower chamber were fixed using methanol, dyed with 5% crystal violet, and imaged under a microscope.

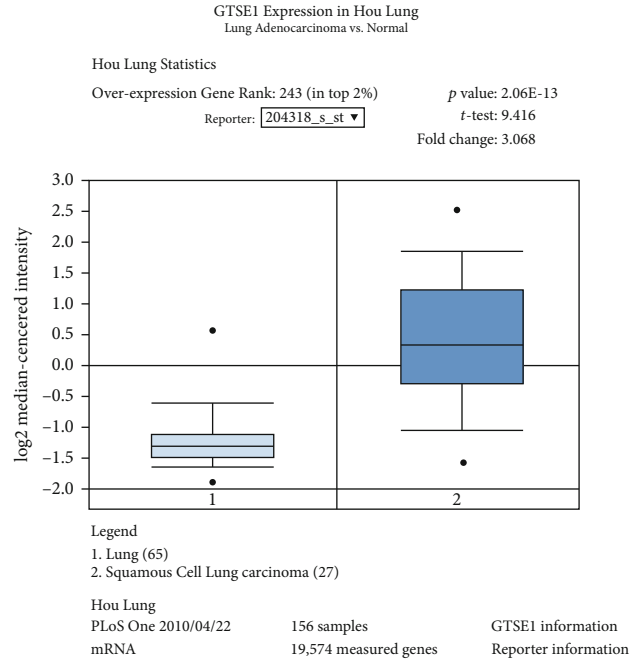
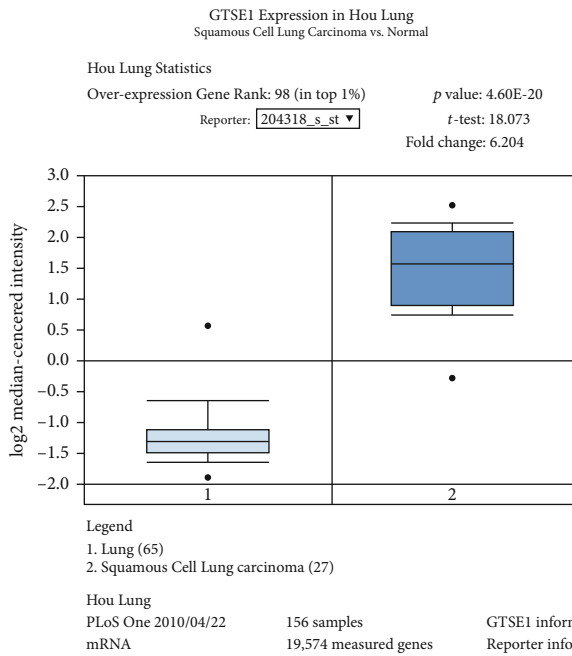
**2.10. Cell Cycle and Apoptosis Analysis.** Based on the manufacturer's instruction, the cell cycle and apoptosis were analyzed by using the PI staining kit and Annexin-V-FITC/PI staining kit (Invitrogen), respectively. After staining, the cells were analyzed by using a flow cytometer (CytoFlex, Beckman Coulter, Fullerton, CA, USA).

**2.11. Statistical Analysis.** All statistical analyses were performed using SPSS 22.0 (SPSS Inc., Chicago, IL). The values are presented as means  $\pm$  SD. The difference between the groups was analyzed by Student's *t*-test or one-way analysis of variance. *p* value < 0.05 was considered statistically significant.

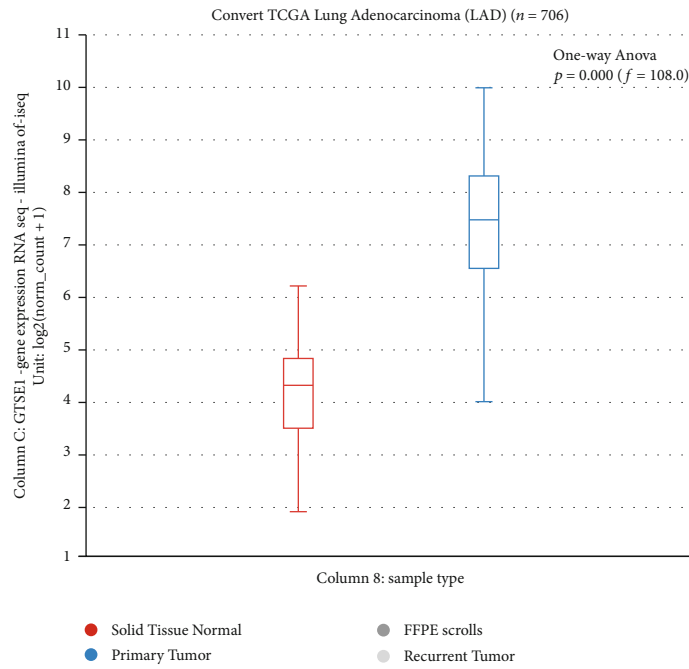
## 3. Results

**3.1. The Prognostic Value of GTSE1 mRNA Level in Lung Cancer.** By consulting the Oncomine database, we found that the mRNA levels of GTSE1 were higher in lung cancer tissues than in normal lung tissues. The mRNA levels of GTSE1 were elevated in squamous cell lung carcinoma and lung adenocarcinoma compared with normal lung tissues (fold change: 6.204 and 3.068, respectively) (Figure 1(a)). From TCGA database, we demonstrated that the levels of GTSE1 were increased in lung cancer tissues compared with normal lung tissues. TCGA database revealed that the GTSE1 expression is also increased in lung tumor samples (Figure 1(b)). Through TCGA database, we also found that the methylation level of the GTSE1 promoter was significantly decreased (Figure 1(c)). We think that the hypomethylation of the GTSE1 promoter might be responsible for its high expression. The Kaplan-Meier plotter analysis database revealed that high GTSE1 expression predicts poorer overall survival of lung cancer patients (Figure 1(d)). Therefore, the GTSE1 mRNA expression can act as a prognostic marker for patients with lung cancer.

**3.2. GTSE1 Is Upregulated in Lung Cancer Samples and Cell Lines.** To investigate the expression of GTSE1 in lung cancer cell lines and samples, the messenger RNA (mRNA) levels of GTSE1 in the tumor samples and corresponding normal tissues were detected by RT-PCR. The mRNA levels of GTSE1 showed significant upregulation in lung cell lines (H146, H82, H460, A549, and H460) compared with the Beas-2b cell line. In accordance with mRNA level changes, the western blotting assay revealed that the protein levels of GTSE1 were significantly increased in these cell lines (H146, H82, H460, A549, and H460) compared with the Beas-2b cell line (Figure 2(b)), especially in A549 and H460 cells. Furthermore, we detected the GTSE1 mRNA expression level in lung cancer tumor tissues. As can be seen from Figure 2(c), the mRNA level of GTSE1 was significantly increased in 3 paired cancer tissues compared with noncancerous tissues. Consistently, the western blotting assay also revealed a significant



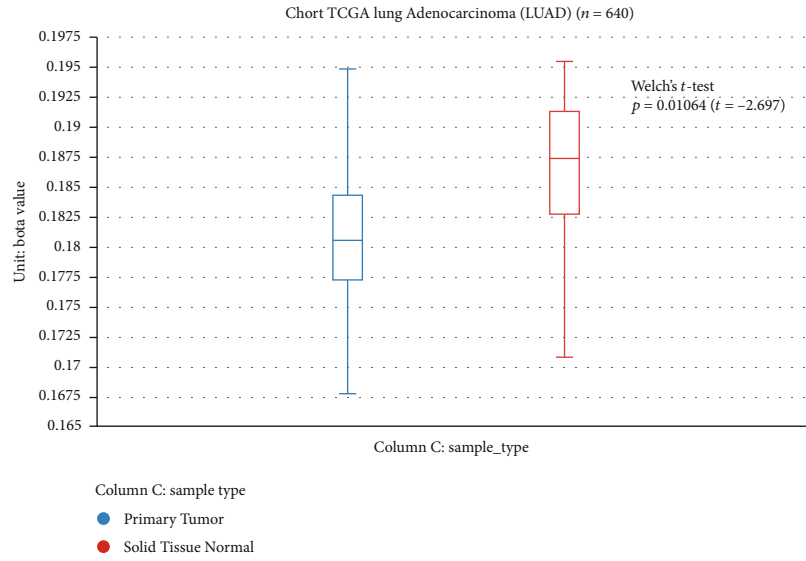
(a)



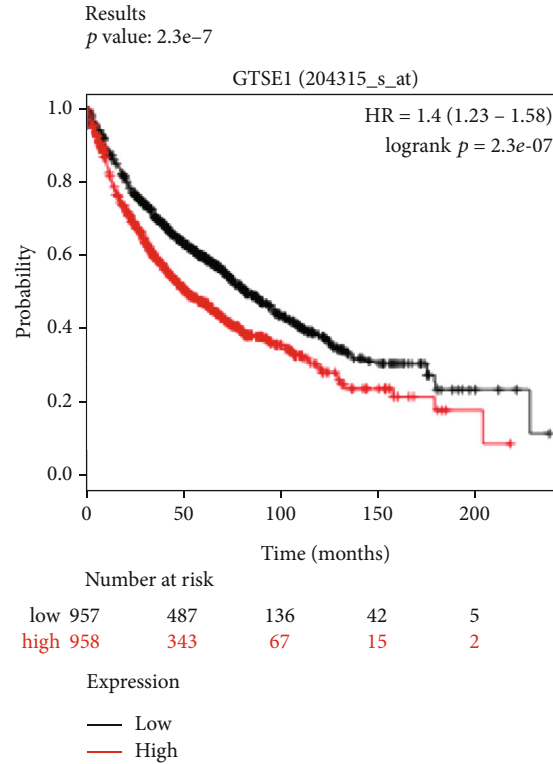
(b)

FIGURE 1: Continued.





(c)



(d)

FIGURE 1: The prognostic role of GTSE1 expression in lung cancer. (a) The mRNA levels of GTSE1 in squamous cell lung carcinoma and lung adenocarcinoma were higher than those in lung normal tissues. (b) TCGA database revealed the GTSE1 expression in lung tumor samples and normal lung samples. (c) TCGA database revealed that the methylation level of the GTSE1 promoter was significantly decreased. (d) The Kaplan-Meier plotter analysis database revealed the overall survival of patients with lung cancer with high or low GTSE1 expression.

increase in the protein level of GTSE1 (Figure 2(d)). All these data demonstrated that GTSE expression was upregulated in lung cancer cell lines and tissue samples.

3.3. Ectopic Expression of GTSE1 Promotes Proliferation, Invasion, and Migration of Lung Cancer Cells A549 and H460. To explore the functions of GTSE1 in the lung cancer

cell line, the lentivirus-mediated expression system was adopted to stably overexpress GTSE1 in A549 and H460 cells. We validated the overexpression of GTSE1 in the two cell lines using the WB assay (Figure 3(a)). The CCK8 assay showed that cell proliferation was promoted by GTSE1 overexpression (Figure 3(b)). The results of the colony formation assay showed that overexpression of GTSE1 increased the

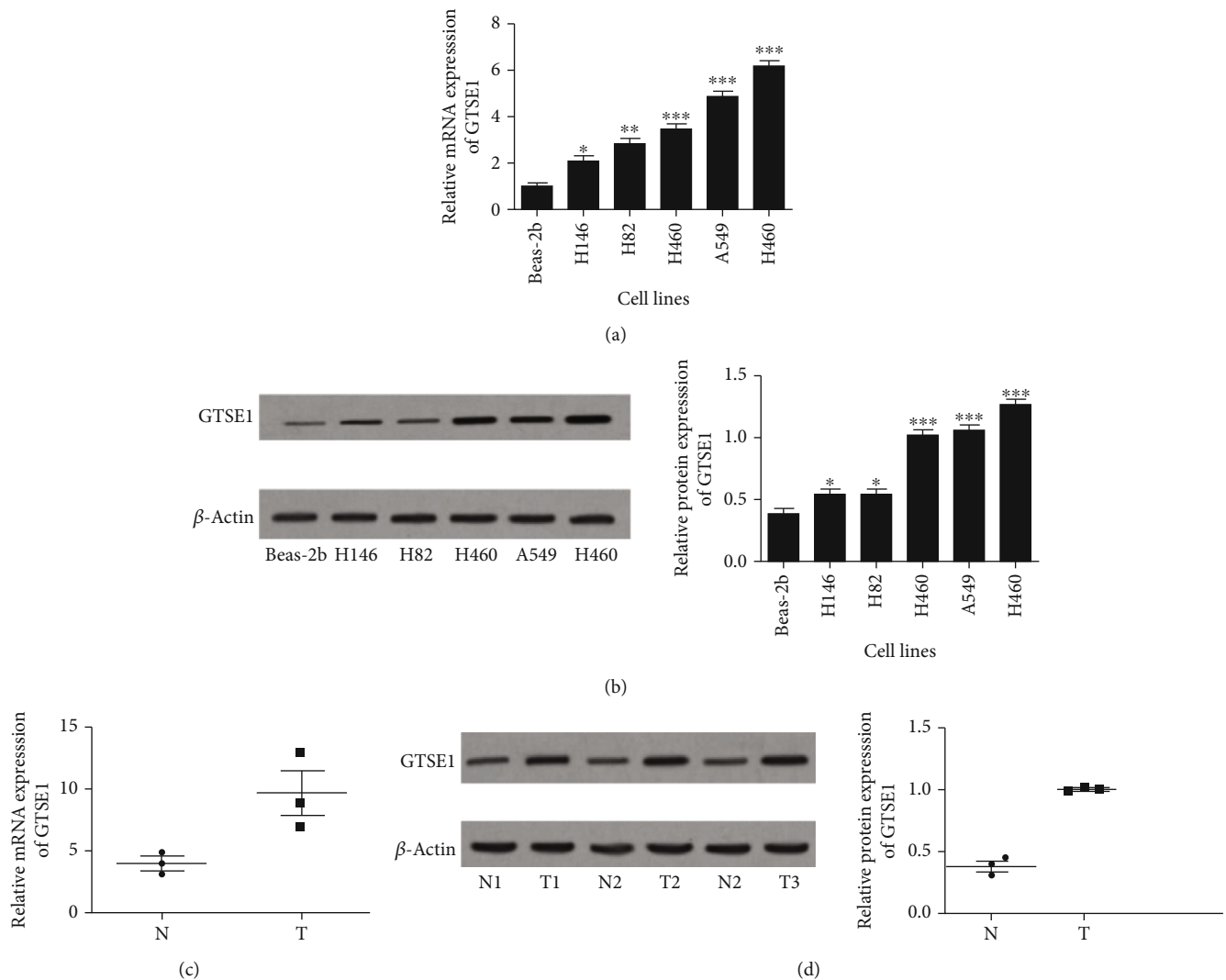


FIGURE 2: GTSE1 expression in lung cancer tissues and cells. (a) RT-PCR analysis of GTSE1 mRNA in lung cell lines. (b) Western blotting analysis of GTSE1 protein in lung cell lines. (c) RT-PCR analysis of GTSE1 mRNA levels in lung cancer tissues. (d) Western blotting analysis of GTSE1 protein in lung cancer tissues. All the values of three independent experiments were presented as means  $\pm$  SD. \* $p < 0.05$  and \*\* $p < 0.01$ .

colony number of A549 and H460 cell lines (Figure 3(c)). The wound healing assay showed that overexpression of GTSE1 promoted the migration of A549 and H460 cell lines (Figure 3(d)). The transwell invasion assay showed that overexpressed GTSE1 significantly increased the A549 and H460 cell invasion (Figure 3(e)). These results revealed that GTSE1 could promote the proliferation, colony formation, cell migration, and invasion in lung cancer.

**3.4. Knockdown of GTSE1 Inhibited Proliferation, Invasion, and Migration of Lung Cancer Cells A549 and H460.** To further confirm the oncogene role of GTSE1, the GTSE1 gene was silenced by shRNAs delivered by lentivirus in the H460 and A549 cell lines. We validated the silence of GTSE1 in both A549 and H460 cell lines by using the WB assay (Figure 4(a)). The results of the CCK8 assay showed that cell proliferation was inhibited by GTSE1 downregulation (Figure 4(b)). In the colony formation assay, low expression

of GTSE1 inhibited the colony number of A549 and H460 cell lines (Figure 4(c)). The wound healing assay showed that low expression of GTSE1 decreased the migration ability of A549 and H460 cell lines (Figure 4(d)). The transwell invasion assay presented that silencing GTSE1 significantly inhibited the invasion of A549 and H460 cell lines (Figure 4(e)). These results demonstrated that silencing the GTSE1 expression suppressed the proliferation, colony formation, invasion, and migration of lung cancer cells.

**3.5. Deletion of GTSE1 Regulated the Cell Cycle and Induced Cell Apoptosis in H460 and A549 Cell Lines.** Next, we explored the effect of GTSE1 on the cell cycle and apoptosis in H460 and A549 cell lines. As shown in Figure 5, the cell cycle and cell apoptosis were measured by flow cytometric analysis. Silencing of GTSE1 inhibited the S of cell cycles and suppressed the cell cycles in H460 and A549 cells (Figures 5(a) and 5(b)). Silencing of GTSE1 induced cell

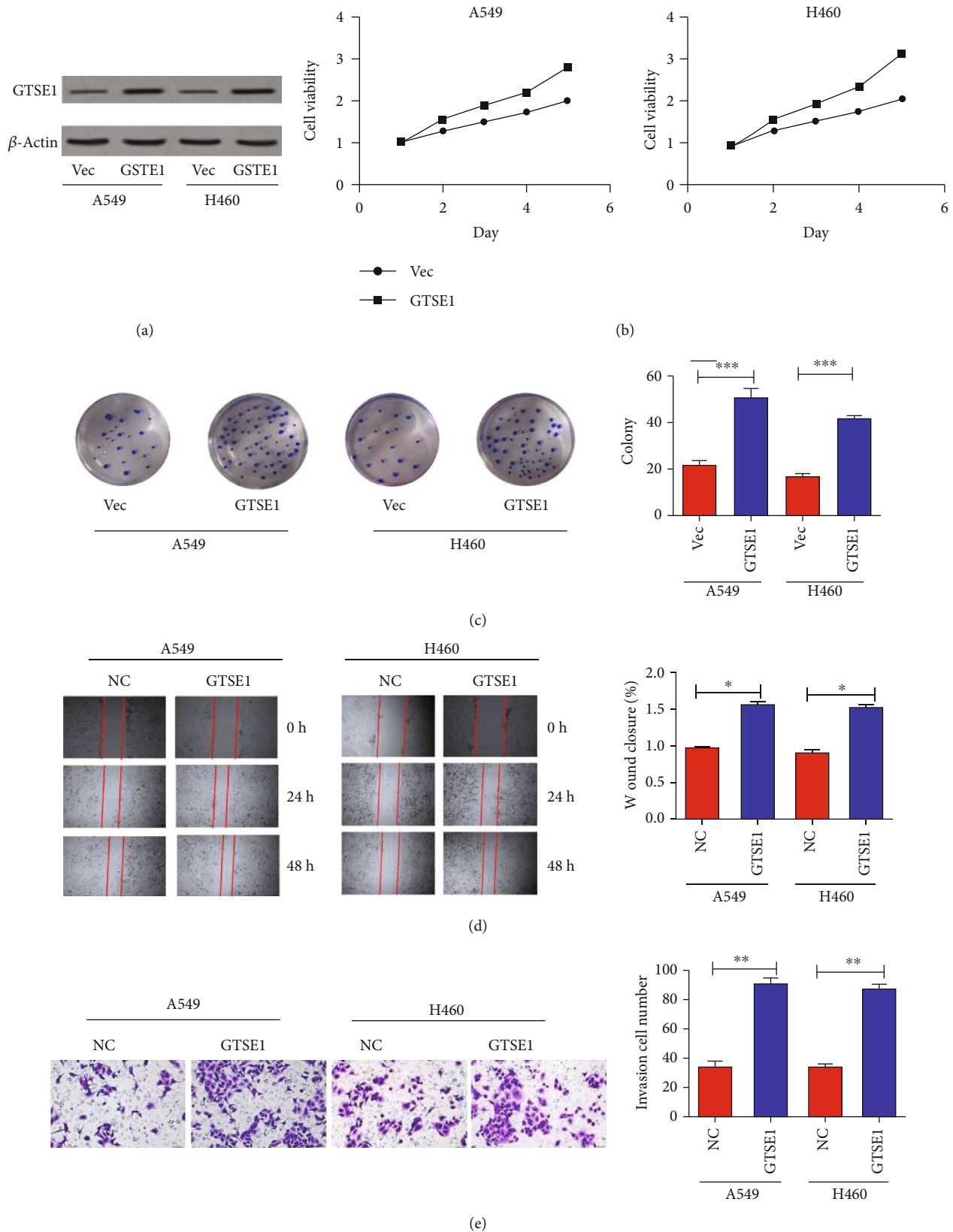


FIGURE 3: Ectopic expression of GTSE1 promotes proliferation, migration, and invasion of lung cancer cells A549 and H460. (a–e) GTSE1 was overexpressed in A549 and H460 cells. (a) The overexpression of GTSE1 in cells A549 and H460 was validated by using the WB assay. The CCK8 assay (b), colony formation (c), wound healing assay (d), and transwell invasion assay (e) were performed to evaluate cell proliferation, migration, and invasion. \* $p < 0.05$  and \*\* $p < 0.01$ .

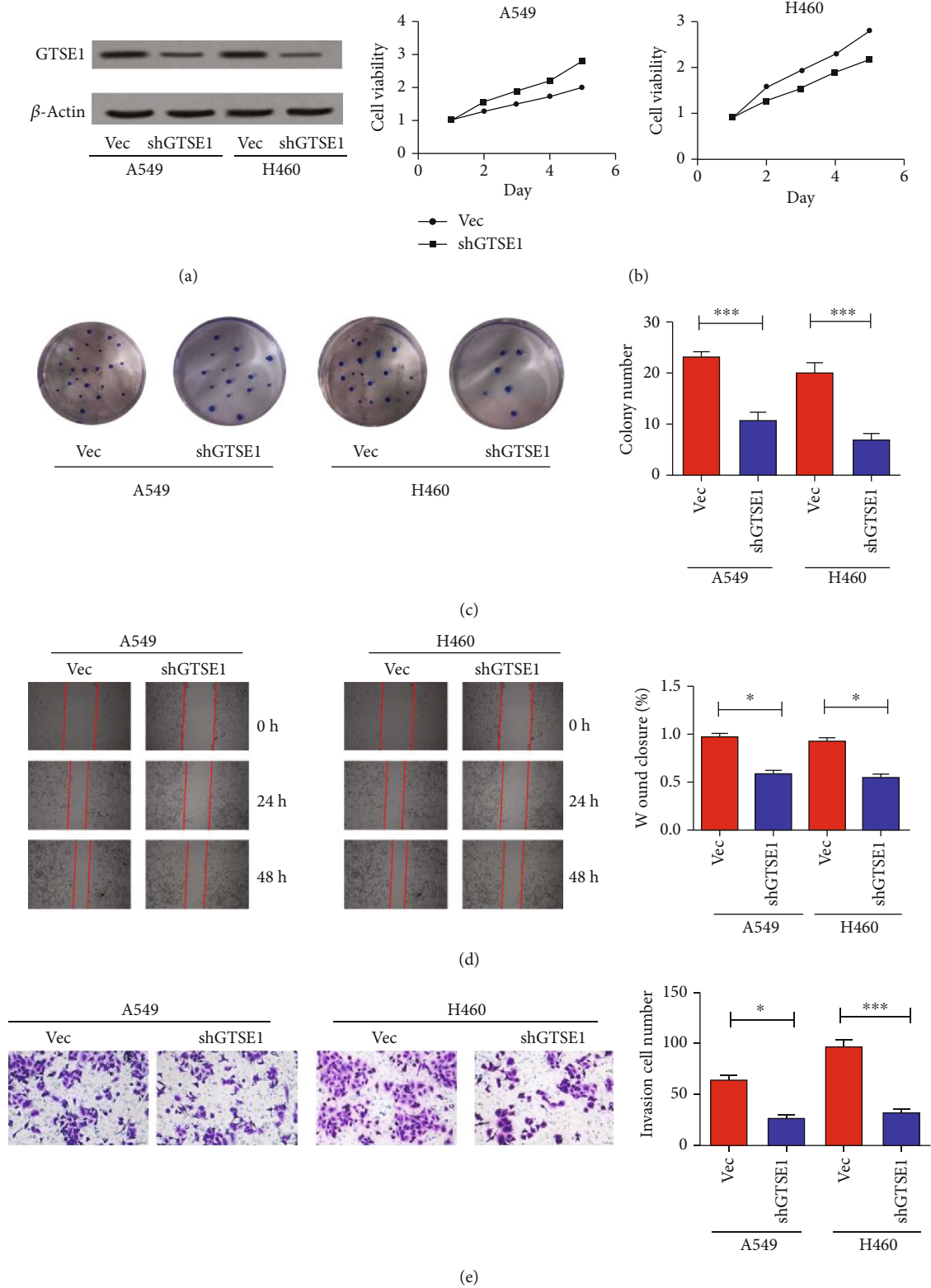


FIGURE 4: Knockdown of GTSE1 inhibited proliferation, migration, and invasion of cells A549 and H460 in lung cancer. (a–e) GTSE1 was silenced in A549 and H460 cells. (a) The silence of GTSE1 in cells A549 and H460 was validated by using the WB assay. The CCK8 assay (b), colony formation (c), wound healing assay (d), and transwell invasion assay (e) were performed to evaluate cell proliferation, migration, and invasion. \* $p < 0.05$  and \*\* $p < 0.01$ .



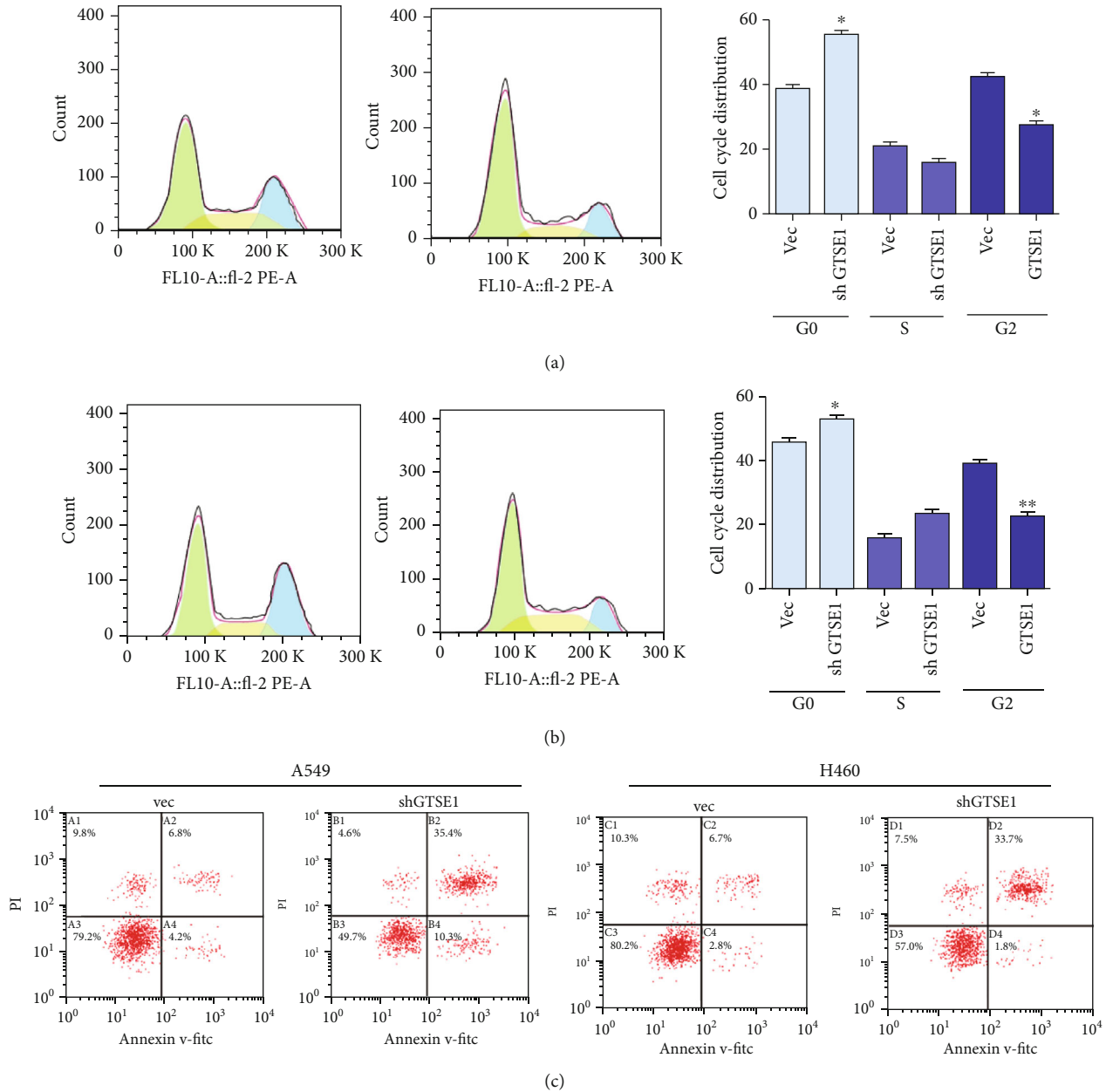


FIGURE 5: Deletion of GTSE1 inhibits the cell cycle and cell apoptosis induced in A549 and H460 cell lines. (a–c) GTSE1 was silenced in A549 and H460 cells. The cell cycle (a, b) and cell apoptosis (c) were analyzed by flow cytometry. \* $p < 0.05$  and \*\* $p < 0.01$ .

apoptosis of H460 and A549 cells (Figures 5(c)). These results indicated that silencing the GTSE1 expression regulated the cell cycle and induced cell apoptosis in H460 and A549 cell lines.

**3.6. GTSE1 Suppressed p53 Expression and Activated AKT/mTOR Signaling in H460 and A549 Cell Lines.** To investigate the potential molecular mechanism of GTSE1 in regulating lung cancer cells' malignant phenotype, we detected the activation of tumor-related signaling pathways. Our data showed that overexpression of GTSE1 significantly downregulated p53 protein level and promoted the phosphorylation of Akt and mTOR in H460 and A549 cell lines (Figure 6(a)). Accordingly, silence of GTSE1 significantly

raised p53 protein level and suppressed the phosphorylation of Akt and mTOR in H460 and A549 cell lines (Figure 6(b)). These results indicated that GTSE1 was able to suppress p53 expression and activate AKT/mTOR signaling in lung cancer cells.

## 4. Discussion

The abnormal expressions of different genes have been explored in many cancer types and play an important role in cancer development [15–18]. In this study, we reported that the expression of GTSE1 was enhanced in lung cancer tissues and cells, and we think that the hypomethylation of the GTSE1 promoter might be responsible for its high

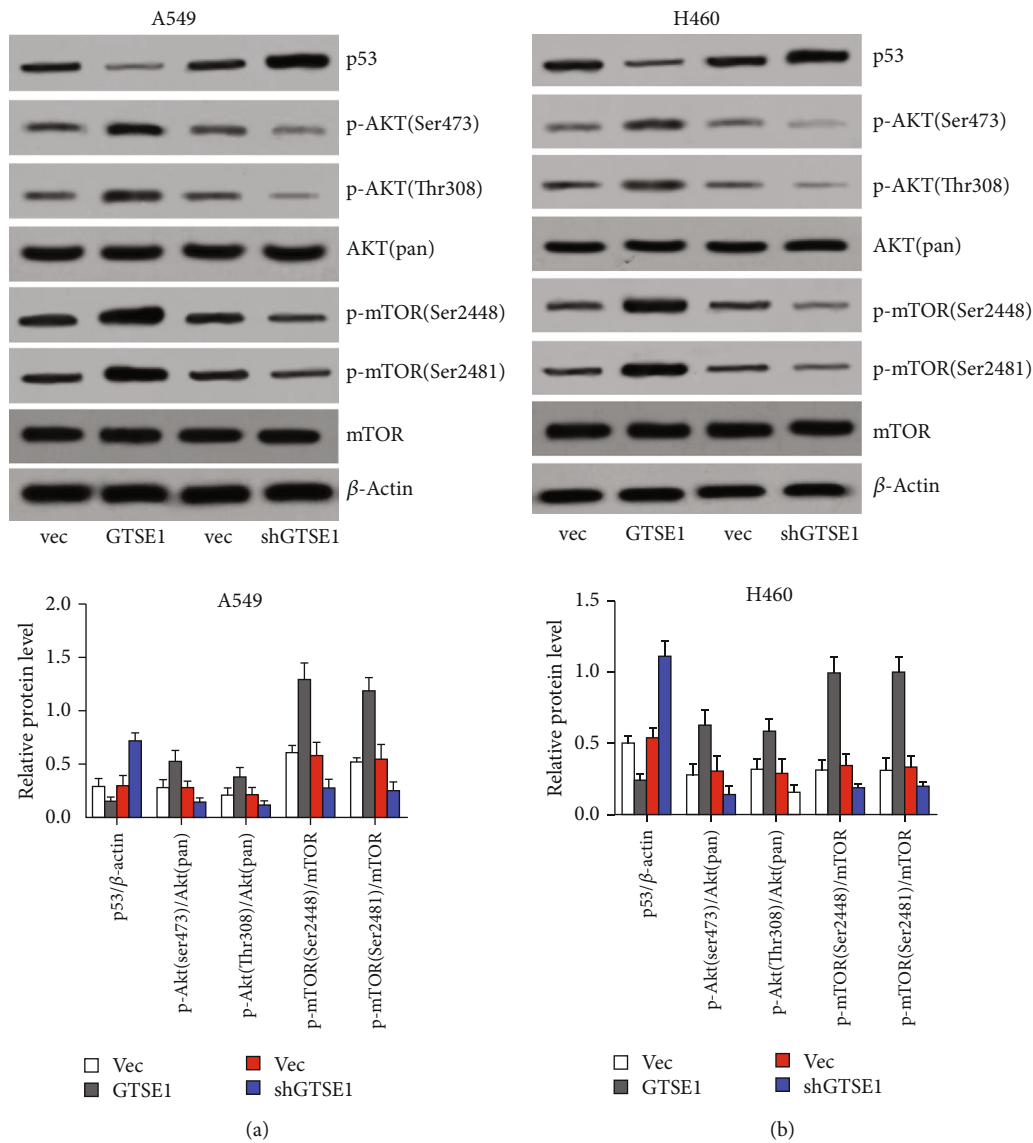


FIGURE 6: GTSE1 activated AKT signaling in H460 and A549 cell lines. (a, b) GTSE1 was overexpressed and silenced in both A549 and H460 cells. p53 protein, phosphorylation of Akt, and mTOR protein level were detected by the western blotting assay. \* $p < 0.05$ .

expression. The upregulated GTSE1 was inseparable from the prognosis of lung cancer. Furthermore, the proliferation, invasion, and migration of H460 and A549 lung cancer cells were promoted by ectopic expression of GTSE1 while being inhibited by knockdown of GTSE1. Our results demonstrated that GTSE1 might function as an oncogenic trigger in the development and progression of lung cancer, which may be useful as a therapeutic target for lung cancer.

GTSE1, a microtubule-localized protein, was reported to overexpress in many kinds of human cancer and negatively regulate the functions of p53 [19, 20]. It has been reported that the high GTSE1 expression contributes to the malignant behavior of human cancer [10, 21]. In neuroendocrine tumors, overexpression of GTSE1 can augment aggressive phenotypes [22]. Consistent with these results, our results indicated that the GTSE1 expression was increased in lung cancer tissues and cell lines, and this outcome is correlated

with the overall survival of patients with lung cancer [12]. In summary, GTSE1 could play a crucial role in the development and progression of lung cancer.

GTSE1 is well correlated with tumor progression [12]. GTSE1 exerts a major effect on clone formation and has direct association with promoting proliferation in hepatocellular carcinoma (HCC) cells [23]. Furthermore, our results also showed that GTSE1 knockdown inhibited cell proliferation and clone formation in A549 and H460 cells, which is in accord with the data on hepatocellular carcinoma and breast cancer. Previous studies have also suggested that GTSE1 regulates the cell cycle via promoting p53 localization to the cytoplasm. In A549 and H460 cells, GTSE1 knockdown resulted in an increased G0/G1 phase while decreased G2/M phase, which indicated that the abnormal expression of GTSE1 affected the distribution of the cell cycle.

In breast cancer, the protein levels of GTSE1 were shown to determine the migratory capacity of nontransformed breast cancer cell lines [24]. Upregulated GTSE1 correlates with tumor stage, invasive potential, and distant metastasis [25]. Consistent with this study, we reported that cell invasion and migration in lung cancer were dependent on the GTSE1 expression levels. The ectopic expression of GTSE1 promoted cellular invasion and migration, while the downregulation of GTSE1 inhibited the cellular abilities of invasion and migration.

Furthermore, we demonstrated that GTSE1 was able to suppress p53 expression and promote the phosphorylation of AKT and mTOR and then activate AKT/mTOR signaling in lung cancer cells. p53 is a well-known cancer suppressor which could inhibit the activation of many carcinogenic signaling pathways including AKT signaling [26]. So we think that GTSE1 may promote the phosphorylation of AKT by downregulating p53. AKT, also known as protein kinase B, is a known oncogene. Its abnormal overexpression or activation has been reported in many cancers and is closely related to cancer cell proliferation, survival, invasion, and migration [27, 28]. The mTOR is a Ser/Thr protein kinase downstream of AKT signaling [29–31]. mTOR is phosphorylated at Ser2448 via the Akt kinase and autophosphorylated at Ser2481 [29–31]. AKT/mTOR signaling plays a key role in promoting malignant processes of cancers [27–31]. So, we consider that GTSE1 may also facilitate tumor cell proliferation, migration, and invasion and suppress apoptosis via activating AKT signaling in lung cancer.

We acknowledged that this study did not include an in vivo assay, which was a limitation of this research. We will further study the role of GTSE1 in animal models of lung cancer in the future.

In conclusion, we defined high GTSE1 expression as a worse prognostic trigger for lung cancer patients and reported that GTSE1 acts as an oncogene by activating AKT/mTOR signaling in the lung cancer. Thus, GTSE1 may serve as a therapeutic target and novel prognostic marker in lung cancer. This study, to our knowledge, is the first to show expounding cellular function of GTSE1 protein.

## Data Availability

The data used to support the findings of this study are included within the article.

## Conflicts of Interest

All authors have no conflicts of interest to declare.

## Authors' Contributions

Fan Zhang and Jingfei Meng contributed equally to this work.

## Acknowledgments

This research was supported by the Zhejiang Provincial Natural Science Foundation of China (No. LY15H160009), Zhe-

jiang Provincial Science and Technology Program (No. 2014C33116), Medical Health Science and Technology Project of Zhejiang Provincial Health Commission (No. 2014KYA173), and Zhejiang Provincial Science and Technology Plan of Traditional Chinese Medicine (No. 2012ZB125).

## References

- [1] F. Nasim, B. F. Sabath, and G. A. Eapen, "Lung cancer," *The Medical Clinics of North America*, vol. 103, no. 3, pp. 463–473, 2019.
- [2] S. Wang, S. Zimmermann, K. Parikh, A. S. Mansfield, and A. A. Adjei, "Current diagnosis and management of small-cell lung cancer," *Mayo Clinic Proceedings*, vol. 94, no. 8, pp. 1599–1622, 2019.
- [3] A. E. Dutkowska and A. Antczak, "Comorbidities in lung cancer," *Pneumonologia i Alergologia Polska*, vol. 84, no. 3, pp. 186–192, 2016.
- [4] A. G. Pallis and K. N. Syrigos, "Lung cancer in never smokers: disease characteristics and risk factors," *Critical Reviews in Oncology/Hematology*, vol. 88, no. 3, pp. 494–503, 2013.
- [5] N. Duma, R. Santana-Davila, and J. R. Molina, "Non-small cell lung cancer: epidemiology, screening, diagnosis, and treatment," *Mayo Clinic Proceedings*, vol. 94, no. 8, pp. 1623–1640, 2019.
- [6] R. Utrera, L. Collavin, D. Lazarević, D. Delia, and C. Schneider, "A novel p53-inducible gene coding for a microtubule-localized protein with G2-phase-specific expression," *The EMBO Journal*, vol. 17, no. 17, pp. 5015–5025, 1998.
- [7] D. R. Bublik, M. Scolz, G. Triolo, M. Monte, and C. Schneider, "Human GTSE-1 regulates p 21 (CIP1/WAF1) stability conferring resistance to paclitaxel treatment," *The Journal of Biological Chemistry*, vol. 285, no. 8, pp. 5274–5281, 2010.
- [8] F. Lin, Y. J. Xie, X. K. Zhang et al., "GTSE1 is involved in breast cancer progression in p 53 mutation-dependent manner," *Journal of Experimental & Clinical Cancer Research*, vol. 38, no. 1, p. 152, 2019.
- [9] Y. Zheng, Y. Shi, S. Yu et al., "GTSE1, CDC20, PCNA, and MCM6 synergistically affect regulations in cell cycle and indicate poor prognosis in liver cancer," *Analytical Cellular Pathology*, vol. 2019, Article ID 1038069, 13 pages, 2019.
- [10] A. Liu, S. Zeng, X. Lu et al., "Overexpression of G2 and S phase-expressed-1 contributes to cell proliferation, migration, and invasion via regulating p53/FoxM1/CCNB1 pathway and predicts poor prognosis in bladder cancer," *International Journal of Biological Macromolecules*, vol. 123, pp. 322–334, 2019.
- [11] X. Wu, H. Wang, Y. Lian et al., "GTSE1 promotes cell migration and invasion by regulating EMT in hepatocellular carcinoma and is associated with poor prognosis," *Scientific Reports*, vol. 7, no. 1, p. 5129, 2017.
- [12] V. V. Subhash, S. H. Tan, W. L. Tan et al., "GTSE1 expression represses apoptotic signaling and confers cisplatin resistance in gastric cancer cells," *BMC Cancer*, vol. 15, no. 1, 2015.
- [13] T. Tian, E. Zhang, F. Fei et al., "Up-regulation of GTSE1 lacks a relationship with clinical data in lung cancer," *Asian Pacific Journal of Cancer Prevention*, vol. 12, no. 8, pp. 2039–2043, 2011.

- [14] X. Zhang, Y. Ning, Y. Xiao et al., "MAEL contributes to gastric cancer progression by promoting ILKAP degradation," *Oncotarget*, vol. 8, no. 69, pp. 113331–113344, 2017.
- [15] H. A. Bircan, N. Gurbuz, A. Pataer et al., "Elongation factor-2 kinase (eEF-2K) expression is associated with poor patient survival and promotes proliferation, invasion and tumor growth of lung cancer," *Lung Cancer*, vol. 124, pp. 31–39, 2018.
- [16] R. Zhang, F. Zhang, Z. Sun et al., "LINE-1 retrotransposition promotes the development and progression of lung squamous cell carcinoma by disrupting the tumor-suppressor gene FGGY," *Cancer Research*, vol. 79, no. 17, pp. 4453–4465, 2019.
- [17] M. Zeng, Y. Xiong, N. Safaee et al., "Exploring targeted degradation strategy for oncogenic KRAS<sup>G12C</sup>," *Cell Chemical Biology*, vol. 27, no. 1, pp. 19–31.e6, 2020.
- [18] H. Huang, D. Wang, W. Guo, X. Zhuang, and Y. He, "Correlated low IGF2BP1 and FOXM1 expression predicts a good prognosis in lung adenocarcinoma," *Pathology, Research and Practice*, vol. 215, no. 7, p. 152433, 2019.
- [19] A. R. Tipton, J. D. Wren, J. R. Daum, J. C. Siefert, and G. J. Gorbisky, "GTSE1 regulates spindle microtubule dynamics to control aurora B kinase and Kif4A chromokinesin on chromosome arms," *The Journal of Cell Biology*, vol. 216, no. 10, pp. 3117–3132, 2017.
- [20] S. Bendre, A. Rondelet, C. Hall et al., "GTSE1 tunes microtubule stability for chromosome alignment and segregation by inhibiting the microtubule depolymerase MCAK," *The Journal of Cell Biology*, vol. 215, no. 5, pp. 631–647, 2016.
- [21] H. Jin, G. Y. Kang, S. Jeon et al., "Identification of molecular signatures involved in radiation-induced lung fibrosis," *Journal of Molecular Medicine*, vol. 97, no. 1, pp. 37–47, 2019.
- [22] J. Lee, C. O. Sung, E. J. Lee et al., "Metastasis of neuroendocrine tumors are characterized by increased cell proliferation and reduced expression of the ATM gene," *PLoS One*, vol. 7, no. 4, article e34456, 2012.
- [23] M. Monte, R. Benetti, G. Buscemi, P. Sandy, G. Del Sal, and C. Schneider, "The cell cycle-regulated protein human GTSE-1 controls DNA damage-induced apoptosis by affecting p53 function," *The Journal of Biological Chemistry*, vol. 278, no. 32, pp. 30356–30364, 2003.
- [24] M. Scolz, P. O. Widlund, S. Piazza et al., "GTSE1 is a microtubule plus-end tracking protein that regulates EB1-dependent cell migration," *PLoS One*, vol. 7, no. 12, article e51259, 2012.
- [25] L. Guo, S. Zhang, B. Zhang et al., "Silencing GTSE-1 expression inhibits proliferation and invasion of hepatocellular carcinoma cells," *Cell Biology and Toxicology*, vol. 32, no. 4, pp. 263–274, 2016.
- [26] M. F. Ladelfa, M. F. Toledo, J. E. Laiseca, and M. Monte, "Interaction of p53 with tumor suppressive and oncogenic signaling pathways to control cellular reactive oxygen species production," *Antioxidants & Redox Signaling*, vol. 15, no. 6, pp. 1749–1761, 2011.
- [27] A. C. Tan, "Targeting the PI3K/Akt/mTOR pathway in non-small cell lung cancer (NSCLC)," *Thoracic Cancer*, vol. 11, no. 3, pp. 511–518, 2020.
- [28] J. Lee, C. Kim, J.-Y. Um, G. Sethi, and K. Ahn, "Castacin-induced inhibition of cell growth and survival are mediated through the dual modulation of Akt/mTOR signaling cascade," *Cancers*, vol. 11, no. 2, p. 254, 2019.
- [29] M. Song, A. M. Bode, Z. Dong, and M. H. Lee, "AKT as a therapeutic target for cancer," *Cancer Research*, vol. 79, no. 6, pp. 1019–1031, 2019.
- [30] P. S. Ong, L. Z. Wang, X. Dai, S. H. Tseng, S. J. Loo, and G. Sethi, "Judicious toggling of mTOR activity to combat insulin resistance and cancer: current evidence and perspectives," *Frontiers in Pharmacology*, vol. 7, p. 395, 2016.
- [31] K. Chen, Z. Shang, A. L. Dai, and P. L. Dai, "Novel PI3K/Akt/mTOR pathway inhibitors plus radiotherapy: strategy for non-small cell lung cancer with mutant RAS gene," *Life Sciences*, vol. 255, p. 117816, 2020.



## Research Article

# Comparison of the Fatty Acid Metabolism Pathway in Pan-Renal Cell Carcinoma: Evidence from Bioinformatics

Ping Wu,<sup>1</sup> Yingkun Xu ,<sup>2</sup> Jiayi Li,<sup>3</sup> Xiaowei Li,<sup>4</sup> Peizhi Zhang,<sup>2</sup> Ningke Ruan,<sup>5</sup> Cong Zhang,<sup>6</sup> Panpan Sun,<sup>7</sup> Qifei Wang ,<sup>4</sup> and Guangzhen Wu <sup>4</sup>

<sup>1</sup>Department of Anesthesiology, The First Affiliated Hospital of Dalian Medical University, Dalian, China

<sup>2</sup>Department of Urology, Shandong Provincial Hospital, Cheeloo College of Medicine, Shandong University, Jinan, China

<sup>3</sup>School of Business, Hanyang University, Seoul, Republic of Korea

<sup>4</sup>Department of Urology, The First Affiliated Hospital of Dalian Medical University, Dalian, China

<sup>5</sup>The Nursing College of Zhengzhou University, Zhengzhou, China

<sup>6</sup>Department of Pain Management, Shandong Provincial Hospital, Cheeloo College of Medicine, Shandong University, Jinan, China

<sup>7</sup>Department of Pain Management, The Second Hospital of Shandong University, Jinan, China

Correspondence should be addressed to Qifei Wang; wangqifei6008@hotmail.com and Guangzhen Wu; wuguang0613@hotmail.com

Received 11 September 2020; Revised 1 February 2021; Accepted 5 February 2021; Published 23 February 2021

Academic Editor: Victor H. Villar

Copyright © 2021 Ping Wu et al. This is an open access article distributed under the Creative Commons Attribution License, which permits unrestricted use, distribution, and reproduction in any medium, provided the original work is properly cited.

This study analyzed and compared the potential role of fatty acid metabolism pathways in three subtypes of renal cell carcinoma. Biological pathways that were abnormally up- and downregulated were identified through gene set variation analysis in the subtypes. Abnormal downregulation of the fatty acid metabolism pathway occurred in all three renal cell carcinoma subtypes. Alteration of the fatty acid metabolism pathway was vital in the development of pan-renal cell carcinoma. Bioinformatics methods were used to obtain a panoramic view of copy number variation, single-nucleotide variation, mRNA expression, and the survival landscape of fatty acid metabolism pathway-related genes in pan-renal cell carcinoma. Most importantly, we used genes related to the fatty acid metabolism pathway to establish a prognostic-related risk model in the three subtypes of renal cell carcinoma. The data will be valuable for future clinical treatment and scientific research.

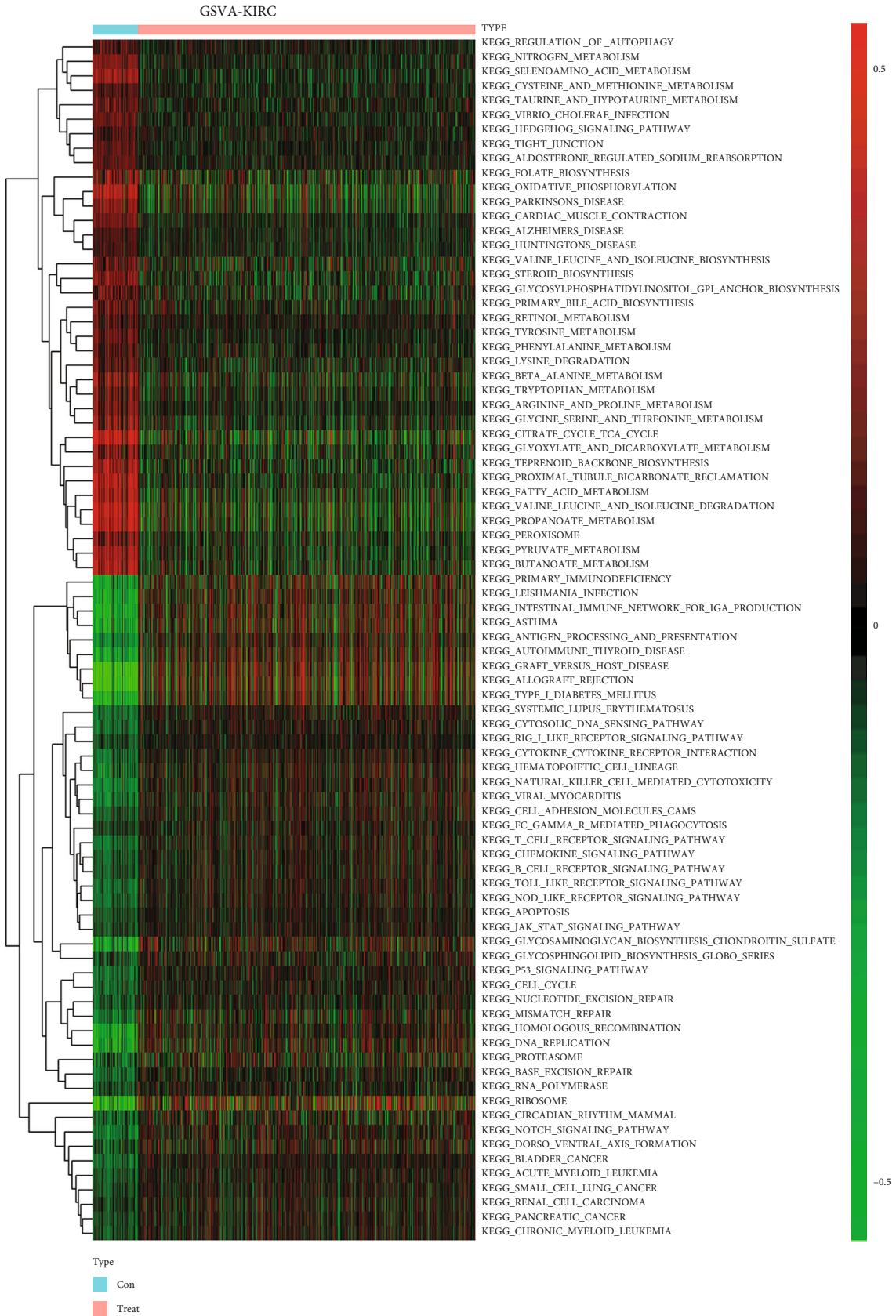
## 1. Introduction

Renal cell carcinoma (RCC) is one of the most common malignancies in the urinary system [1]. The incidence of kidney cancer has been increasing worldwide in recent years [2]. In the United States, nearly 64,000 patients were diagnosed as having RCC in 2017, with an annual increase of 2-4% [3, 4]. The primary treatment for RCC is radical resection of the kidney. However, there is no effective treatment for patients with metastatic and recurrent kidney cancer. Increasing evidence suggests that metabolic gene perturbations are a significant feature of RCC [5-7]. Epigenetic interference genes in RCC are good candidate targets for the development of powerful prognostic and diagnostic tools and novel therapies [8, 9]. The common pathological types of RCC mainly include

kidney renal clear cell carcinoma (KIRC), kidney renal papillary cell carcinoma (KIRP), and kidney chromophobe (KICH).

It is unclear whether there are differences in fatty acid metabolism pathways between these three RCC subtypes. To explore this, we used gene set variation analysis (GSVA) to perform pathway analysis in pan-RCC. The approach sensitively detected subtle changes in pathway activity between tumor tissue and normal tissue [10].

The present data indicate that fatty acid metabolism pathways may be essential in the three RCC subtypes, with significant differences between subtypes. Metabolism is influential in RCC. Changes in fatty acid metabolism pathways may have an essential role in the development of RCC [11, 12]. A characteristic feature of cancer cells is that they can



(a)

FIGURE 1: Continued.

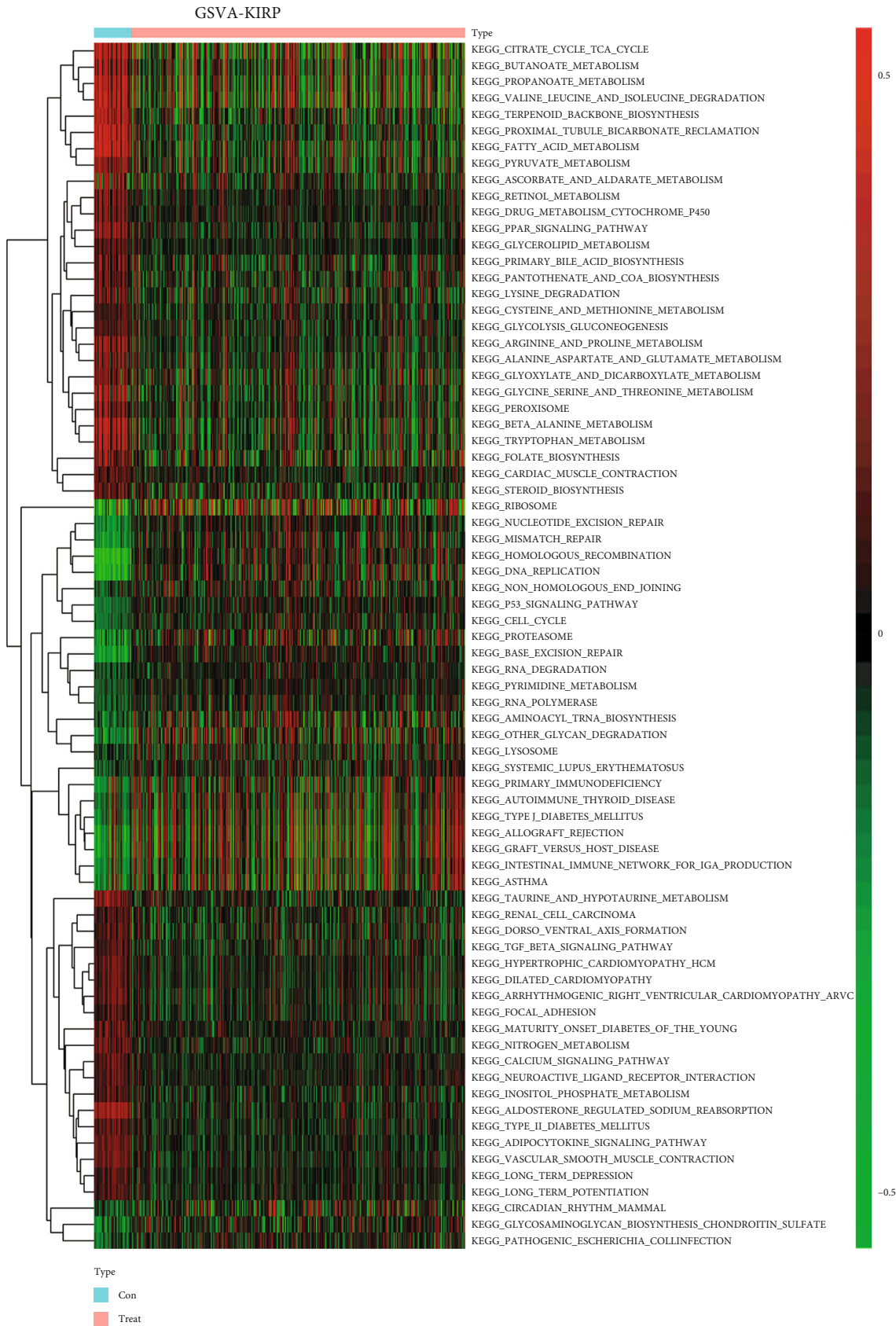
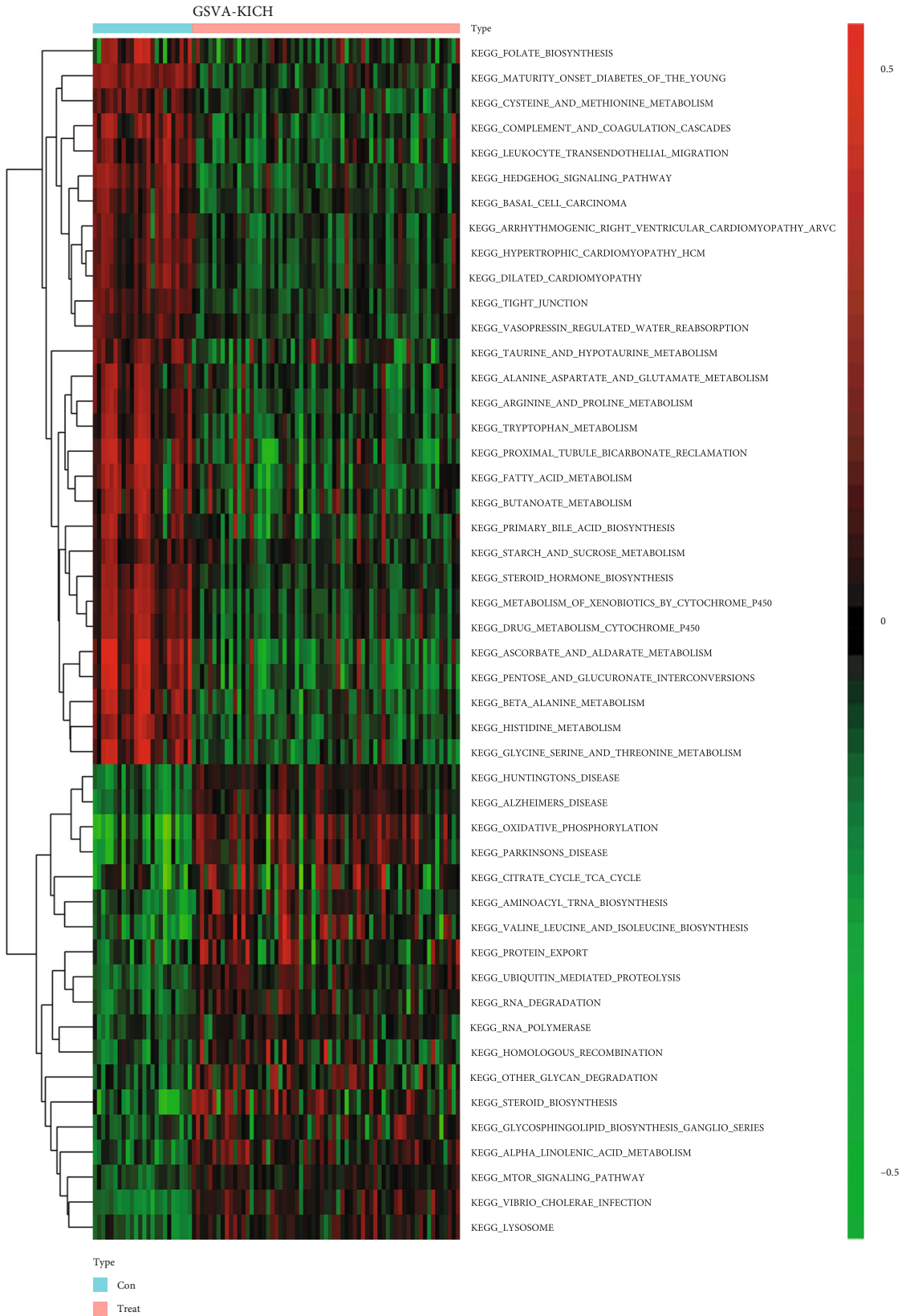


FIGURE 1: Continued.



(c)

FIGURE 1: Overview of GSVA in pan-renal cell carcinoma. (a) KIRC, (b) KIRP, and (c) KICH. The redder the color, the stronger the activation of the corresponding pathway. The greener the color, the stronger the suppression of the relevant pathway.



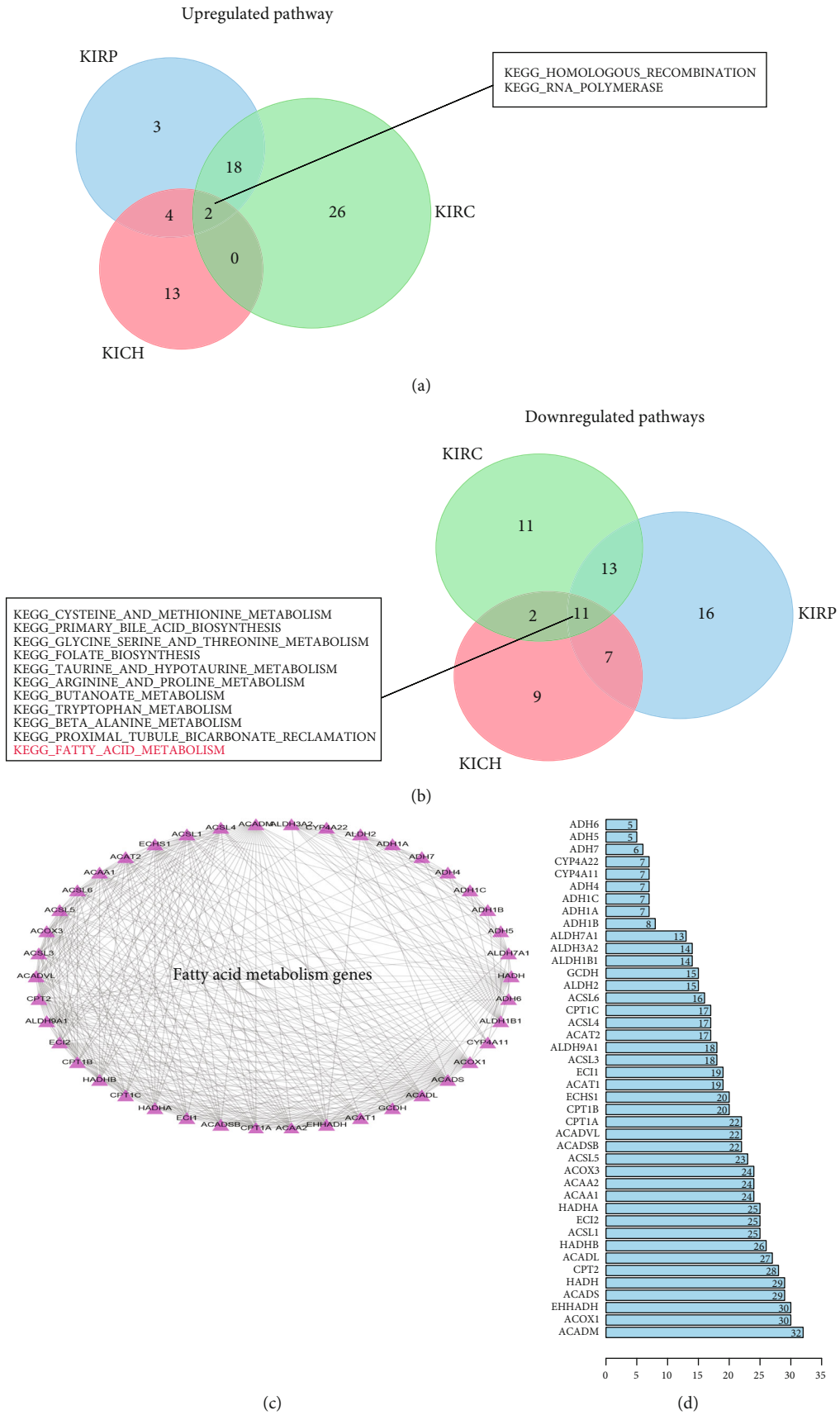


FIGURE 2: Continued.

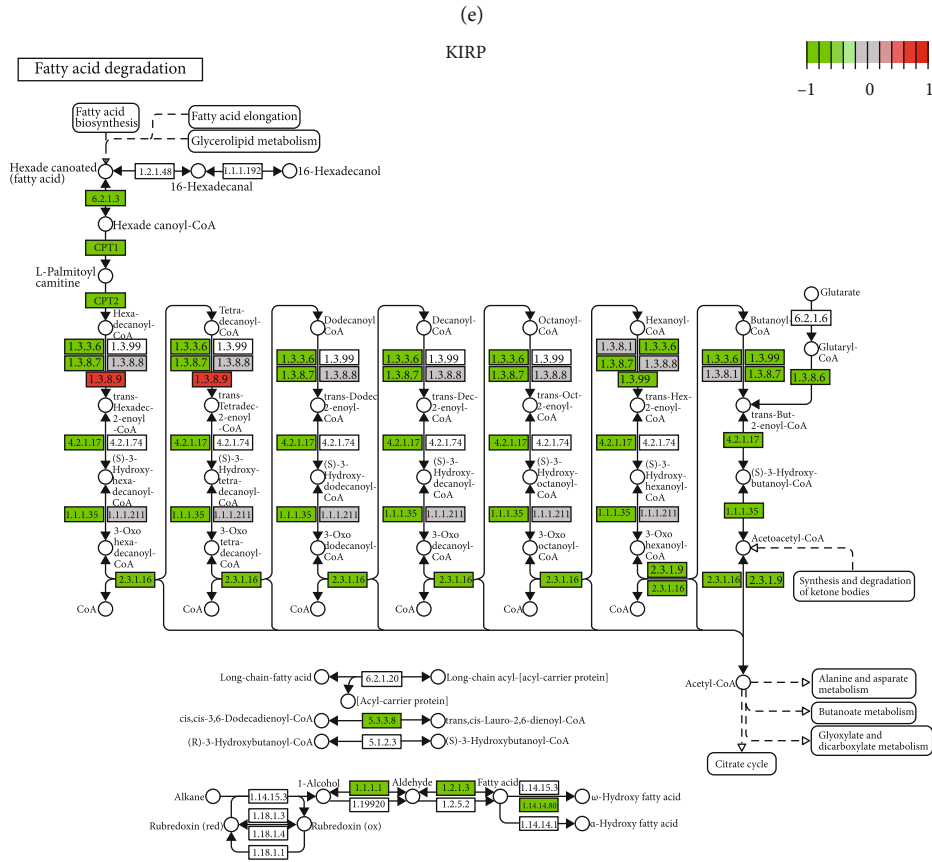
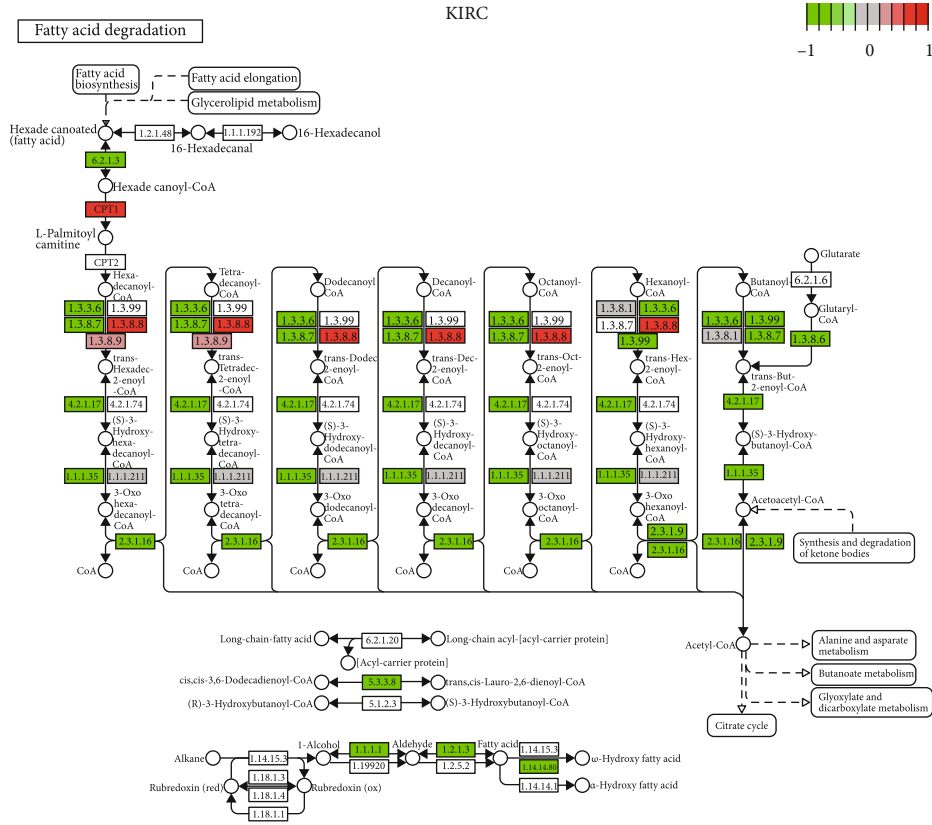


FIGURE 2: Continued.

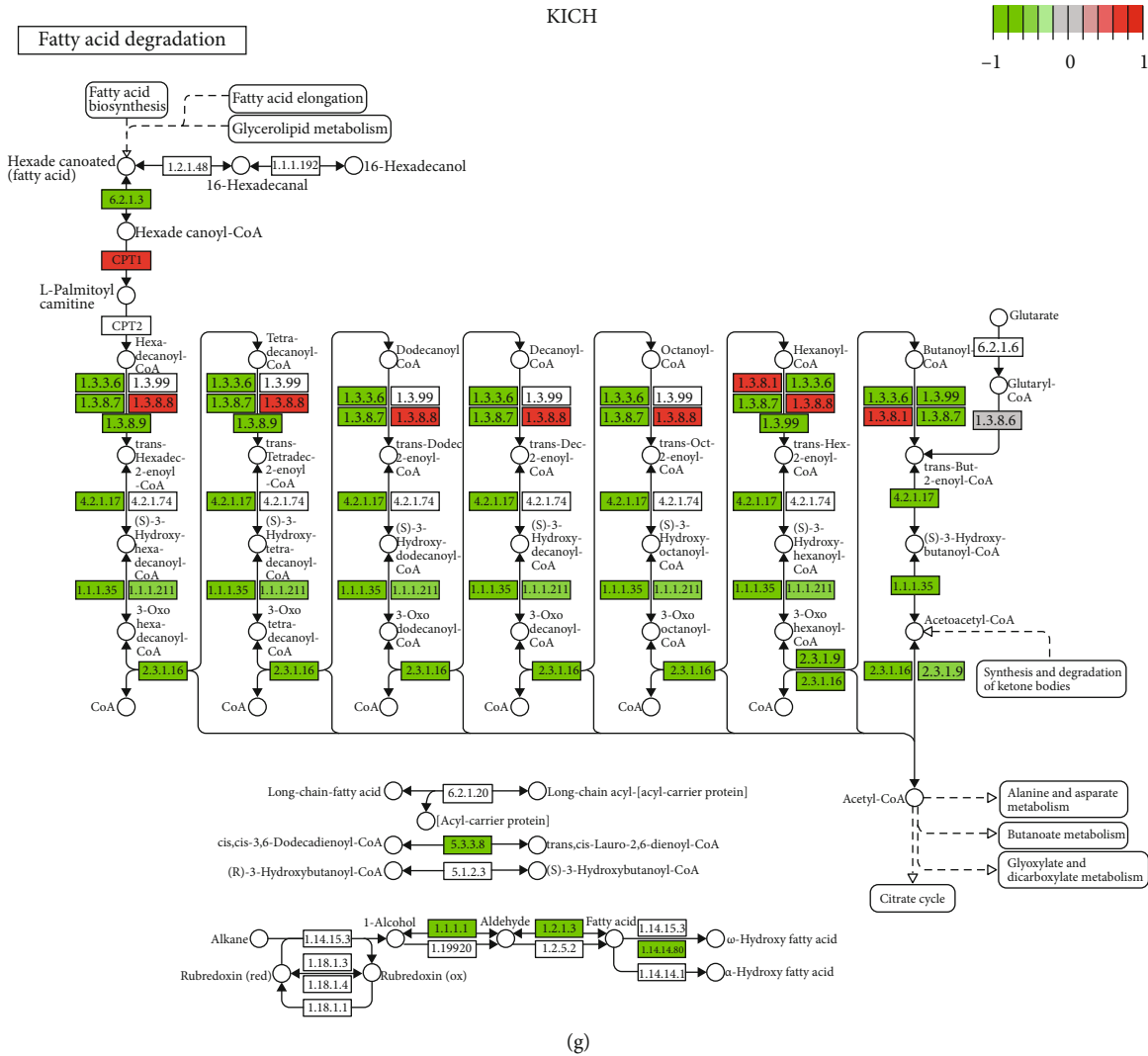


FIGURE 2: Overview of the fatty acid metabolism pathway in pan-renal cell carcinoma. (a) Venn diagrams of downregulated pathways in pan-renal cell carcinoma. (b) Venn diagrams of upregulated pathways in pan-renal cell carcinoma. (c) Interaction diagram between fatty acid metabolism genes. (d) The weight of each fatty acid metabolism gene in all the biological processes. The larger the value, the more critical is its biological role. (e) Inhibition or activation of related biological processes on fatty acid metabolism pathways in KIRC. (f) Inhibition or activation of relevant biological processes on fatty acid metabolism pathways in KIRP. (g) Inhibition or activation of related biological processes on fatty acid metabolism pathways in KICH. The redder the color, the more potent is the activation. The greener the color, the more influential is the inhibition.

readjust their metabolism to maintain ATP production and the growth, division, and survival of the cancer cells. Notably, abnormally, fatty acid metabolism occurs in the development of RCC and in most tumors. The importance of abnormal changes in fatty acid metabolism in cancer has attracted the attention of many researchers, since these metabolites can be used as structural components of the cell membrane matrix and critical secondary messengers and as fuel sources for energy production [13–15].

In this study, to fully understand the genetic variation and clinicopathological correlation of these fatty acid metabolic genes in pan-RCC, we obtained a panorama of copy number variation (CNV), single-nucleotide variation (SNV), messenger RNA (mRNA) expression, and the survival landscape. Subsequently, we used the R language to generate heat maps of these genes in the three RCC subtypes and

explored the correlation between these molecules. In particular, the fatty acid metabolism genes were used to establish three risk signatures related to patient prognosis in the three RCC subtypes. The findings should be valuable information for future scientific research and clinical diagnosis and treatment of RCC.

## 2. Materials and Methods

**2.1. Data Acquisition.** The Cancer Genome Atlas (TCGA) program is sponsored by the National Cancer Institute and National Human Genome Research Institute and was jointly launched in 2006. TCGA uses a large-scale gene sequence analysis technology to build a complete set of maps related to all cancer genome changes. In February 2020, we downloaded the CNV, SNV, and mRNA expression data of the

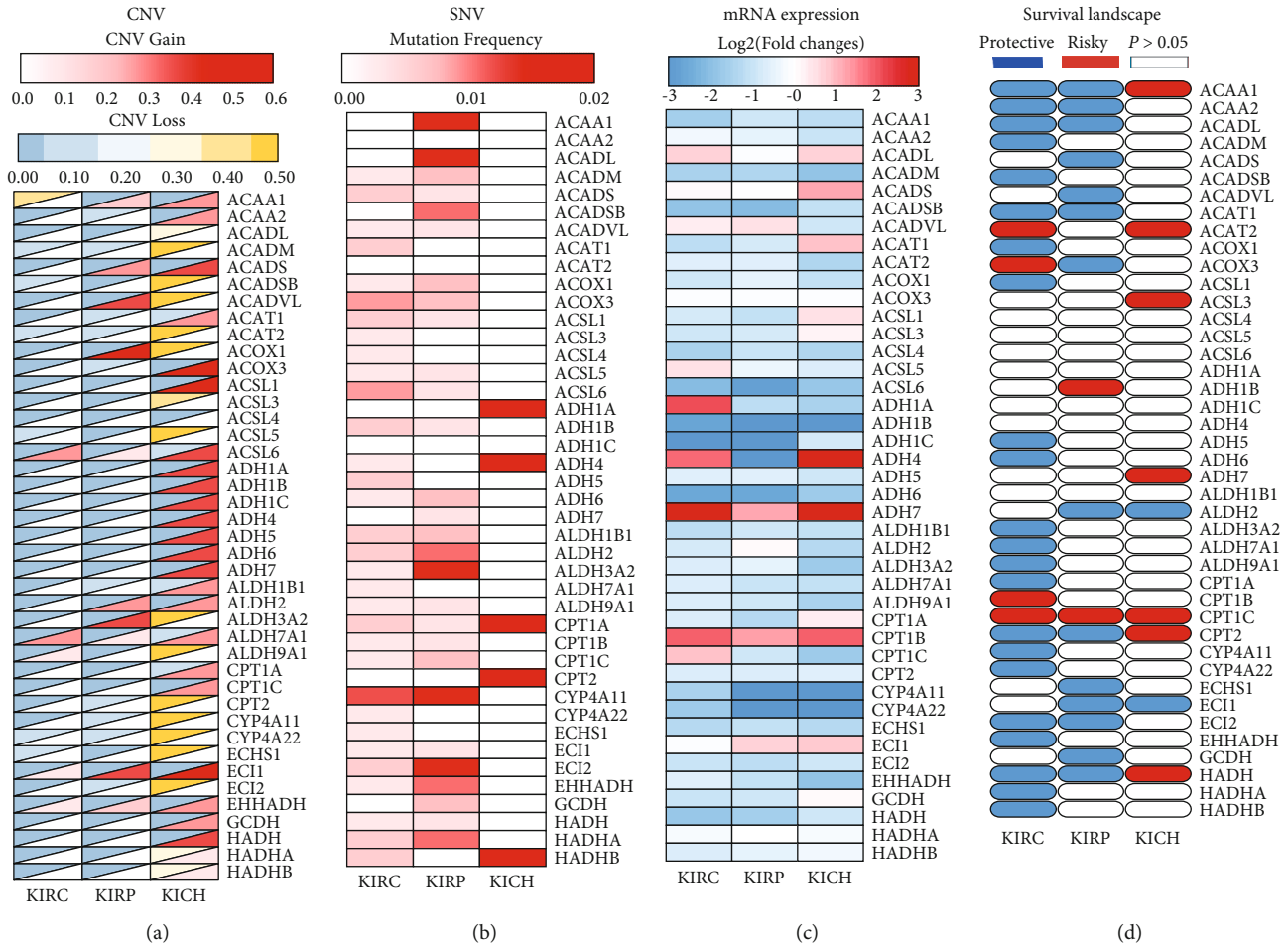


FIGURE 3: Overview of fatty acid metabolism genes in pan-renal cell carcinoma. (a) CNV in pan-renal cell carcinoma. The lower half of the rectangle represents the CNV gain. The redder the color, the higher the frequency of variation. The upper part represents the CNV loss. The yellower the color, the higher the frequency of variation. (b) SNV in pan-renal cell carcinoma. The redder the color, the higher the frequency of variation. (c) The mRNA expression of fatty acid metabolism genes in pan-renal cell carcinoma. Red indicates that the corresponding gene is upregulated in the tumor tissue. Blue indicates that the corresponding gene is downregulated in the tumor tissue. (d) The survival landscape of fatty acid metabolism genes in pan-renal cell carcinoma. Blue represents protective factors, red represents risk factors, and white represents a  $P$  value  $> 0.05$ , which is not statistically significant.

KIRC, KIRP, and KICH datasets in the TCGA database. Clinical parameters and survival data of the corresponding cases were extracted. The KIRC database contains 539 tumor tissues and 72 normal tissues. The KIRP database contains 289 tumor tissues and 32 normal tissues. The KICH database contains 65 tumor tissues and 24 normal tissues.

**2.2. GSVA.** GSVA is an open-source software package for R [10]. GSVA can sensitively detect subtle pathway activity changes in samples and can be used to build path-centric biological models. We used this data packet for the three RCC subtypes.

**2.3. Protein-Protein Interaction (PPI) Network Analysis.** Genes related to fatty acid metabolism were identified through the GSEA website [16, 17]. STRING is a high-coverage, high-quality PPI network platform with a wide range of applications in interpreting large-scale biomedical data and visualization in the context of systems biology [18]. The

STRING online database was used to map these fatty acid metabolism genes on the PPI network. Cytoscape visualization software was used to draw the PPI network [19].

**2.4. Data Processing and Analysis.** The R language has powerful data analysis processing and visual drawing functions. It can be used on Windows, Linux, and Mac systems. Writing a new code or adjusting an existing code can quickly achieve the requirements of data presentation and graphic drawing in scientific research. The R language was used to draw a heat map of the path changes in KIRC, KIRP, and KICH, where the defining criteria were  $P < 0.05$  and  $\log_{2}FC > 0.2$ . We then plotted Venn diagrams of the upregulated and downregulated pathways between the three subtypes of RCC and found pathways common to all three. The R language was additionally used to map the activation or inhibition of genes related to fatty acid metabolism pathways in KIRC, KIRP, and KICH. We plotted the heat maps of CNV, SNV, mRNA expression, and the survival landscape of fatty acid



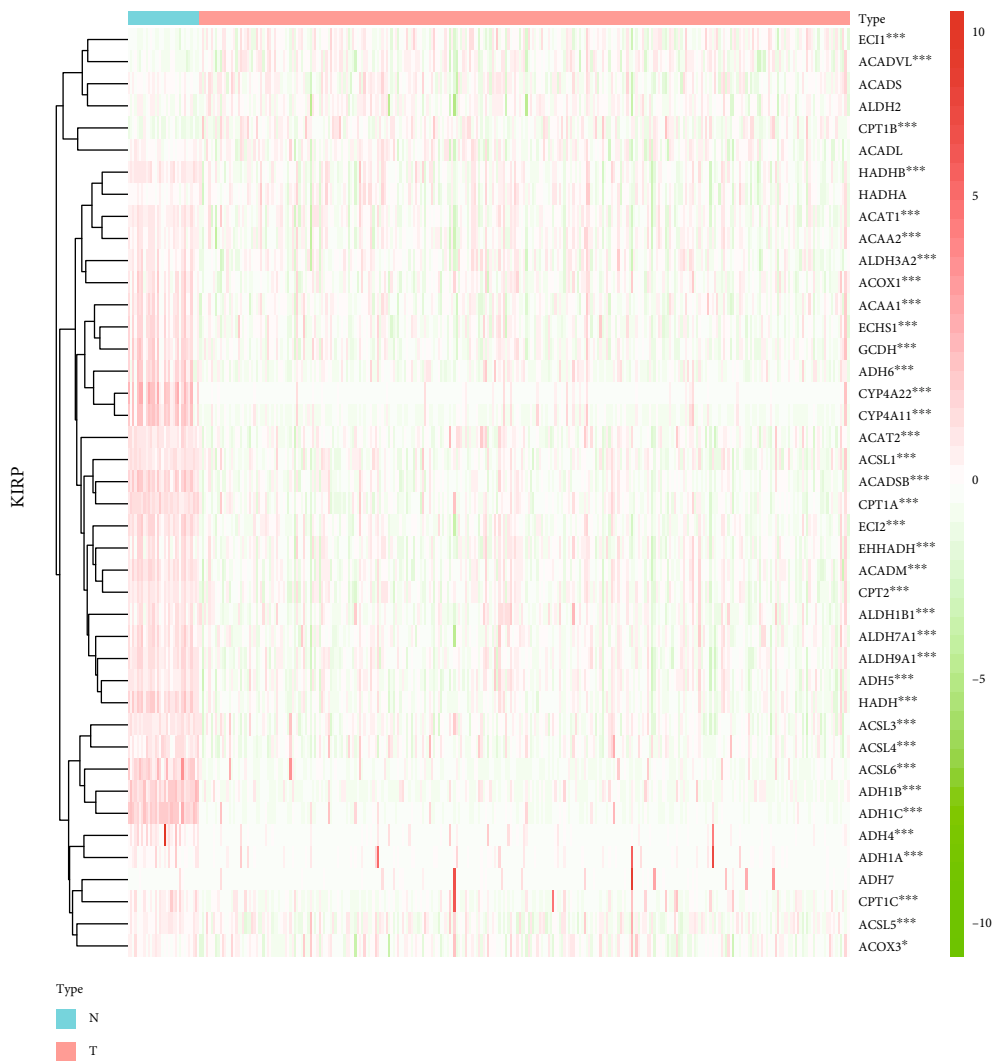


(a)

(b)

FIGURE 4: Continued.





(d)

FIGURE 4: Continued.



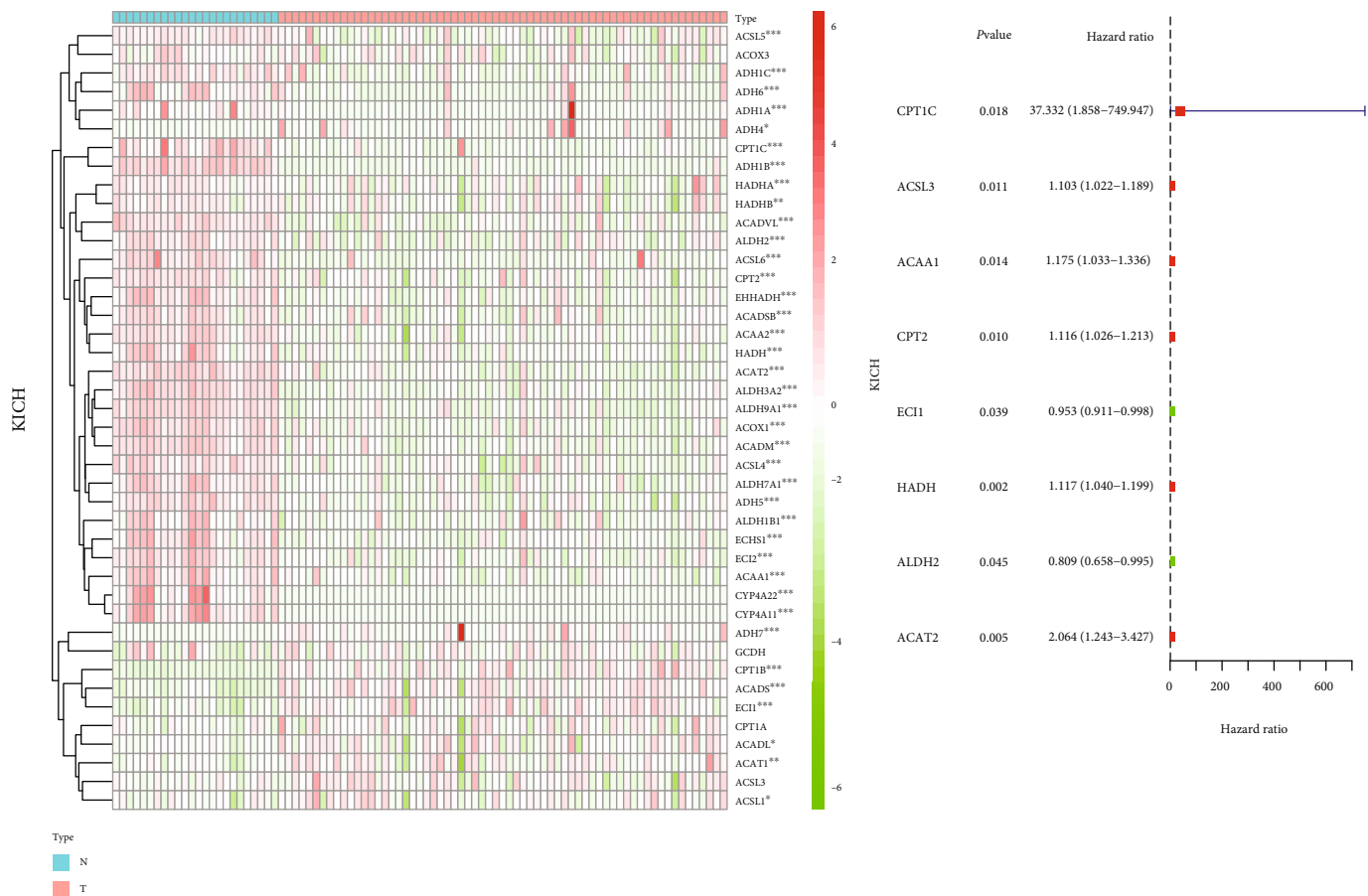


FIGURE 4: Continued.



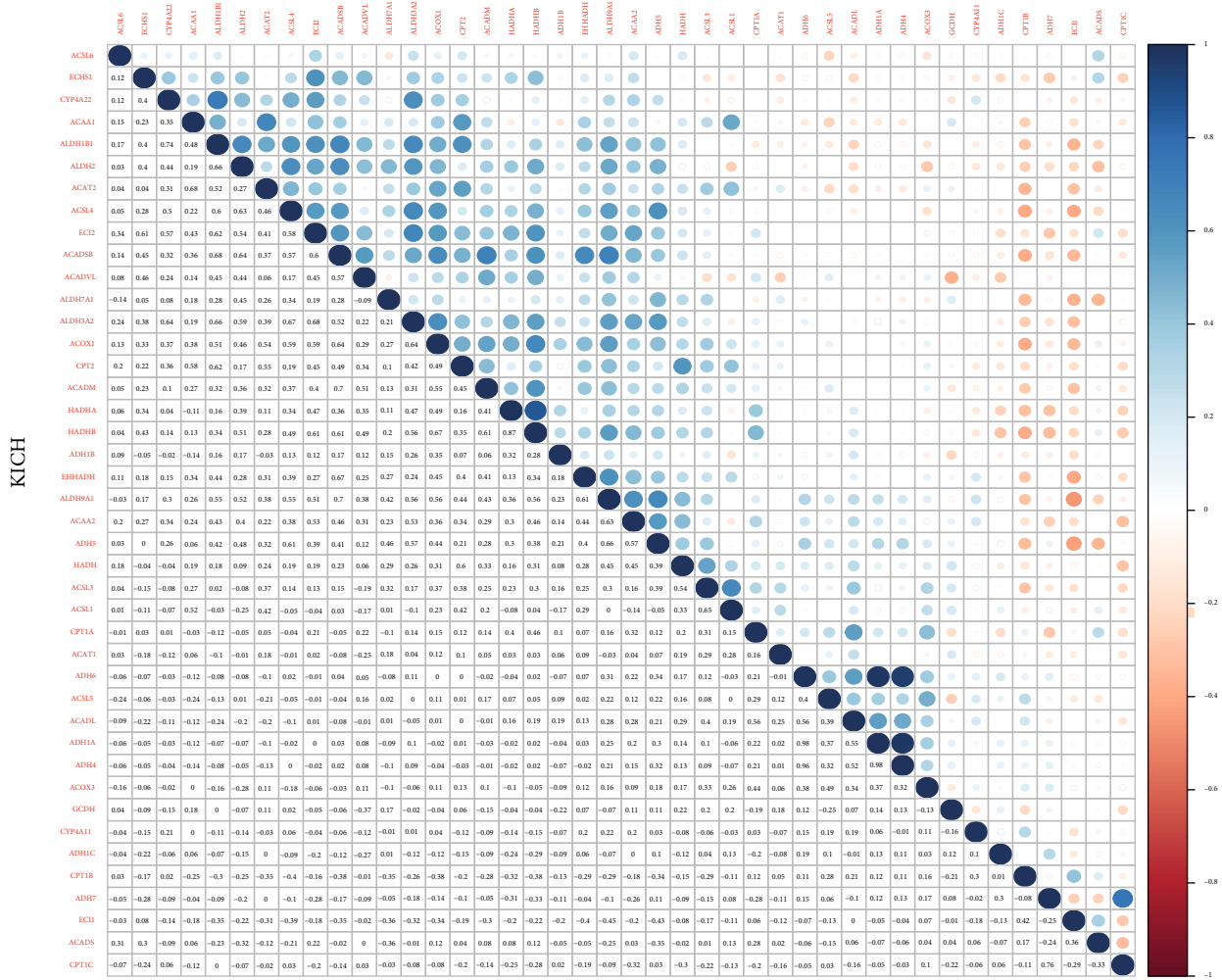


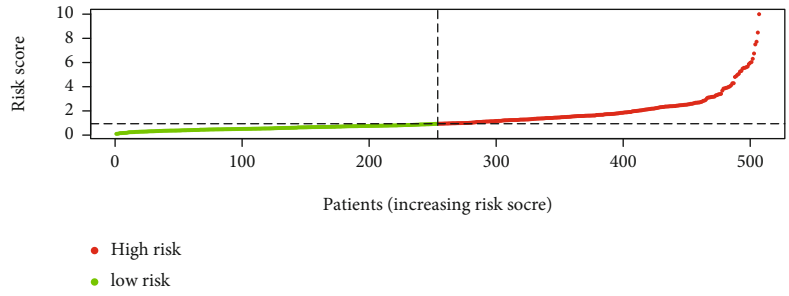
FIGURE 4: Correlation between two fatty acid metabolism genes in pan-renal cell carcinoma. (a, d, g) Expression of fatty acid metabolism-related genes between cancer tissues and normal tissues in KIRC, KIRP, and KICH. The redder the color, the higher the expression. The greener the color, the lower the expression. (b, e, h) Univariate analysis of fatty acid metabolism-related genes in KIRC, KIRP, and KICH. When the hazard ratio of this gene is >1, it means that the gene is a risk factor in the corresponding tumor and vice versa. (c, f, i) Correlation analysis of fatty acid metabolism-related genes in KIRC, KIRP, and KICH. Red represents a positive correlation and blue represents a negative correlation. \* $P < 0.05$ , \*\* $P < 0.01$ , and \*\*\* $P < 0.001$ .

metabolism genes in these three RCC subtypes. Next, to reveal the changes in mRNA levels more clearly, the R language was used to draw a heat map of the expression of these fatty acid metabolic genes in KIRC, KIRP, and KICH. Univariate Cox analysis of these genes was performed in the three RCC subtypes to explore the gene correlations. Finally, these fatty acid metabolism genes were used to establish risk signatures related to prognosis. Multiple data packages were used coordinately. The limma software package performed different analyses of the data. The corplot software package performed the coexpression analysis. The pheatmap software package was used to construct heat maps. The survival software package was used to analyze and construct survival curves. The survivalROC software package was used to explain and illustrate the receiver operating characteristic (ROC) curve. In addition, in order to verify the results that we obtained by analyzing the TCGA database, we used the

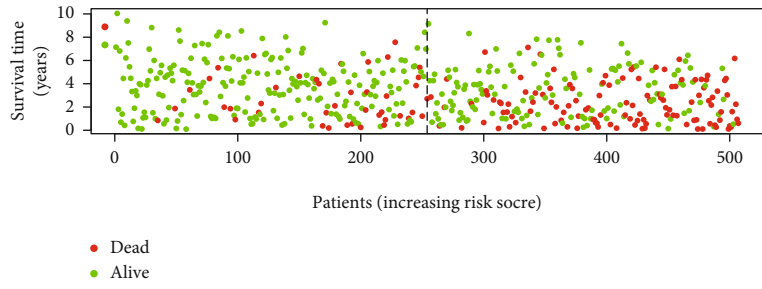
data in the GEO database to verify the expression levels of fatty acid metabolism-related genes in KIRC, KIRP, and KICH and drew the corresponding heat map (Supplementary materials Fig. S1A-C). Among them, the GEO chip number of KIRC is GSE11151 and the GEO chip number of KIRP and KICH is GSE15641 [20–23]. Because chip GSE15641 contains both KIRP data and KICH data, therefore, we will select the KIRP and KICH data contained in this chip for subsequent verification. A  $P$  value < 0.05 denoted statistical significance.

### 3. Results

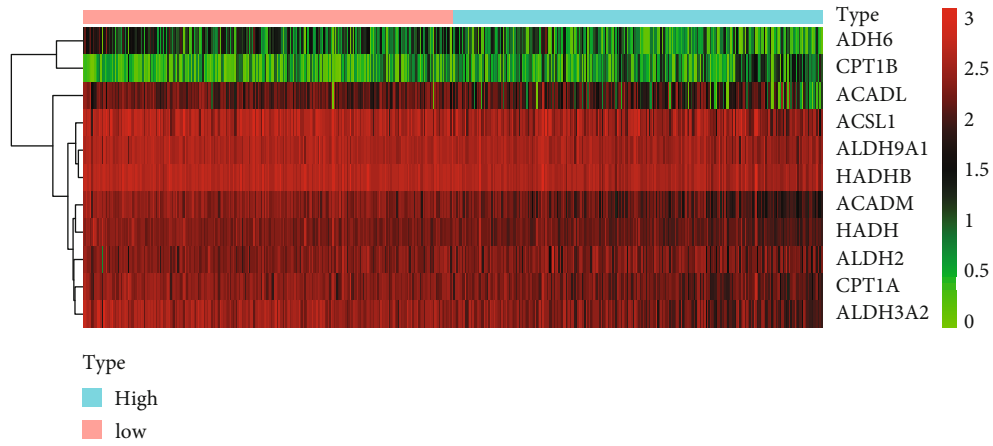
3.1. A Panoramic View of GSVA in Pan-RCC. The R language was first used to perform GSVA on pan-RCC and the corresponding heat map was generated. In KIRC, the pathways that were inhibited included folate biosynthesis, oxidative



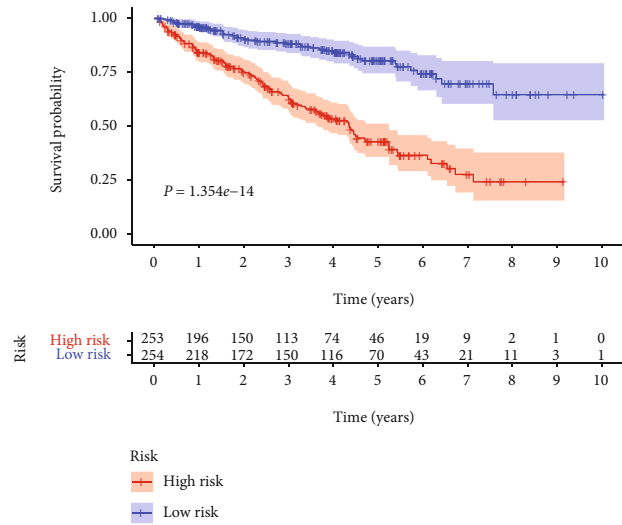
(a)



(b)

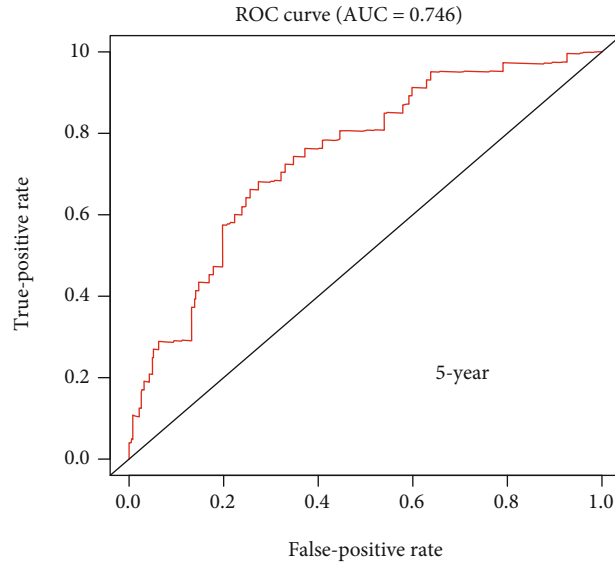


(c)

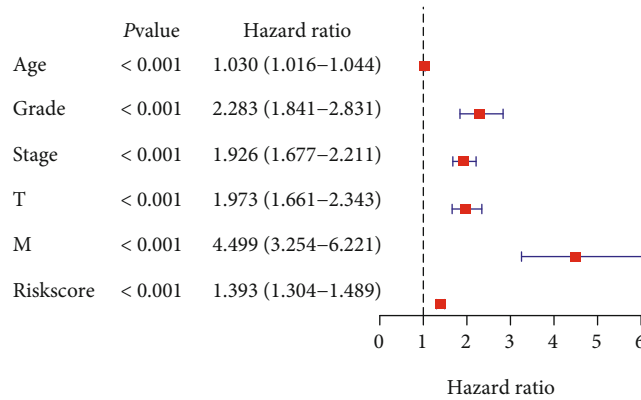


(d)

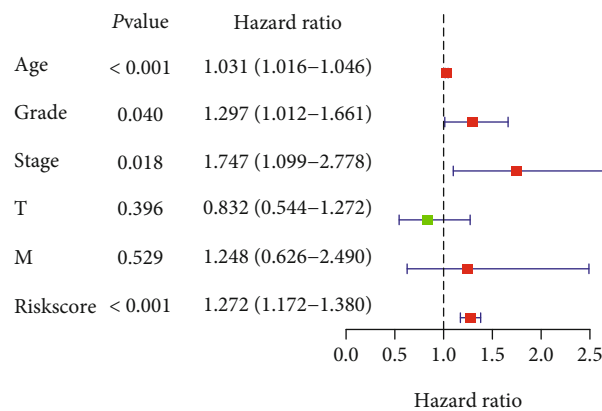
FIGURE 5: Continued.



(e)



(f)



(g)

FIGURE 5: Establishment of the risk signature in KIRC and its correlation with clinical characteristics. (a–c) The process of building the risk signature containing 11 genes in KIRC. (d) Survival curve drawn based on the model. (e) Five-year ROC curve. Results of (f) univariate Cox analysis and (g) multivariate Cox analysis.

phosphorylation, steroid biosynthesis, citrate cycle, tricarboxylic acid (TCA) cycle, and fatty acid metabolism. Activated pathways included apoptosis, DNA replication, cell cycle, Notch signaling pathway, JAK/STAT signaling pathway, and P53 signaling pathway (Figure 1(a)). In KIRP, the

inhibited pathways included citrate cycle, TCA cycle, fatty acid metabolism, peroxisome proliferator-activated receptor signaling pathway, transforming growth factor-beta (TGF- $\beta$ ) signaling pathway, calcium signaling pathway, and adipocytokine signaling pathway. Activated pathways included

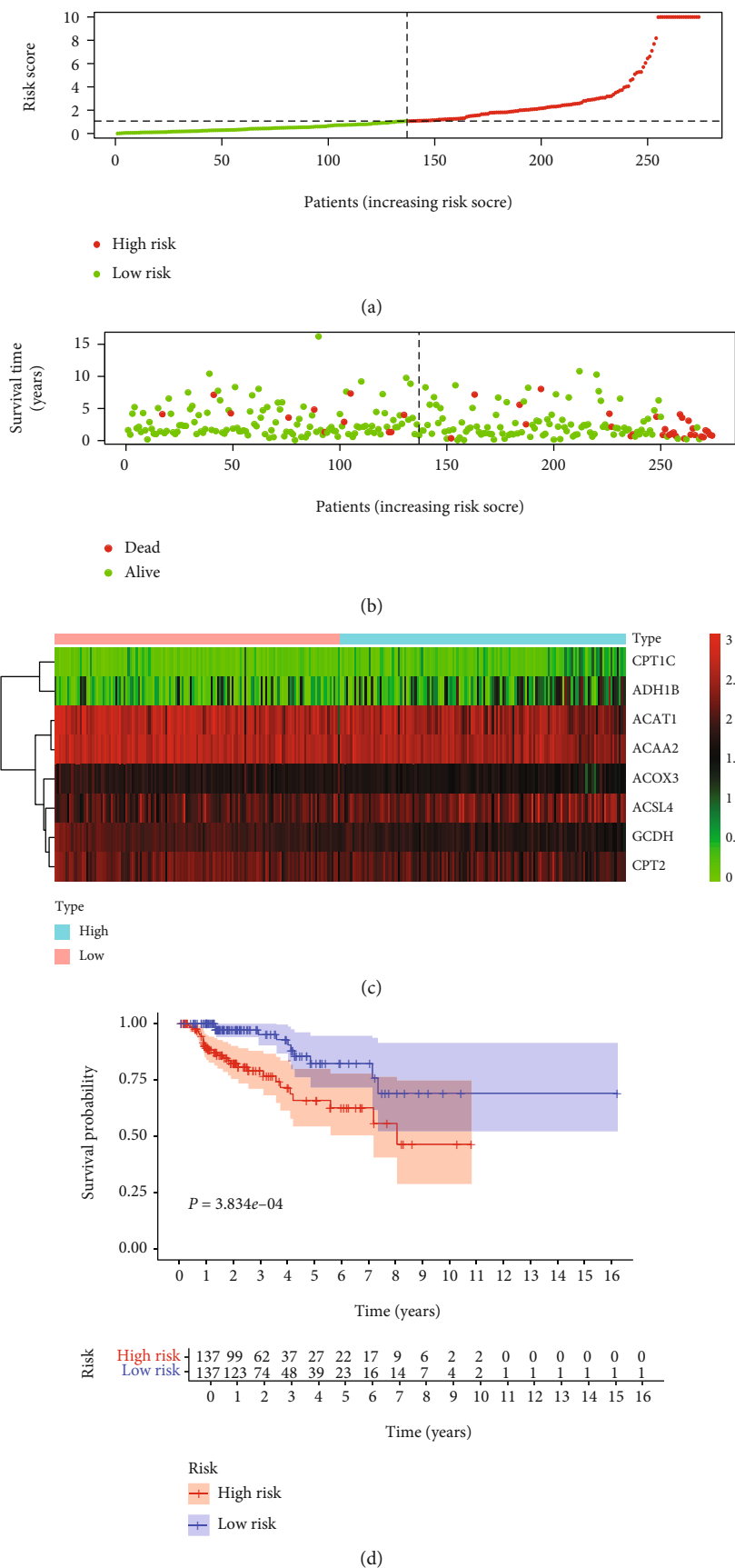


FIGURE 6: Continued.

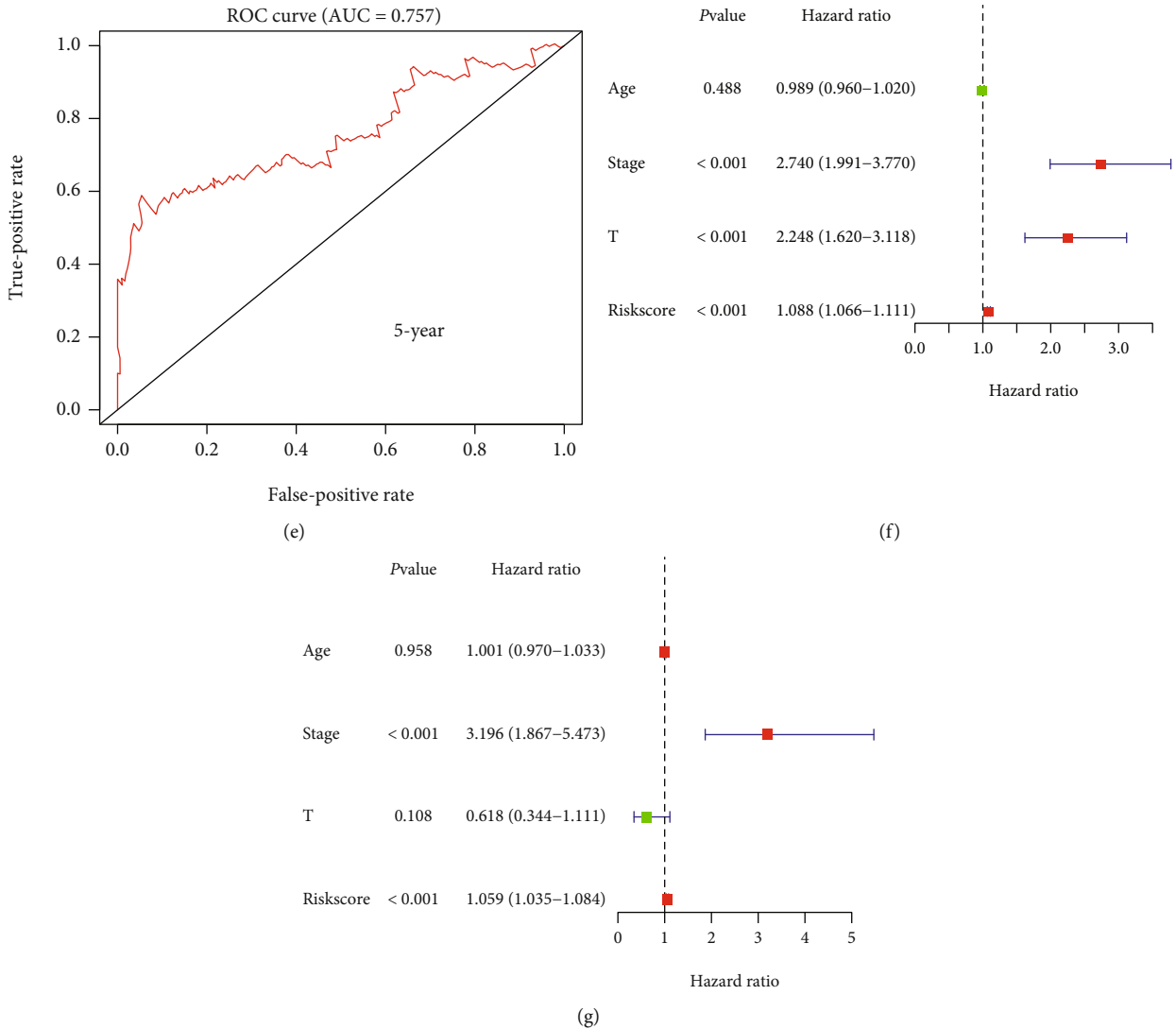


FIGURE 6: Risk signature in KIRP and its correlation with clinical characteristics. (a–c) The process of building the risk signature containing eight genes in KIRP. (d) Survival curve drawn based on the model. (e) Five-year ROC curve. Results for (f) univariate Cox analysis and (g) multivariate Cox analysis.

nucleotide excision repair, DNA replication, P53 signaling pathway, cell cycle, proteasome, and RNA degradation (Figure 1(b)). In KICH, the inhibited pathways included folate biosynthesis, hedgehog signaling pathway, tight junction, fatty acid metabolism, and drug metabolism cytochrome p450. Activated pathways included oxidative phosphorylation, citrate cycle, TCA cycle, protein export, RNA degradation, and mammalian target of rapamycin signaling pathway (Figure 1(c)).

3.2. Panoramic View of Genes Related to Fatty Acid Metabolism Pathways in RCC. Venn diagram construction identified up- and downregulated pathways in the three RCC subtypes. The homologous recombination and RNA polymerase pathways were upregulated (Figure 2(a)). The cysteine and methionine metabolism, primary bile biosynthesis, glycine serine and threonine metabolism, folate biosynthesis, taurine and hypotaurine metabolism, arginine and proline metabolism, butanoate metabolism, tryptophan

metabolism, beta-alanine metabolism, proximal tubule bicarbonate reclamation, and fatty acid metabolism pathways were downregulated (Figure 2(b)). Fatty acid metabolism has an essential role in RCC. We identified genes related to fatty acid metabolism using the GSEA website. These genes were used to draw a PPI network map and quantify the data (Figures 2(c) and 2(d)). The findings revealed potentially critical roles of the acyl-CoA dehydrogenase medium chain (ACADM), acyl-CoA oxidase 1 (ACOX1), and enoyl-CoA hydratase and 3-hydroxyacyl-CoA dehydrogenase (EHHADH) genes in the biological process. We then assessed the expression of the fatty acid metabolism genes in three RCC subtypes and plotted a panoramic view. The plot revealed significant differences in the expression of these genes in the different RCC subtypes (Figures 2(e)–2(g)). The data highlighted the heterogeneity between the genes.

3.3. Molecular Changes in Fatty Acid Metabolism Genes in Pan-RCC. The R language was used to generate CNV, SNV,



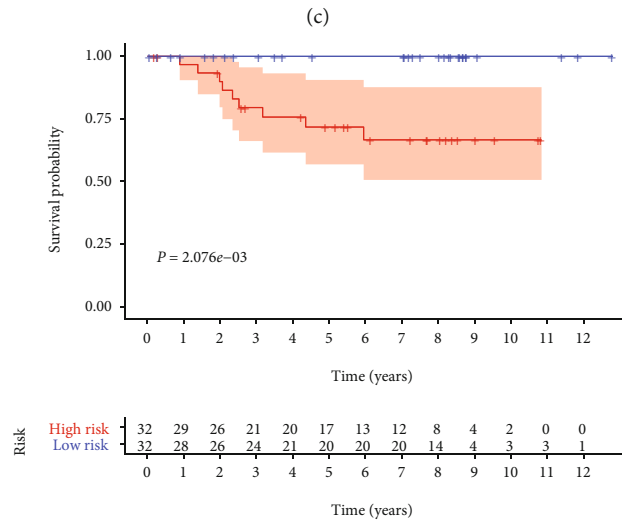
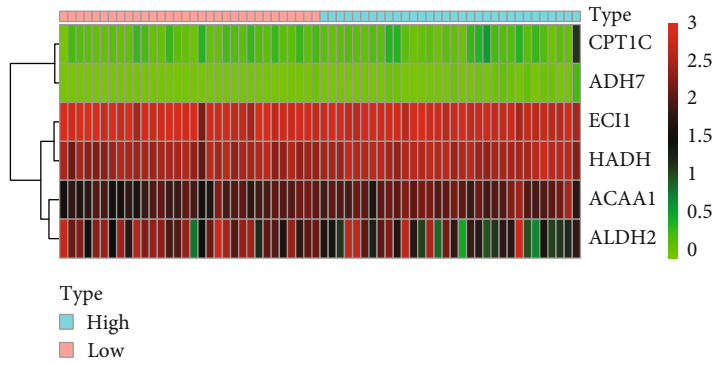
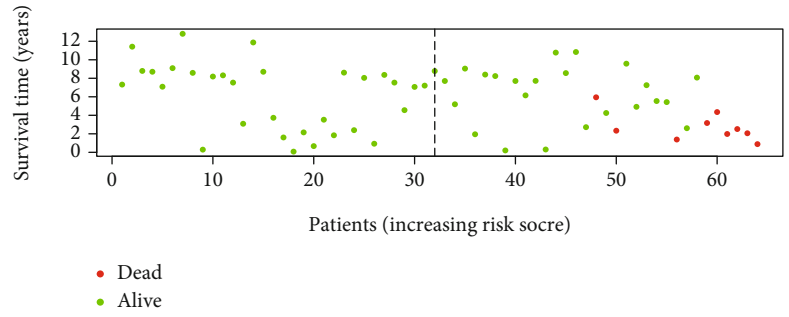
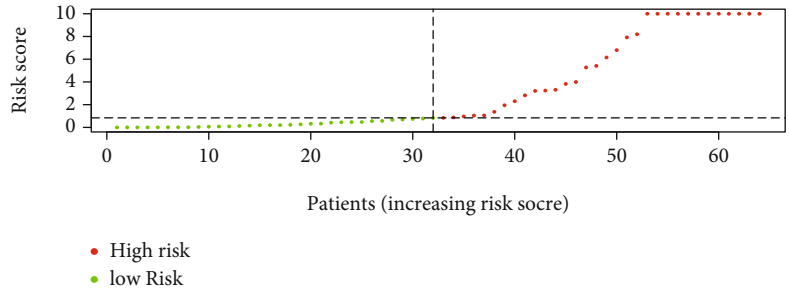
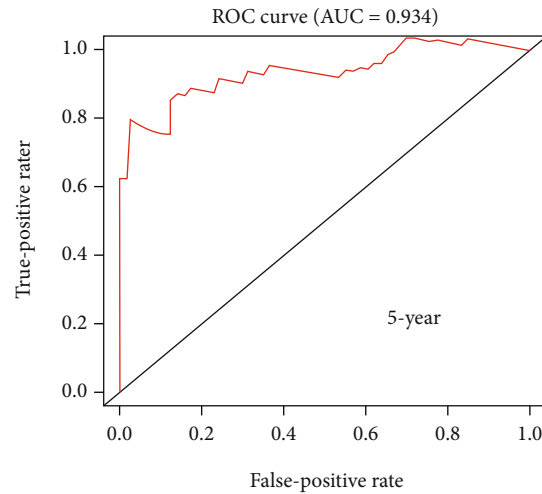
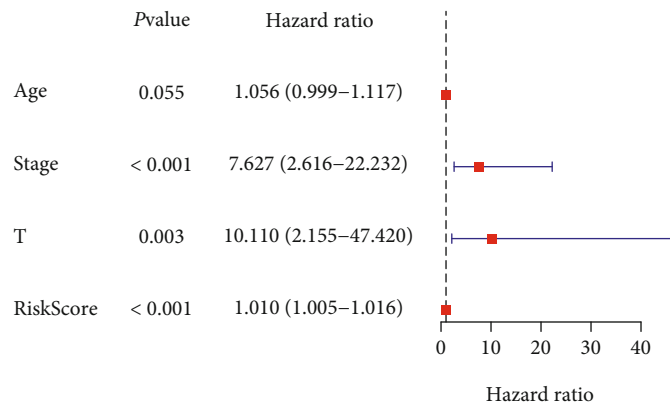


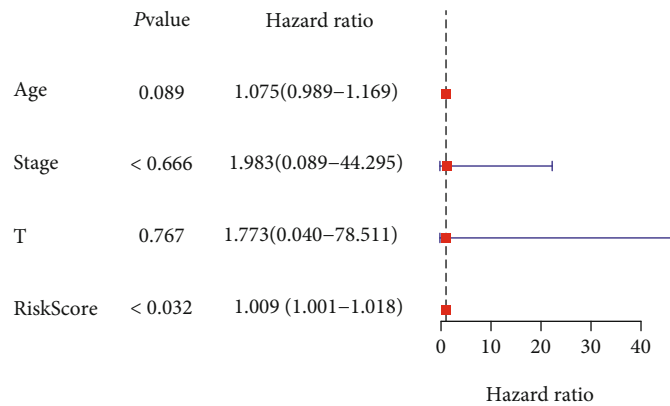
FIGURE 7: Continued.



(e)



(f)



(g)

FIGURE 7: Risk signature in KICH and its correlation with clinical characteristics. (a–c) The process of building the risk signature containing six genes in KICH. (d) Survival curve drawn based on the model. (e) Five-year ROC curve. Results of (f) univariate Cox analysis and (g) multivariate Cox analysis.

mRNA expression, and survival landscape panoramas of the fatty acid metabolism genes in the three RCC subtypes. The survival landscape was drawn by TBtools (<http://cj-chen.github.io/tbtools/>). In CNV, the related genes in KICH displayed higher acquired and deletion mutation frequencies than KIRC and KIRP (Figure 3(a)). In SNV, related genes

displayed higher mutation frequencies in KIRP than KIRC and KICH (Figure 3(b)). Concerning subsequent mRNA expression, ADH7 and CPT1B were upregulated in all three RCC subtypes. In contrast, ADH1B, CYP4A11, and CYP4A22 are downregulated (Figure 3(c)). Finally, in the survival landscape panorama, blue denoted a protective

factor and red denoted a risk factor. Many fatty acid metabolism genes have a protective role in KIRC. The vast majority of statistically significant genes were risk factors in KICH (Figure 3(d)). Interestingly, ACCA1 and HADH were protective factors in KIRC and KIRP but were risk factors in KICH.

**3.4. Clinical Relevance of Fatty Acid Metabolism Genes in Pan-RCC.** To understand whether these genes were protective or a risk factor in tumorigenesis and development, the R language was used to generate heat maps of the expression of these fatty acid metabolic genes in the three RCC subtypes (Figures 4(a), 4(d), and 4(g)). In the figure, progressively redder and greener color indicated progressively higher and lower expression levels, respectively. To verify these results, we chose to use the data in the GEO database to verify our results. In the GEO database, we selected chips corresponding to KIRC, KIRP, and KICH. Among them, KIRC's GEO chip number is GSE11151 and KIRP and KICH's GEO chip number is GSE15641 [20–23]. Because chip GSE15641 contains both KIRP data and KICH data, therefore, we will select the KIRP and KICH data contained in this chip for subsequent verification. We use the information on these GEO chips to explore the expression of fatty acid metabolism-related genes in KIRC, KIRP, and KICH and draw the corresponding heat maps (Supplementary materials Fig. S1A–C). Subsequently, we carefully compared the expression of these fatty acid metabolism-related genes in the GEO database with the expression in the TCGA database and found that the results of the two databases are basically consistent with each other. And then, univariate Cox regression analysis of these fatty acid metabolic genes was performed in the three RCC subtypes. The hazard ratios of ACOX3, CPT1B, and CPT1C in KIRC exceeded 1, implicating the genes as risk factors in the development of KIRC (Figure 4(b)). Similarly, CPT1C and ADH1B were risk factors in the occurrence and development of KIRP (Figure 4(e)). CPT1C, ACSL3, ACAA1, CPT2, HADH, and ACAT2 were identified as risk factors in the development of KICH (Figure 4(h)). To understand the correlation between these genes, we drew a panoramic view of the relationship between the two molecules. In the upper right of these panoramic pictures, progressively bluer colors and progressively larger bubble sizes indicated increasingly stronger positive correlations between the two molecules. Progressively redder colors and progressively larger bubble sizes indicated stronger negative relationships between the two. The bottom left of these panoramas displays a quantitative value of the correlation. A value closer to 1 and  $-1$  indicated a progressively stronger positive correlation and negative correlation, respectively. Strong positive correlations were evident between ADH4 and ADH1C in KIRC (Figure 4(c)), between HADHA and HADHB in KIRP (Figure 4(f)) and between ADH6 and ADH1A in KICH (Figure 4(i)).

**3.5. The Prognostic Risk Signature in KIRC.** In order to explore the potential clinical application value of fatty acid metabolism genes in KIRC, we use fatty acid metabolism

genes to establish a prognostic-related risk signature in KIRC (Figures 5(a) and 5(b)). This risk signature consisted of ADH6, CPT1B, ACADL, ACSL1, ALDH9A1, HADHB, ACADM, HADH, ALDH2, CPT1A, and ALDH3A2 (Figure 5(c)). This risk signature was used to divide KIRC patients into high-risk and low-risk groups. A statistically significant difference was evident between the risk signature and overall survival ( $P = 1.354e - 14$ ; Figure 5(d)). An ROC curve was drawn. The area under the ROC curve (AUC) was 0.746 (Figure 5(e)). Subsequently, we used RT-qPCR to detect the mRNA expression of the ADH6 gene in three KIRC tumor samples and three normal kidney samples and plotted relative histograms (Supplementary materials Fig. S2). The results showed that the expression level of the ADH6 gene in KIRC tumor tissue was significantly lower than that in normal kidney tissue. Finally, univariate and multivariate Cox regression analyses were performed. The age, grade, stage, and risk score were independent risk factors in KIRC (Figure 5(f) and 5(g)).

**3.6. The Prognostic Risk Signature in KIRP.** Similarly, a prognostic risk signature was established in KIRP (Figures 6(a) and 6(b)). This risk signature consisted of CPT1C, ADH1B, ACAT1, ACAA2, ACOX3, ACSL4, GCDH, and CPT2 (Figure 6(c)). The allocation of KIRP patients into high- and low-risk groups also proved to be statistically significant with overall survival ( $P = 3.834e - 04$ ; Figure 6(d)). The AUC of the ROC curve was 0.757 (Figure 6(e)). The univariate and multivariate Cox regression analyses revealed that the stage and risk score were independent risk factors in KIRP (Figures 6(f) and 6(g)).

**3.7. The Prognostic Risk Signature in KICH.** The similarly constructed prognostic-related risk signature in KICH (Figures 7(a) and 7(b)) consisted of CPT1C, ADH7, ECI1, HADH, ACAA1, and ALDH2 (Figure 7(c)). The allocation of KICH patients into high- and low-risk groups also was statistically significant with overall survival ( $P = 2.076e - 03$ ; Figure 7(d)). Then, AUC of the ROC curve was 0.934 (Figure 7(e)). Finally, univariate and multivariate Cox regression analyses determined that the risk score was an independent risk factor in KICH (Figures 7(f) and 7(g)).

## 4. Discussion

RCC is a common malignant tumor in the urinary system. RCC accounts for approximately 3% of all adult cancer patients [24, 25]. Once RCC has metastasized, the five-year survival rate is only 12% and approximately 20–40% of patients with primary kidney cancer experience distant metastases [26, 27]. Understanding the molecular mechanisms of the development and progression of RCC is increasingly important, and detailed and comprehensive data on the three RCC subtypes are urgently needed. Big data analysis by a high-throughput sequencing technology has identified potential diagnostic and therapeutic targets in disease progression [28, 29].

This study analyzed TCGA sequence data to discover effective prognostic models of pan-RCC. The findings could

potentially guide future clinical and basic medical research. First, GSVA was used to analyze the three RCC subtypes. This analysis revealed the joint downregulation of fatty acid metabolism pathways in the three subtypes. The finding highlighted the important role of fatty acid metabolism in the three RCC subtypes. Tumor cells usually use aerobic glycolysis (Warburg effect) to meet their energy and membrane structure needs. These are precisely the key factors that drive cancer growth, immune escape, survival, and disease development. These glycolysis products are used to synthesize lipids and provide a material basis for cell proliferation. Targeted fatty acid metabolism pathways can play a substantial role in RCC [12, 30, 31]. Focusing on the fatty acid metabolism pathways, we explored the genetic variation and clinical relevance in the three RCC subtypes.

In univariate Cox regression, ACOX3, CPT1B, CPT1C, and five clinical characteristics (age, grade, stage, T, and M) were significant predictors of survival in KIRC patients. Multivariate Cox regression suggested that three clinical characteristics (age, grade, and stage) were independent prognostic factors for KIRC. Similarly, in KIRP, univariate Cox regression showed that CPT1C, ADH1B, and two clinical characteristics (stage and T) were significant predictors of survival. Multivariate Cox regression suggested that the clinical stage was an independent prognostic factor. Univariate Cox regression in KICH showed that CPT1C, ACSL3, ACAA1, CPT2, HADH, ACAT2 and two clinical characteristics (stage and T) were significant predictors of survival. However, the multivariate Cox regression did not reveal any independent prognostic factors. The collective findings revealed that the three RCC subtypes have common and different risk factors. Thus, while the subtypes are all RCC, they are heterogeneous. CPT1C was identified as having a risk factor role in all three RCC subtypes. CPT1C is the last member of the CPT1 family to be identified. The protein is mainly expressed in the endoplasmic reticulum of cells and can interact with different proteins to produce a wide range of biological effects. The most important is the interaction with Atlastin-1, which maintains the endoplasmic reticulum integrity of sex-related proteins. There is increasing evidence for the role of CPT1C in regulating lipid metabolism. The protein is highly expressed in specific tumor cells, which confers resistance to low glucose and hypoxia [32, 33]. Therefore, CPT1C may be a promising target for the treatment of cancer [34].

Finally, we used the fatty acid metabolism genes to establish prognostic risk signatures in the three RCC subtypes. The risk signature constructed in KIRC patients consists of eleven genes: ADH6, CPT1B, ACADL, ACSL1, ALDH9A1, HADHB, ACADM, HADH, ALDH2, CPT1A, and ALDH3A2. The risk signature constructed in KIRP patients consists of eight genes: CPT1C, ADH1B, ACAT1, ACAA2, ACOX3, ACSL4, GCDH, and CPT2. The risk signature created in KICH patients consists of six genes: CPT1C, ADH7, ECI1, HADH, ACAA1, and ALDH2. The possible underlying mechanisms of ADH6 in pancreatic cancer have been discovered in previous studies. These include fatty acid metabolism, retinol metabolism, primary alcohol metabolic processes, and drug metabolism cytochrome P450 [35]. Fatty

acid oxidation may affect tumor progression by affecting lymphangiogenesis, and CPT1B may participate [36]. Interest in ACADL in tumor biology has focused mainly on prostate cancer, breast cancer, and esophageal squamous cell carcinoma, primarily to study its influence on the occurrence, development, and treatment of tumors. However, many potential functions are still unclear and require further research [37–39]. Studies in hepatocellular carcinoma have shown that long-chain noncoding RNA HULC can activate ACSL1 by upregulating the transcription factor PPARA to affect the proliferation of liver cancer cells [40]. Mutations in the ALDH9A1 gene may be a potential risk factor in RCC [41]. The ACADM gene can be regulated by microRNA-224 to affect the apoptosis of breast epithelial cells through the production of triglycerides [42]. After the downregulation of HADH,  $\beta$ -oxidation was inhibited in gastric cancer cells, which led to the accumulation of fatty acids. This inhibited the transcription of phosphatase and tensin homolog and promoted the proliferation and invasion of gastric cancer cells [43–45]. ALDH2 is related to the occurrence and development of liver cancer, gastric cancer, and colon cancer [46]. As a critical rate-limiting enzyme for fatty acid oxidation, CPT1A plays a role in transporting fatty acids into the mitochondria for oxidative phosphorylation. CPT1A has also been associated with the occurrence and very early development of various tumors [47–50]. ADH1B mutations have also been extensively studied and have been associated with esophageal, head and neck, ovarian, and colorectal cancer [51–54]. Acsl4 may induce ferroptosis by altering the lipid composition [55]. From previous research, it is clear that we can see that the vast majority of genes used to establish risk signatures are related to cancer research and to some extent support our findings.

In many cancers, gene expression signatures and prognostic-related risk signatures have proven to function based on their roles in driving pathogenesis, which is useful for predicting the clinical outcome and prognostic value [56–60]. The multiple models that we constructed using genes related to fatty acid metabolism can effectively predict the survival of kidney cancer patients. Even so, data from large-scale, multicenter, evidence-based medical studies are needed for verification.

## 5. Conclusions

In summary, we used TCGA data to draw a panoramic view of CNV, SNV, mRNA expression, and survival landscape of fatty acid metabolism genes in KIRC, KIRP, and KICH patients. Based on the fatty acid metabolism genes, we identified a variety of prognostic risk signatures for KIRC, KIRP, and KICH. But it must be admitted that there are still some shortcomings in this research. There is a lack of exploring the functions and molecular mechanisms of these new mRNAs in vivo and in vitro. In the future, we will continue to explore in depth along these important clues. We believe that the current data can provide help for future scientific research and the clinical diagnosis and treatment of RCC.

## Abbreviations

RCC:	Renal cell carcinoma
GSVA:	Gene set variation analysis
KEGG:	Kyoto encyclopedia of genes and genomes
CNV:	Copy number variation
SNV:	Single-nucleotide variation
KIRC:	Kidney renal clear cell carcinoma
KIRP:	Kidney renal papillary cell carcinoma
KICH:	Kidney chromophobe
TCGA:	The Cancer Genome Atlas
ADH6:	Alcohol dehydrogenase 6
CPT1B:	Carnitine palmitoyltransferase 1B
ACADL:	Acyl-CoA dehydrogenase long chain
ACSL1:	Acyl-CoA synthetase long-chain family member 1
ALDH9A1:	Aldehyde dehydrogenase 9 family member A1
HADHB:	Hydroxyacyl-CoA dehydrogenase trifunctional multienzyme complex subunit beta
ACADM:	Acyl-CoA dehydrogenase medium chain
HADH:	Hydroxyacyl-CoA dehydrogenase
ALDH2:	Aldehyde dehydrogenase 2
CPT1A:	Carnitine palmitoyltransferase 1A
ALDH3A2:	Aldehyde dehydrogenase 3 family member A2
CPT1C:	Carnitine palmitoyltransferase 1C
ADH1B:	Alcohol dehydrogenase 1B
ACAT1:	Acetyl-CoA acetyltransferase 1
ACAA2:	Acetyl-CoA acyltransferase 2
ACOX3:	Acyl-CoA oxidase 3
ACSL4:	Acyl-CoA synthetase long-chain family member 4
GCDH:	Glutaryl-CoA dehydrogenase
CPT2:	Carnitine palmitoyltransferase 2
ADH7:	Alcohol dehydrogenase 7
ECI1:	Enoyl-CoA delta isomerase 1
ACAA1:	Acetyl-CoA acyltransferase 1.

## Data Availability

The data used to support the findings of this study are available from the corresponding author upon request.

## Disclosure

Ping Wu and Yingkun Xu are the co-first authors.

## Conflicts of Interest

The authors declare no potential conflicts of interest.

## Authors' Contributions

Ping Wu and Yingkun Xu contributed equally to this study. Qifei Wang and Guangzhen Wu designed the research; Ping Wu and Yingkun Xu analyzed the data and wrote the paper. Jiayi Li, Ningke Ruan, and Cong Zhang performed the data analysis and interpreted the data. Xiaowei Li, Peizhi Zhang, and Panpan Sun help to revise the manuscript in the article. All authors read and approved the final manuscript.

## Acknowledgments

This project is supported by the Scientific Research Fund of Liaoning Provincial Education Department (No. LZ2020071).

## Supplementary Materials

Figure S1: verification process from GEO database; Figure S2: RT-qPCR technology verifies the expression of the ADH6 gene in KIRC tumors and normal tissues. (*Supplementary Materials*)

## References

- [1] U. Capitanio and F. Montorsi, "Renal cancer," *Lancet*, vol. 387, no. 10021, pp. 894–906, 2016.
- [2] A. Znaor, J. Lortet-Tieulent, M. Laversanne, A. Jemal, and F. Bray, "International variations and trends in renal cell carcinoma incidence and mortality," *European Urology*, vol. 67, no. 3, pp. 519–530, 2015.
- [3] D. J. Sanchez and M. C. Simon, "Genetic and metabolic hallmarks of clear cell renal cell carcinoma," *Biochimica Et Biophysica Acta. Reviews on Cancer*, vol. 1870, no. 1, pp. 23–31, 2018.
- [4] K. Guo, Q. Chen, X. He et al., "Expression and significance of cystatin-C in clear cell renal cell carcinoma," *Biomedicine & Pharmacotherapy*, vol. 107, pp. 1237–1245, 2018.
- [5] The Cancer Genome Atlas Research Network, "Comprehensive molecular characterization of clear cell renal cell carcinoma," *Nature*, vol. 499, no. 7456, pp. 43–49, 2013.
- [6] F. Gatto, I. Nookaew, and J. Nielsen, "Chromosome 3p loss of heterozygosity is associated with a unique metabolic network in clear cell renal carcinoma," *Proceedings of the National Academy of Sciences of the United States of America*, vol. 111, no. 9, pp. E866–E875, 2014.
- [7] A. A. Hakimi, E. Reznik, C. H. Lee et al., "An integrated metabolic atlas of clear cell renal cell carcinoma," *Cancer Cell*, vol. 29, no. 1, pp. 104–116, 2016.
- [8] M. R. Morris and F. Latif, "The epigenetic landscape of renal cancer," *Nature Reviews. Nephrology*, vol. 13, no. 1, pp. 47–60, 2017.
- [9] L. S. Schmidt and W. M. Linehan, "Genetic predisposition to kidney cancer," *Seminars in Oncology*, vol. 43, no. 5, pp. 566–574, 2016.
- [10] S. Hänzelmann, R. Castelo, and J. Guinney, "GSVA: gene set variation analysis for microarray and RNA-seq data," *BMC Bioinformatics*, vol. 14, no. 1, p. 7, 2013.
- [11] G. Wu, Q. Wang, Y. Xu et al., "Targeting the transcription factor receptor LXR to treat clear cell renal cell carcinoma: agonist or inverse agonist?," *Cell Death & Disease*, vol. 10, no. 6, p. 416, 2019.
- [12] G. Wu, Y. Xu, Q. Wang et al., "FABP5 is correlated with poor prognosis and promotes tumour cell growth and metastasis in clear cell renal cell carcinoma," *European Journal of Pharmacology*, vol. 862, p. 172637, 2019.
- [13] F. Röhrig and A. Schulze, "The multifaceted roles of fatty acid synthesis in cancer," *Nature Reviews. Cancer*, vol. 16, no. 11, pp. 732–749, 2016.
- [14] K. Vriens, S. Christen, S. Parik et al., "Evidence for an alternative fatty acid desaturation pathway increasing cancer plasticity," *Nature*, vol. 566, no. 7744, pp. 403–406, 2019.



- [15] N. Koundouros and G. Poulogiannis, "Reprogramming of fatty acid metabolism in cancer," *British Journal of Cancer*, vol. 122, no. 1, pp. 4–22, 2020.
- [16] V. K. Mootha, C. M. Lindgren, K. F. Eriksson et al., "PGC-1 $\alpha$ -responsive genes involved in oxidative phosphorylation are coordinately downregulated in human diabetes," *Nature Genetics*, vol. 34, no. 3, pp. 267–273, 2003.
- [17] A. Subramanian, P. Tamayo, V. K. Mootha et al., "Gene set enrichment analysis: a knowledge-based approach for interpreting genome-wide expression profiles," *Proceedings of the National Academy of Sciences of the United States of America*, vol. 102, no. 43, pp. 15545–15550, 2005.
- [18] D. Szklarczyk, A. L. Gable, D. Lyon et al., "STRING v11: protein-protein association networks with increased coverage, supporting functional discovery in genome-wide experimental datasets," *Nucleic Acids Research*, vol. 47, no. D1, pp. D607–d613, 2019.
- [19] P. Shannon, A. Markiel, O. Ozier et al., "Cytoscape: a software environment for integrated models of biomolecular interaction networks," *Genome Research*, vol. 13, no. 11, pp. 2498–2504, 2003.
- [20] J. Jones, H. Otu, D. Spentzos et al., "Gene signatures of progression and metastasis in renal cell cancer," *Clinical Cancer Research*, vol. 11, no. 16, pp. 5730–5739, 2005.
- [21] M. V. Yusenko, R. P. Kuiper, T. Boethe, B. Ljungberg, A. G. van Kessel, and G. Kovacs, "High-resolution DNA copy number and gene expression analyses distinguish chromophobe renal cell carcinomas and renal oncocytomas," *BMC Cancer*, vol. 9, no. 1, p. 152, 2009.
- [22] M. V. Yusenko, D. Zubakov, and G. Kovacs, "Gene expression profiling of chromophobe renal cell carcinomas and renal oncocytomas by affymetrix genechip using pooled and individual tumours," *International Journal of Biological Sciences*, vol. 5, no. 6, pp. 517–527, 2009.
- [23] M. V. Yusenko, T. Ruppert, and G. Kovacs, "Analysis of differentially expressed mitochondrial proteins in chromophobe renal cell carcinomas and renal oncocytomas by 2-D gel electrophoresis," *International Journal of Biological Sciences*, vol. 6, no. 3, pp. 213–224, 2010.
- [24] S. Del Vecchio and R. J. Ellis, "Cabozantinib for the management of metastatic clear cell renal cell carcinoma," *Journal of Kidney Cancer and VHL*, vol. 5, no. 4, pp. 1–5, 2018.
- [25] W. Majer, K. Kluzek, H. Bluysen, and J. Wesoly, "Potential approaches and recent advances in biomarker discovery in clear-cell renal cell carcinoma," *Journal of Cancer*, vol. 6, no. 11, pp. 1105–1113, 2015.
- [26] M. B. Atkins and N. M. Tannir, "Current and emerging therapies for first-line treatment of metastatic clear cell renal cell carcinoma," *Cancer Treatment Reviews*, vol. 70, pp. 127–137, 2018.
- [27] Q. Cao, H. Ruan, K. Wang et al., "Overexpression of PLIN2 is a prognostic marker and attenuates tumor progression in clear cell renal cell carcinoma," *International Journal of Oncology*, vol. 53, no. 1, pp. 137–147, 2018.
- [28] Y. Xu, G. Wu, J. Li et al., "Screening and identification of key biomarkers for bladder cancer: a study based on TCGA and GEO data," *BioMed Research International*, vol. 2020, Article ID 8283401, 20 pages, 2020.
- [29] G. Wu, Z. Zhang, Q. Tang et al., "Study of FABP's interactome and detecting new molecular targets in clear cell renal cell carcinoma," *Journal of Cellular Physiology*, vol. 235, no. 4, pp. 3776–3789, 2019.
- [30] K. D. Courtney, D. Bezwada, T. Mashimo et al., "Isotope Tracing of Human Clear Cell Renal Cell Carcinomas Demonstrates Suppressed Glucose Oxidation *In Vivo*," *Cell Metabolism*, vol. 28, no. 5, pp. 793–800.e2, 2018.
- [31] V. Fritz, Z. Benfodda, G. Rodier et al., "Abrogation of de novo lipogenesis by stearoyl-CoA desaturase 1 inhibition interferes with oncogenic signaling and blocks prostate cancer progression in mice," *Molecular Cancer Therapeutics*, vol. 9, no. 6, pp. 1740–1754, 2010.
- [32] K. Zaugg, Y. Yao, P. T. Reilly et al., "Carnitine palmitoyltransferase 1C promotes cell survival and tumor growth under conditions of metabolic stress," *Genes & Development*, vol. 25, no. 10, pp. 1041–1051, 2011.
- [33] P. T. Reilly and T. W. Mak, "Molecular pathways: tumor cells co-opt the brain-specific metabolism gene CPT1C to promote survival," *Clinical Cancer Research*, vol. 18, no. 21, pp. 5850–5855, 2012.
- [34] N. Casals, V. Zammit, L. Herrero, R. Fadó, R. Rodríguez-Rodríguez, and D. Serra, "Carnitine palmitoyltransferase 1C: From cognition to cancer," *Progress in Lipid Research*, vol. 61, pp. 134–148, 2016.
- [35] X. Liao, R. Huang, X. Liu et al., "Distinct prognostic values of alcohol dehydrogenase mRNA expression in pancreatic adenocarcinoma," *Oncotargets and Therapy*, vol. Volume 10, pp. 3719–3732, 2017.
- [36] B. W. Wong, X. Wang, A. Zecchin et al., "The role of fatty acid  $\beta$ -oxidation in lymphangiogenesis," *Nature*, vol. 542, no. 7639, pp. 49–54, 2017.
- [37] B. X. Xie, H. Zhang, J. Wang et al., "Analysis of differentially expressed genes in LNCaP prostate cancer progression model," *Journal of Andrology*, vol. 32, no. 2, pp. 170–182, 2011.
- [38] Z. Li, J. Heng, J. Yan et al., "Integrated analysis of gene expression and methylation profiles of 48 candidate genes in breast cancer patients," *Breast Cancer Research and Treatment*, vol. 160, no. 2, pp. 371–383, 2016.
- [39] D. L. Yu, H. W. Li, Y. Wang et al., "Acyl-CoA dehydrogenase long chain expression is associated with esophageal squamous cell carcinoma progression and poor prognosis," *Oncotargets and Therapy*, vol. Volume 11, pp. 7643–7653, 2018.
- [40] M. Cui, Z. Xiao, Y. Wang et al., "Long noncoding RNA HULC modulates abnormal lipid metabolism in hepatoma cells through an miR-9-mediated RXRA signaling pathway," *Cancer Research*, vol. 75, no. 5, pp. 846–857, 2015.
- [41] M. Y. R. Henrion, M. P. Purdue, G. Scelo et al., "Common variation at 1q24.1 (ALDH9A1) is a potential risk factor for renal cancer," *PLoS One*, vol. 10, no. 3, article e0122589, 2015.
- [42] B. Shen, Q. Pan, Y. Yang et al., "miR-224 affects mammary epithelial cell apoptosis and triglyceride production by downregulating ACADM and ALDH2 genes," *DNA and Cell Biology*, vol. 36, no. 1, pp. 26–33, 2017.
- [43] D. Huang, T. Li, X. Li et al., "HIF-1-mediated suppression of acyl-CoA dehydrogenases and fatty acid oxidation is critical for cancer progression," *Cell Reports*, vol. 8, no. 6, pp. 1930–1942, 2014.
- [44] K. Yin, L. Wang, X. Zhang et al., "Netrin-1 promotes gastric cancer cell proliferation and invasion via the receptor neogenin through PI3K/AKT signaling pathway," *Oncotarget*, vol. 8, no. 31, pp. 51177–51189, 2017.

- [45] C. Shen, Y. H. Song, Y. Xie et al., “Downregulation of HADH promotes gastric cancer progression via Akt signaling pathway,” *Oncotarget*, vol. 8, no. 44, pp. 76279–76289, 2017.
- [46] R. Li, Z. Zhao, M. Sun, J. Luo, and Y. Xiao, “ALDH2 gene polymorphism in different types of cancers and its clinical significance,” *Life Sciences*, vol. 147, pp. 59–66, 2016.
- [47] Y. N. Wang, Z. L. Zeng, J. Lu et al., “CPT1A-mediated fatty acid oxidation promotes colorectal cancer cell metastasis by inhibiting anoikis,” *Oncogene*, vol. 37, no. 46, pp. 6025–6040, 2018.
- [48] Y. Xiong, Z. Liu, X. Zhao et al., “CPT1A regulates breast cancer-associated lymphangiogenesis via VEGF signaling,” *Biomedicine & Pharmacotherapy*, vol. 106, pp. 1–7, 2018.
- [49] J. Shi, H. Fu, Z. Jia, K. He, L. Fu, and W. Wang, “High expression of CPT1A predicts adverse outcomes: a potential therapeutic target for acute myeloid leukemia,” *eBioMedicine*, vol. 14, pp. 55–64, 2016.
- [50] M. Joshi, G. E. Stoykova, M. Salzmänn-Sullivan et al., “CPT1A supports castration-resistant prostate cancer in androgen-deprived conditions,” *Cells*, vol. 8, no. 10, p. 1115, 2019.
- [51] K. M. Gharpure, O. D. Lara, Y. Wen et al., “ADH1B promotes mesothelial clearance and ovarian cancer infiltration,” *Oncotarget*, vol. 9, no. 38, pp. 25115–25126, 2018.
- [52] H. Gu, D. Gong, G. Ding et al., “A variant allele of ADH1B and ALDH2, is associated with the risk of esophageal cancer,” *Experimental and Therapeutic Medicine*, vol. 4, no. 1, pp. 135–140, 2012.
- [53] M. Crous-Bou, G. Rennert, D. Cuadras et al., “Polymorphisms in alcohol metabolism genes ADH1B and ALDH2, alcohol consumption and colorectal cancer,” *PLoS One*, vol. 8, no. 11, article e80158, 2013.
- [54] Y. Zhang, N. Gu, L. Miao, H. Yuan, R. Wang, and H. Jiang, “Alcohol dehydrogenase-1B Arg47His polymorphism is associated with head and neck cancer risk in Asian: a meta-analysis,” *Tumour Biology*, vol. 36, no. 2, pp. 1023–1027, 2015.
- [55] S. Doll, B. Proneth, Y. Y. Tyurina et al., “ACSL4 dictates ferroptosis sensitivity by shaping cellular lipid composition,” *Nature Chemical Biology*, vol. 13, no. 1, pp. 91–98, 2017.
- [56] E. J. Askeland, V. A. Chehval, R. W. Askeland et al., “Cell cycle progression score predicts metastatic progression of clear cell renal cell carcinoma after resection,” *Cancer Biomarkers*, vol. 15, no. 6, pp. 861–867, 2015.
- [57] B. I. Rini, B. Escudier, J. F. Martini et al., “Validation of the 16-gene recurrence score in patients with locoregional, high-risk renal cell carcinoma from a phase III trial of adjuvant sunitinib,” *Clinical Cancer Research*, vol. 24, no. 18, pp. 4407–4415, 2018.
- [58] S. A. Brooks, A. R. Brannon, J. S. Parker et al., “ClearCode34: a prognostic risk predictor for localized clear cell renal cell carcinoma,” *European Urology*, vol. 66, no. 1, pp. 77–84, 2014.
- [59] Y. Xu, X. Li, Y. Han et al., “A New Prognostic Risk Model Based on PPAR Pathway-Related Genes in Kidney Renal Clear Cell Carcinoma,” *PPAR Research*, vol. 2020, Article ID 6937475, 13 pages, 2020.
- [60] Y. Zhang, M. Chen, M. Liu, Y. Xu, and G. Wu, “Glycolysis-related genes serve as potential prognostic biomarkers in clear cell renal cell carcinoma,” *Oxidative Medicine and Cellular Longevity*, vol. 2021, article 6699808, 20 pages, 2021.

## Research Article

# p300-Catalyzed Lysine Crotonylation Promotes the Proliferation, Invasion, and Migration of HeLa Cells via Heterogeneous Nuclear Ribonucleoprotein A1

Xuesong Han,<sup>1</sup> Xudong Xiang,<sup>2,3</sup> Hongying Yang,<sup>2,3</sup> Hongping Zhang,<sup>2,3</sup> Shuang Liang,<sup>4</sup> Jie Wei,<sup>2,3</sup> and Jing Yu<sup>2,3</sup> 

<sup>1</sup>The First Affiliated Hospital of Kunming Medical University, Kunming, China

<sup>2</sup>The Third Affiliated Hospital of Kunming Medical University, Kunming, China

<sup>3</sup>Yunnan Cancer Center, Kunming, China

<sup>4</sup>Pu'er People's Hospital, Pu'er, China

Correspondence should be addressed to Jing Yu; [yu\\_jing\\_yn@163.com](mailto:yu_jing_yn@163.com)

Xuesong Han and Xudong Xiang contributed equally to this work.

Received 1 July 2020; Revised 13 October 2020; Accepted 28 November 2020; Published 7 December 2020

Academic Editor: Juan F. Santibanez

Copyright © 2020 Xuesong Han et al. This is an open access article distributed under the Creative Commons Attribution License, which permits unrestricted use, distribution, and reproduction in any medium, provided the original work is properly cited.

Cervical carcinoma is the third most common cause of cancer in women with a significant challenge in clinical treatment. Human papillomavirus (HPV) is strongly responsible for cervical carcinoma. Here, we show the increased expression level of heterogeneous nuclear ribonucleoprotein A1 (HNRNPA1) in HPV-associated cervical cancer cells including HeLa, Caski, and SiHa cells, especially in HeLa cells. We provide the evidence that the expression of HNRNPA1 is closely related to HeLa cell proliferation, invasion, and migration. Emerging evidence show that histone modifications account for gene expression. Moreover, our results indicate that HNRNPA1 could be regulated by p300 through p300-mediated lysine crotonylation. Inhibition of p300 downregulated both the lysine crotonylation level and the HNRNPA1 expression. And p300-mediated lysine crotonylation participates in the regulation of HNRNPA1 on HeLa cell proliferation, invasion, and migration. Collectively, our study uncovers that p300-mediated lysine crotonylation enhances expression of HNRNPA1 to promote the proliferation, invasion, and migration of HeLa cells.

## 1. Introduction

Cervical carcinoma is the third most common cause of cancer in women worldwide [1]. Human papillomavirus (HPV) infection is supposed to be a major risk factor of cervical carcinoma [2], and about 95% of cases are caused by infections with high-risk HPV. However, there are limited therapeutic advances for HPV-associated cervical carcinoma. Thus, the prognosis marker of cervical cancers warrants further investigation.

As an oncogene, heterogeneous nuclear ribonucleoprotein A1 (HNRNPA1) was associated with cancer development and was supposed to be a promising therapeutic target in cancer. HNRNPA1 was involved in apoptosis of

colon cancer cells [3]. In oral squamous cancer, HNRNPA1 could modulate the cell cycle and proliferation [4]. HNRNPA1 expression was related to the metastasis of breast cancer [5]. And HNRNPA1 activity affected the therapy of hepatocarcinoma [6]. Thus, the function of HNRNPA1 in HPV-associated cervical carcinoma warranted further investigation. Here, we show that HNRNPA1 was upregulated in HPV-associated cervical cells. And inhibition of HNRNPA1 attenuated the proliferation, invasion, and migration of HeLa cells, which indicated that HNRNPA1 represented a potential target for HPV-associated cervical carcinoma.

Proteins such as histones and nonhistones are subject to a vast range of posttranslation modifications (PTMs) which mainly include methylation, phosphorylation, ubiquitination,

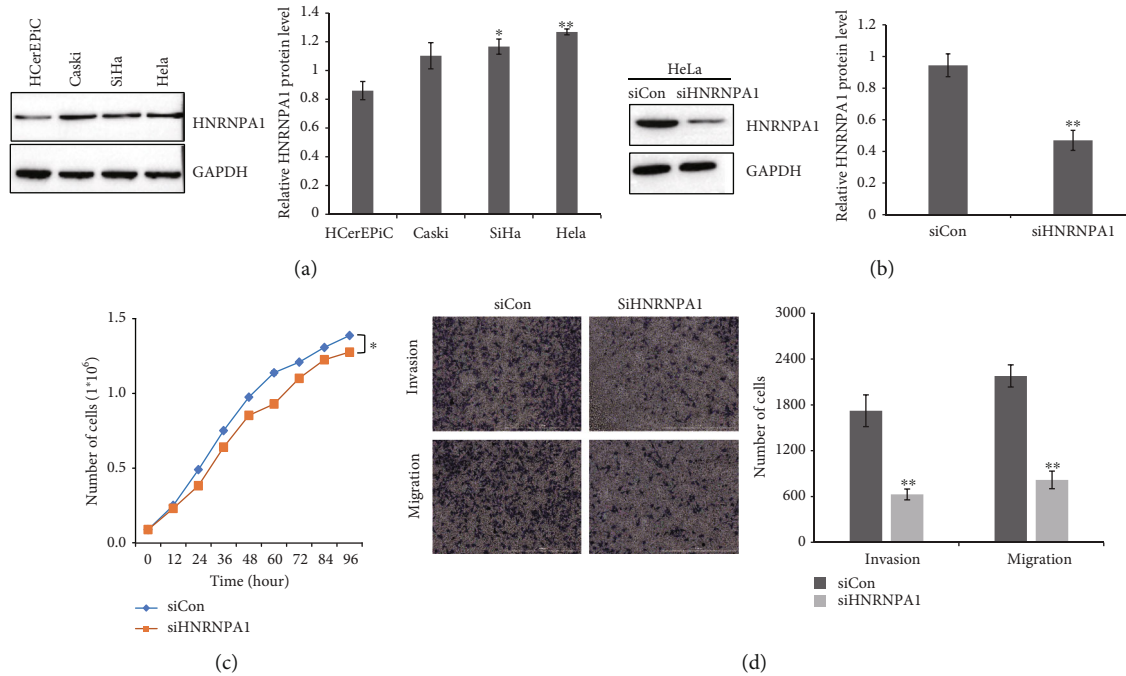


FIGURE 1: Knockdown of HNRNPA1 attenuated the proliferation, invasion, and migration of HeLa cells. (a) Western blot results showed the expression of HNRNPA1 in normal cervical epithelial cells (HCrEPiC) and HPV-associated cervical cancer cells (HeLa cells, Caski cells, and SiHa cells). The relative intensities of HNRNPA1/GAPDH were quantified using ImageJ. \* $P < 0.05$ ; \*\* $P < 0.01$ . (b) HNRNPA1 expression was measured by western blot in HeLa cells stably expressing nontargeting control (siCon) and siHNRNPA1. The relative intensities of HNRNPA1/GAPDH were quantified using ImageJ. \*\* $P < 0.01$ . (c) Effects of HNRNPA1 on HeLa cell proliferation were determined by CCK-8 kits. \* $P < 0.05$ . (d) Transwell assay was performed to determine the invasion and migration of HeLa cells. The invasion and migration of HeLa cells were quantified using Image-Pro Plus 6.0. \* $P < 0.05$ ; \*\* $P < 0.01$ .

and acylation. The protein PTMs are identified to play roles in cancer progression such as tumorigenesis [7], oncogenic transformation [8], recurrence [9], and cancer therapy [10]. Moreover, protein PTMs were closely related to gene transcription. Besides acetylation, short-chain Lys acylations have been identified mainly including butyrylation (Kbu), propionylation (Kpr), and crotonylation (Kcr) [11]. More and more evidence demonstrated the role of Kcr in gene transcription [12, 13].

Different protein PTMs were carried out by different enzymes; these enzymes are frequently mutated or dysregulated in various types of cancer [14]. p300, as a transcriptional coactivator, contributed to cell proliferation [15], differentiation [16], apoptosis [17], and autophagy [18]. Except for histone acetyltransferase (HAT) activity of p300 [19], recent studies have illuminated that the histone crotonyltransferase activity of p300 and p300-mediated Kcr directly stimulates transcription [20]. A study has shown that p300 and p300-mediated Kcr participated in HNRNPA1 regulation [21]. However, the role of p300-mediated Kcr in HeLa cell proliferation, invasion, and migration which are regulated by HNRNPA1 remained obscure.

In present study, we investigated the effect of HNRNPA1 on proliferation, invasion, and migration of HeLa cells. Moreover, our results indicated that p300-mediated lysine crotonylation was able to regulate the expression of HNRNPA1 and in turn affect cell development.

## 2. Materials and Methods

**2.1. Cell Culture.** Human cervical cell lines (HeLa cells, Caski cells, and SiHa cells) and the normal cervical epithelial cell line HCrEPiC were purchased from ATCC (American Type Culture Collection, USA). Cells were maintained in Dulbecco's modified Eagle's medium (DMEM) supplemented with 10% fetal bovine serum (FBS) and 1% of penicillin solution. For sodium crotonate (NaCr, Alfa, B22235) treatment, cells were grown to 40% confluency and 20 mM NaCr was added to the medium [22]. Cells were treated with the same concentration of NaCl in parallel as the control.

**2.2. Cell Transfection.** Stable knockdown of target genes was achieved by siRNA. The siRNA sequences used in this study were as follows: sip300 forward: AGAUACAAGCG AGGAAAACCA; reverse: GUUUUCCUCGCUUGUAUCU CC. siACSS2 forward: UUCUAAAUAUCUAACUCCAA; reverse: GGAGUUAGAUUUUAAGAAUC. siHNRNPA1 was purchased from Santa Cruz Biotechnology (Santa Cruz, CA). Cells were transfected with siRNA using Lipofectamine 3000 (Invitrogen, # L3000-015) for 24h according to the manufacturer's protocol. The knockdown efficiency was measured by western blots. For sodium crotonate treatment, transfected cells were grown to 40% confluency and 20 mM NaCr added to medium.

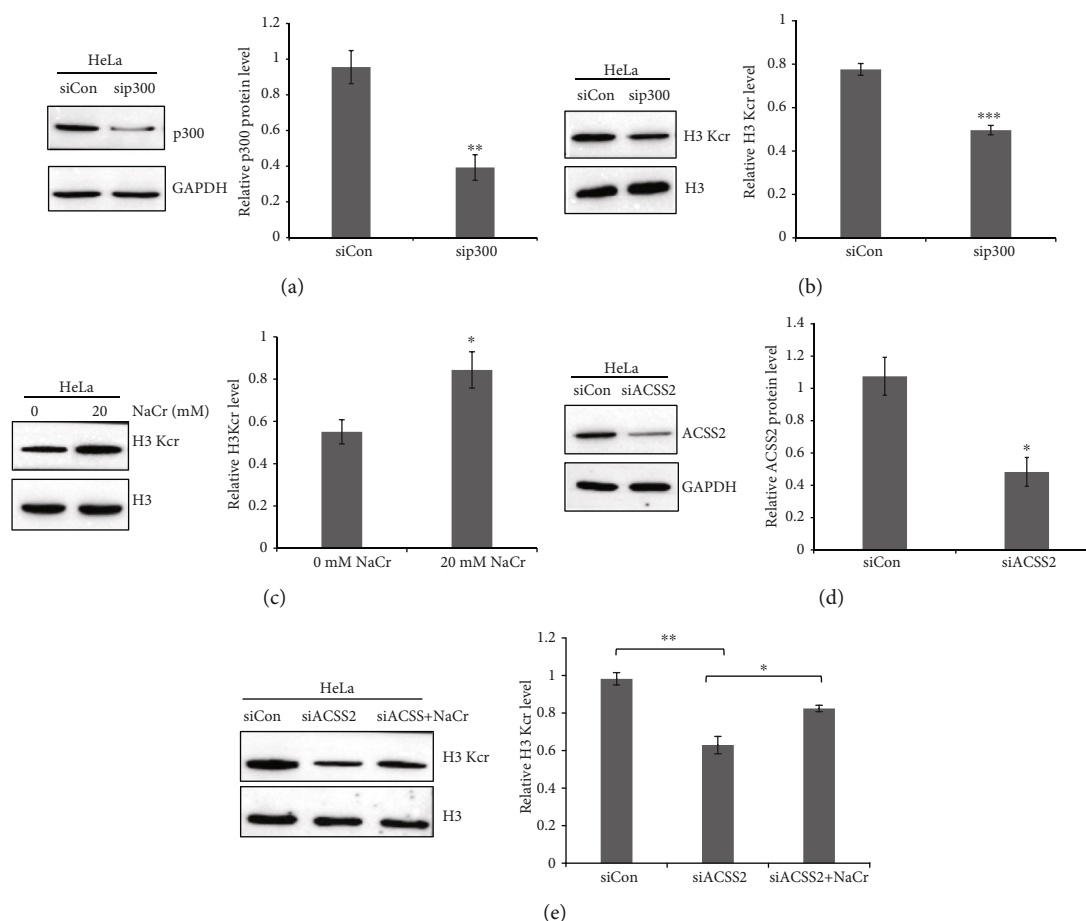


FIGURE 2: p300-mediated lysine crotonylation in HeLa cells. (a) p300 expression was measured by western blot in HeLa cells stably expressing nontargeting control (siCon) and sip300. The relative intensities of p300/GAPDH were quantified using ImageJ.  $^{**}P < 0.01$ . (b) H3 Kcr expression was measured by western blot in HeLa cells stably expressing nontargeting control (siCon) and sip300. The relative intensities of H3 Kcr/H3 were quantified using ImageJ.  $^{***}P < 0.001$ . (c) Effect of NaCr on H3 Kcr expression was determined by western blot. The relative intensities of H3 Kcr/H3 were quantified using ImageJ.  $^{*}P < 0.05$ . (d) ACSS2 expression was measured by western blot in HeLa cells stably expressing nontargeting control (siCon) and siACSS2. The relative intensities of ACSS2/GAPDH were quantified using ImageJ.  $^{**}P < 0.01$ . (e) H3 Kcr expression was determined by western blot in HeLa cell-treated siACSS2 or/and NaCr. The relative intensities of H3 Kcr/H3 were quantified using ImageJ.  $^{*}P < 0.05$ ;  $^{**}P < 0.01$ .

**2.3. Western Blots.** Western blot analysis for a specific protein expression was performed. The protein was separated by sodium dodecyl sulfonate polyacrylamide gel electrophoresis (SDS-PAGE). The protein was transferred to a PVDF membrane by the wet transfer. After being blocked 1 hour in room temperature, the membrane was incubated by primary antibodies incorporating anti-histone H3 (ABclonal, A2348, 1:5000), anti-GAPDH (ABclonal, A19056, 1:5000), anti-panKcr (PTM-501, 1:1000), anti-p300 (Abcam, ab59240, 1:2000), anti-ACSS2 (Abcam, ab234689, 1:2000), and anti-HNRNPA1 (Abcam, ab4791, 1:1000) at room temperature for 2 hours and then incubated with HRP-conjugated anti-rabbit (Abcam, 205717, 1:5000) and anti-mouse (Abcam, 205718, 1:5000) at room temperature for 1 hour.

**2.4. Cell Counting Kit (CCK-8) Assay.** CCK-8 kit (Solarbio, # CA1210) was used to determine the cell proliferation. HeLa cells (5,000 cells/well) with or without HNRNPA1 knock-down and NaCr treatment were cultured. CCK-8 solution was added, and cell numbers were then counted at 0, 24,

48, 72, and 96 h. Then, the optical density at 450 nm was measured by a microtiter plate reader.

**2.5. Cell Migration and Invasion Assay.** The cell migration and invasion assays were performed with Transwell chambers (Corning). For the migration assay, HeLa cells ( $2 \times 10^4$  in each well) with or without treatments were seeded in the upper Transwell chambers, and the lower chamber was filled with a medium containing 10% FBS. For the invasion assay, the upper compartment was precoated with 100  $\mu$ l of Matrigel. After 24 h incubation, the cells in the upper surface were removed. Cells in the lower chamber were fixed with methanol and stained with Giemsa (Solarbio, # G4640). The invasion and migration of HeLa cells were quantified using the Image-Pro Plus 6.0.

**2.6. Statistical Analysis.** All quantitative data are presented as the mean  $\pm$  SEM, and the differences were analyzed by two-tailed Student's *t* test or one-way ANOVA. One-way



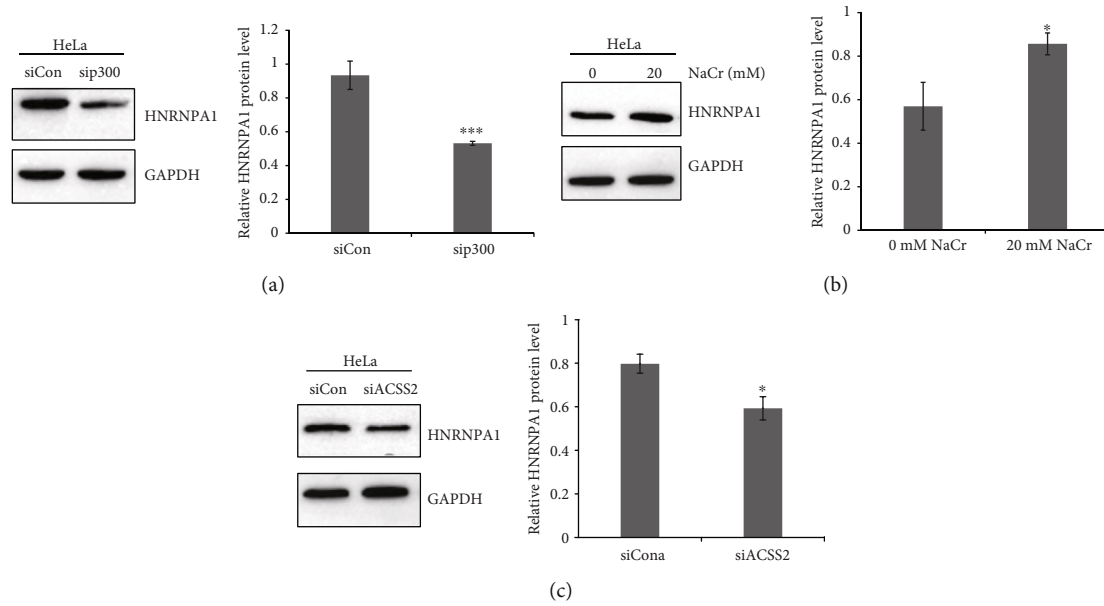


FIGURE 3: p300-mediated lysine crotonylation is responsible for HNRNPA1 expression in HeLa cells. (a) HNRNPA1 expression was measured by western blot in HeLa cells stably expressing nontargeting control (siCon) and sip300. The relative intensities of HNRNPA1/GAPDH were quantified using ImageJ. \*\*\* $P < 0.001$ . (b) HNRNPA1 expression was measured by western blot in NaCr-treated HeLa cells. The relative intensities of HNRNPA1/GAPDH were quantified using ImageJ. \* $P < 0.05$ . (c) HNRNPA1 expression was measured by western blot in HeLa cells stably expressing nontargeting control (siCon) and siACSS2. The relative intensities of HNRNPA1/GAPDH were quantified using ImageJ. \* $P < 0.05$ .

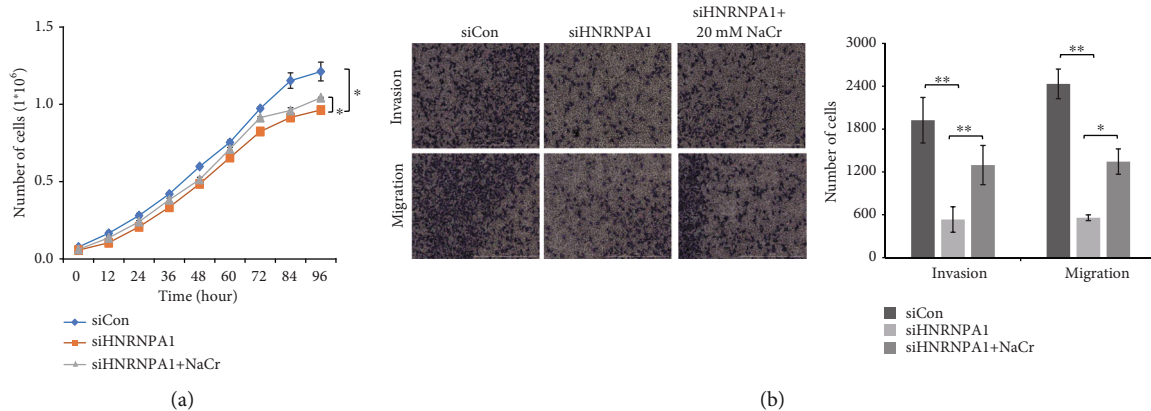


FIGURE 4: p300-mediated lysine crotonylation is involved in the regulation of HNRNPA1 on proliferation, invasion, and migration of HeLa cells. (a) Effects of HNRNPA1 or/and NaCr on HeLa cell proliferation were determined by CCK-8 kit. \* $P < 0.05$ . (b) Transwell assay was performed to determine the invasion and migration of HeLa cells treated with siHNRNPA1 or/and NaCr. The invasion and migration of HeLa cells were quantified using Image-Pro Plus 6.0. \* $P < 0.05$ ; \*\* $P < 0.01$ ; \*\*\* $P < 0.001$ .

ANOVA with the Tukey post hoc test was used to analyze the differences among the different groups. Student's  $t$  test was used for comparisons between two groups. Significance was accepted at  $P < 0.05$ .

### 3. Results and Discussion

**3.1. Knockdown of HNRNPA1 Attenuated the Proliferation, Invasion, and Migration of HeLa Cells.** To identify the HNRNPA1 level in HPV-associated cervical cancer cells, we performed western blot assays to detect the protein level of HNRNPA1 in HeLa cells, Caski cells, SiHa cells, and HCrEPiC cells. As shown in Figure 1(a), the elevated level of HNRNPA1

could be observed in HPV-associated cervical cancer cells, particularly in HeLa cells. In order to determine the role of HNRNPA1 in HeLa cell development, HeLa cells expressing siRNA targeting HNRNPA1 were used (Figure 1(b)). As shown in Figure 1(c), inhibition of HNRNPA1 attenuated HeLa cell proliferation. In addition, HNRNPA1 silencing suppressed invasion and migration of HeLa cells (Figure 1(d)). Thus, our studies indicated that HNRNPA1 was involved in HeLa cell progression.

**3.2. p300-Mediated Lysine Crotonylation in HeLa Cells.** In order to determine whether p300 is responsible for Kcr in HeLa cells as reported, HeLa cells expressing siRNA targeting

p300 were used. The knockdown efficiency of p300 was validated by western blot (Figure 2(a)). And p300 deficiency reduced the Kcr level in HeLa cells (Figure 2(b)). Based on the former result, p300-mediated Kcr could be induced by additional crotonyl-CoA, which was generated from NaCr [20]. When HeLa cells were treated with different concentrations of NaCr, the increased level of Kcr could be observed (Figure 2(c)). Oppositely, knockdown acyl-CoA synthetase (ACSS2), which was known to produce acetyl-CoA, resulted in reduced Kcr level (Figures 2(d) and 2(e)). And NaCr administration in ACSS2-deficient HeLa cells could rescue the Kcr level (Figure 2(e)).

**3.3. p300 and Lysine Crotonylation Is Responsible for HNRNPA1 Expression in HeLa Cells.** Accumulating evidence indicated the effect of Kcr on gene transcription [23, 24]. It has been demonstrated that HNRNPA1 was a p300-regulated lysine crotonylation protein [21]. In order to validate whether the expression of HNRNPA1 could be affected by Kcr, we performed a western blot assay to detect the HNRNPA1 protein level under p300 knockdown. The expression level of HNRNPA1 was significantly decreased in HeLa cell transfected sip300 (Figure 3(a)). In addition, the expression level of HNRNPA1 could be upregulated by NaCr treatment (Figure 3(b)). And inhibition of ACSS2 led to decreased HNRNPA1 expression level (Figure 3(c)). In a word, our studies suggested that p300-catalyzed Kcr was involved in regulation of HNRNPA1 expression.

**3.4. p300-Mediated Lysine Crotonylation Is Involved in the Regulation of HNRNPA1 on Proliferation, Invasion, and Migration of HeLa Cells.** In order to determine the role of p300-catalyzed Kcr on the regulation of HNRNPA1 on HeLa cell progression, NaCr was used to treat HeLa cells with siHNRNPA1. As shown in Figure 4(a), NaCr administration rescued the inhibitory effect of HNRNPA1 knockdown on cell proliferation. Moreover, NaCr treatment also recovered the invasion and migratory abilities of HeLa cells with siHNRNPA1 (Figures 4(b) and 4(c)).

## 4. Conclusions

In the present work, we have demonstrated the function of HNRNPA1 in HPV-associated cervical cancer. The expression of HNRNPA1 was responsible for the development of HeLa cells. Knockdown of HNRNPA1 attenuated cell proliferation, invasion, and migration. We then detect the effect of p300 and p300-mediated Kcr on HNRNPA1 and HeLa cell development. Inhibition of p300 dampened the Kcr level and HNRNPA1 expression. However, as we can see from Figure 2(b), knockdown of p300 could not completely abolish the histone H3 Kcr level, which indicated that the involvement of CBP on Kcr. NaCr administration was able to induce Kcr and promote HNRNPA1 expression. On the contrary, the inhibition of crotonyl-CoA provider ACSS2 led to Kcr and HNRNPA1 reduction. Thus, our results indicated that p300-mediated Kcr was involved in HNRNPA1 expression. In order to identify the role of p300-mediated Kcr in HNRNPA1-regulated HeLa cell development, we performed

proliferation assay and migration assay under NaCr administration. NaCr treatment attenuated the inhibitory effect of HNRNPA1 knockdown in HeLa cell proliferation, invasion, and migration.

Taken together, our investigation demonstrated that HNRNPA1 enhanced cell proliferation, invasion, and migration of HeLa cells through p300-mediated lysine crotonylation.

## Data Availability

No data were used to support this study.

## Conflicts of Interest

The authors declare that they have no competing interests.

## Acknowledgments

The present study was funded by the Joint Project of the Yunnan Provincial Science and Technology Department—Kunming Medical University (grant no. 2017FE467-075).

## References

- [1] L. Shen, J. M. O'Shea, M. R. Kaadige et al., "Metabolic reprogramming in triple-negative breast cancer through Myc suppression of TXNIP," *Proceedings of the National Academy of Sciences of the United States of America*, vol. 112, pp. 5425–5430, 2015.
- [2] M. Ngoma and P. Autier, "Cancer prevention: cervical cancer," *ecancermedicalscience*, vol. 13, p. 952, 2019.
- [3] M. Fujiya, H. Konishi, M. K. M. Kamel et al., "MicroRNA-18a induces apoptosis in colon cancer cells via the autophagolysosomal degradation of oncogenic heterogeneous nuclear ribonucleoprotein A1," *Oncogene*, vol. 33, pp. 4847–4856, 2014.
- [4] C. Yu, J. Guo, Y. Liu, J. Jia, R. Jia, and M. Fan, "Oral squamous cancer cell exploits hnRNP A1 to regulate cell cycle and proliferation," *Journal of Cellular Physiology*, vol. 230, pp. 2252–2261, 2015.
- [5] T. J. Loh, H. Moon, S. Cho et al., "CD44 alternative splicing and hnRNP A1 expression are associated with the metastasis of breast cancer," *Oncology Reports*, vol. 34, pp. 1231–1238, 2015.
- [6] S. Li, W. Wang, H. Ding et al., "Aptamer BC15 against heterogeneous nuclear ribonucleoprotein A1 has potential value in diagnosis and therapy of hepatocarcinoma," *Nucleic Acid Therapeutics*, vol. 22, pp. 391–398, 2012.
- [7] Y. Xia, W. Yang, M. Fa et al., "RNF8 mediates histone H3 ubiquitylation and promotes glycolysis and tumorigenesis," *Journal of Experimental Medicine*, vol. 214, pp. 1843–1855, 2017.
- [8] H. Aihara, T. Nakagawa, H. Mizusaki et al., "genic transformation via upregulation of cyclin D1," *Molecular Cell*, vol. 64, pp. 176–188, 2016.
- [9] L. M. Katz, T. Hielscher, B. Liechty et al., "Loss of histone H3K27me3 identifies a subset of meningiomas with increased risk of recurrence," *Acta Neuropathologica*, vol. 135, pp. 955–963, 2018.
- [10] Q. Q. Li, J.-J. Hao, Z. Zhang et al., "Proteomic analysis of proteome and histone post-translational modifications in heat shock protein 90 inhibition-mediated bladder cancer therapeutics," *Scientific Reports*, vol. 7, article 201, 2017.

- [11] S. Zhao, X. Zhang, and H. Li, "Beyond histone acetylation—writing and erasing histone acylations," *Current Opinion in Structural Biology*, vol. 53, pp. 169–177, 2018.
- [12] L. Kollenstart, A. J. L. de Groot, G. M. C. Janssen et al., "Gcn5 and Esa1 function as histone crotonyltransferases to regulate crotonylation-dependent transcription," *Journal of Biological Chemistry*, vol. 294, pp. 20122–20134, 2019.
- [13] G. J. Gowans, J. B. Bridgers, J. Zhang et al., "Recognition of histone crotonylation by Taf14 links metabolic state to gene expression," *Molecular cell*, vol. 76, pp. 909–921.e3, 2019.
- [14] R. Wang, M. Xin, Y. Li, P. Zhang, and M. Zhang, "The functions of histone modification enzymes in cancer," *Current Protein & Peptide Science*, vol. 17, pp. 438–445, 2016.
- [15] X. Hou, R. Gong, J. Zhan et al., "p300 promotes proliferation, migration, and invasion via inducing epithelial-mesenchymal transition in non-small cell lung cancer cells," *BMC Cancer*, vol. 18, p. 641, 2018.
- [16] M. E. Rieger, B. Zhou, N. Solomon et al., "p300/ $\beta$ -catenin interactions regulate adult progenitor cell differentiation downstream of WNT5a/protein kinase C (PKC)," *Journal of Biological Chemistry*, vol. 291, pp. 6569–6582, 2016.
- [17] Z. Chen, W. Li, F. Qiu et al., "Aspirin cooperates with p300 to activate the acetylation of H3K9 and promote FasL-mediated apoptosis of cancer stem-like cells in colorectal cancer," *Theranostics*, vol. 8, pp. 4447–4461, 2018.
- [18] S. Qian, Y. Han, Y. Shi et al., "Benzene induces haematotoxicity by promoting deacetylation and autophagy," *Journal of Cellular and Molecular Medicine*, vol. 23, pp. 1022–1033, 2019.
- [19] X. Liu, L. Wang, K. Zhao et al., "The structural basis of protein acetylation by the p300/CBP transcriptional coactivator," *Nature*, vol. 451, pp. 846–850, 2008.
- [20] B. R. Sabari, Z. Tang, H. Huang et al., "Intracellular crotonyl-CoA stimulates transcription through p300-catalyzed histone crotonylation," *Molecular Cell*, vol. 58, pp. 203–215, 2015.
- [21] H. Huang, D.-L. Wang, and Y. Zhao, "Quantitative crotonylome analysis expands the roles of p300 in the regulation of lysine crotonylation pathway," *Proteomics*, vol. 18, article e1700230, 2018.
- [22] W. Wei, A. Mao, B. Tang et al., "Large-scale identification of protein crotonylation reveals its role in multiple cellular functions," *Journal of Proteome Research*, vol. 16, pp. 1743–1752, 2017.
- [23] S. Liu, C. Xue, Y. Fang et al., "Global involvement of lysine crotonylation in protein modification and transcription regulation in rice," *Molecular & Cellular Proteomics*, vol. 17, pp. 1922–1936, 2018.
- [24] B. R. Sabari, Z. Tang, H. Huang et al., "Intracellular crotonyl-CoA stimulates transcription through p300-catalyzed histone crotonylation," *Molecular Cell*, vol. 69, p. 533, 2018.

## Research Article

# FKBP4 Accelerates Malignant Progression of Non-Small-Cell Lung Cancer by Activating the Akt/mTOR Signaling Pathway

Wen Meng <sup>1</sup>, Jingfei Meng,<sup>2</sup> Hong Jiang,<sup>1</sup> Xing Feng,<sup>1</sup> Dongshan Wei,<sup>1</sup> and Qingsong Ding<sup>1</sup>

<sup>1</sup>Department of cardiothoracic surgery, Affiliated Hangzhou First People's Hospital, Zhejiang University School of Medicine, Hangzhou, Zhejiang 310006, China

<sup>2</sup>The Second Affiliated Hospital of Xi'an Jiaotong University, Xi'an, Shaanxi 710061, China

Correspondence should be addressed to Wen Meng; mengwentaian@163.com

Received 31 July 2020; Revised 17 November 2020; Accepted 23 November 2020; Published 7 December 2020

Academic Editor: Victor H. Villar

Copyright © 2020 Wen Meng et al. This is an open access article distributed under the Creative Commons Attribution License, which permits unrestricted use, distribution, and reproduction in any medium, provided the original work is properly cited.

**Objective.** To study the expression, biological function, and mechanism of FKBP4 in non-small-cell lung cancer (NSCLC). **Methods.** First of all, the expression of FKBP4 in NSCLC tissues and cell lines was detected by qRT-PCR; then, the effects of FKBP4 on proliferation, apoptosis, migration, and invasion of NSCLC were studied by CCK-8 assays, flow cytometry assays, wound-healing assays, and Transwell assays. After that, tumor xenografts were used to explore the effect of FKBP4 on NSCLC tumor growth in vivo, and the phosphorylation of Akt and mTOR was measured by western blot. **Results.** FKBP4 was highly expressed in NSCLC tissues and cells, and its expression was closely related to NSCLC tumor size, lymph node metastasis, and patient prognosis. In vitro, FKBP4 can promote NSCLC cell proliferation, migration, and invasion and inhibit NSCLC cell apoptosis. In vivo, FKBP4 can promote NSCLC tumor growth. Furthermore, FKBP4 can promote Akt and mTOR phosphorylation and activate the Akt/mTOR signaling pathway and an mTOR inhibitor can neutralize the functions of FKBP4 in NSCLC cells. **Conclusion.** FKBP4 serves as an oncogene to promote malignant processes in NSCLC, and it has the potential to be used as a biological marker and therapeutic target for NSCLC.

## 1. Introduction

Lung cancer is the most common cause of cancer-related deaths worldwide [1, 2]. Non-small-cell lung cancer (NSCLC) accounts for about 85% of lung cancer cases and is mainly divided into several common subtypes: squamous cell carcinoma, adenocarcinoma, and large cell carcinoma [3]. Although great progress has been made in chemotherapy and molecular targeted therapy for NSCLC, the 5-year survival rate of the disease is still lower than 15%, due to limited treatment options and tumor metastasis and recurrence. There is no doubt that a better understanding of the pathogenesis of NSCLC is essential to improve the diagnosis and prognosis of patients with non-small-cell lung cancer. In the occurrence and development of NSCLC, a variety of oncogenes and tumor suppressor genes are abnormally expressed, and they have been involved in the malignant process of tumor cells. Moreover, in recent years,

many research and studies focused on oncogenes and tumor suppressor genes have been reported.

FKBP4, also known as FKBP52, is a member of the immunophilin family, which plays a role in immune regulation, protein folding, and transportation. The encoded protein of FKBP4 is a cis-trans-proline isomerase, which can interact with immunosuppressant FK506 and rapamycin [4]. Studies have shown that FKBP4 has a potential role in tumorigenesis and is considered as a possible biomarker. FKBP4 is expressed in most tissues, with the lowest expression in the breast, bladder, and testis [5, 6]. The expression of FKBP4 was elevated in several cell lines of hormone-dependent cancers, including breast cancer cell lines [7, 8] and prostate cancer cell lines [9]. Moreover, the expression of FKBP4 in breast cancer tissues and preinfiltration breast cancers was higher than that in normal breast tissues [8, 10]. Similar observations have also been made in prostate biopsy tissues [11] and liver cancer tissues [12], which

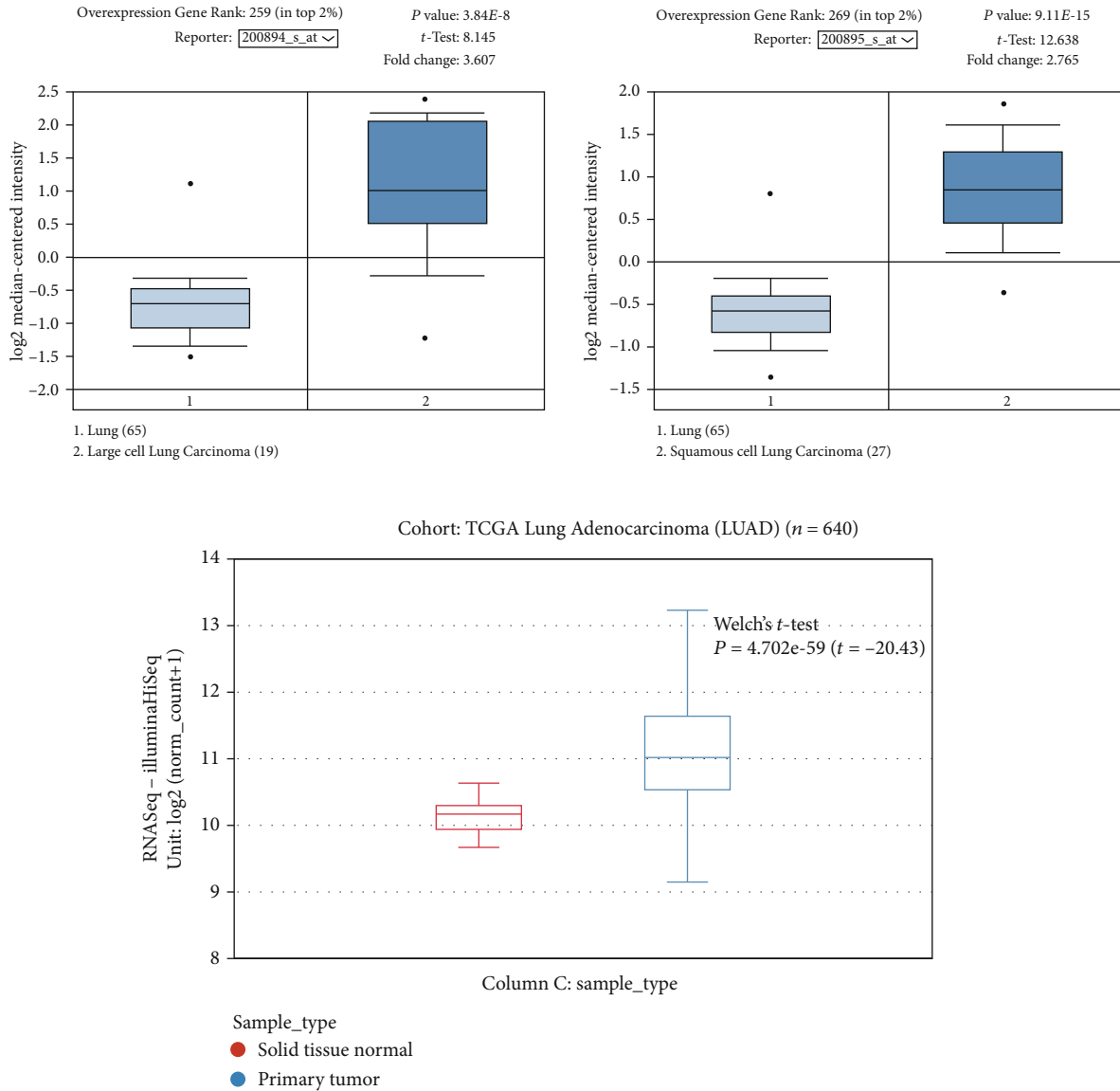


FIGURE 1: Bioinformatics analysis of FKBP4 expression in NSCLC: (a) expression analysis of FKBP4 in large cell lung cancer; (b) expression analysis of the FKBP4 gene in squamous cell lung cancer; (c) expression analysis of FKBP4 lung adenocarcinoma ( $N = 640$ , Welch's  $t$ -test,  $P = 4.702e - 59$ ).

indicates that FKBP4 might be a potential biomarker for tumors. Recent studies illustrated that the expression of FKBP4 is related to breast cancer progression and prognosis. It was illustrated that FKBP4 can promote the growth of triple-negative breast cancer cell models and xenograft tumor models [13]. It also reported that the amplification and overexpression of FKBP4 are potential mechanisms for castration resistance to prostate cancer development, and the interaction of FKBP4 with androgen receptors may provide potential therapeutic targets in prostate cancer [14]. Therefore, FKBP4 may act as an oncogene in tumors and promote the malignant progression of tumors.

In this study, first, it was found that FKBP4 expression was significantly upregulated in NSCLC through bioinformatics analysis, then verified by qRT-PCR in NSCLC tissues and cell lines, and finally, the clinical relevance of FKBP4

expression was analyzed. Subsequently, the function of FKBP4 in NSCLC cell lines and animals were investigated, and the relevant mechanisms of FKBP4 affecting tumor progression were also explored.

## 2. Material and Methods

**2.1. Clinical Samples and Ethics.** Primary NSCLC tissues and adjacent normal tissues were obtained from NSCLC patients who underwent surgical resection in our hospital. All patients did not receive radiation or chemotherapy before surgery. All tumor and adjacent normal lung tissue specimens were frozen immediately after resection and stored in liquid nitrogen until total RNA was extracted. All tumors and matched normal tissues were confirmed by pathology. The clinical characteristics of each patient were also collected, and written informed



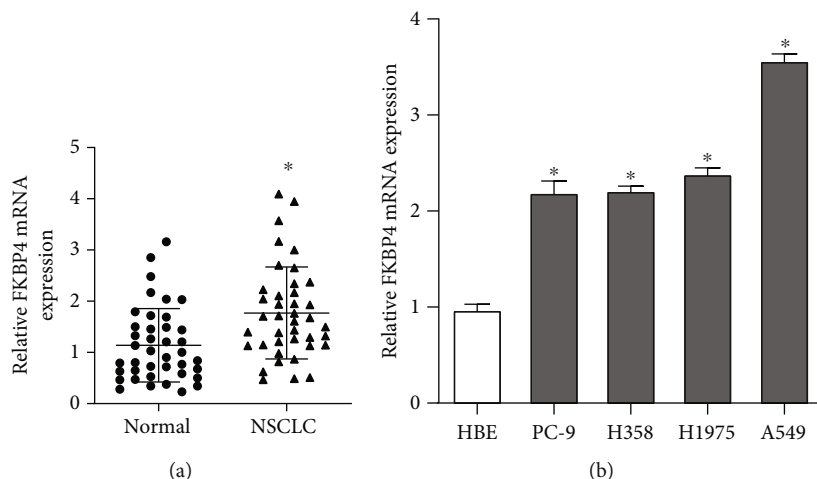


FIGURE 2: FKBP4 expression in NSCLC tissues and cells: (a) FKBP4 expression in NSCLC tissues,  $N = 40$ ; (b) FKBP4 expression in NSCLC tissues; data were compared using ANOVA followed by the Dunnett  $t$ -test,  $N = 3$ ; \* $P < 0.05$  vs. normal or HBE.

TABLE 1: Correlation between clinicopathological factors and FKBP4 expression in patients with NSCLC.

Factors	Number of patients	Upregulated FKBP4	Downregulated FKBP4	$P$ value
Gender				
Male	26	12	14	0.507
Female	14	8	6	
Age				
<65	23	12	11	0.749
$\geq 65$	17	8	9	
Tumor size				
<3 cm	21	6	15	0.004
$\geq 3$ cm	19	14	5	
Lymph node metastasis				
N0	25	9	16	0.022
N1-3	15	11	4	
Grading				
Low	24	11	13	0.519
Medium/advanced	16	9	7	
TNM staging				
I-II	27	11	16	0.091
III-IV	13	9	4	
Smoking history				
No	11	6	5	0.723
Yes	29	14	15	

The chi-square test was used for statistical analysis.

consent was obtained from all patients participating in the study. This study was approved by our ethics committee.

2.2. *Bioinformatics Analysis.* The Oncomine database (<https://www.Oncomine.org/>) was used to analyze the differential

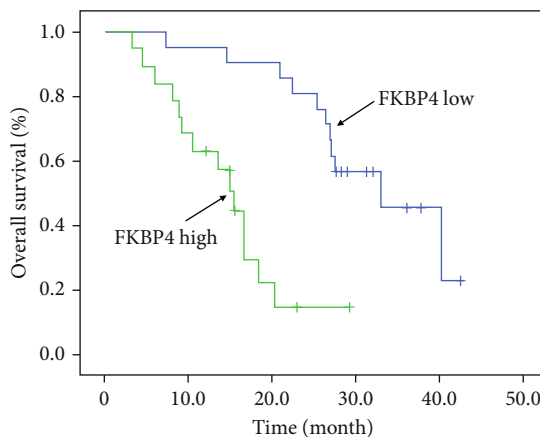


FIGURE 3: Survival analysis of patients with high and low FKBP4 expression groups; log-rank test,  $N = 40$ ,  $P < 0.001$ .

expression of the FKBP4 gene in large cell lung cancer, squamous cell lung cancer, and normal tissues. The Cancer Genome Atlas (TCGA) Lung Cancer (LUNG) database (<http://cancer.genome.nih.gov/>) was used to investigate the differential expression of the FKBP4 gene between lung adenocarcinoma and normal tissues. The significantly differentially expressed genes were determined if the fold change between tumor samples and normal samples is greater than 2 and  $P < 0.05$ .

2.3. *Cell Culture.* All NSCLC cell lines (A549, H1975, H358, and PC-9) and human bronchial epithelial cells (HBE) were purchased from ATCC. The cells were cultured in DMEM (Invitrogen); 10% fetal bovine serum (Invitrogen), 100 U/ml penicillin, and 100 mg/ml streptomycin were added. All cell lines were cultured in a humidified cell incubator with 5% carbon dioxide at 37°C.

2.4. *Cell Transfection.* The overexpressed plasmid and shRNA were transfected into the cells with Lipofectamine 3000 reagent (Invitrogen), and further experiment was

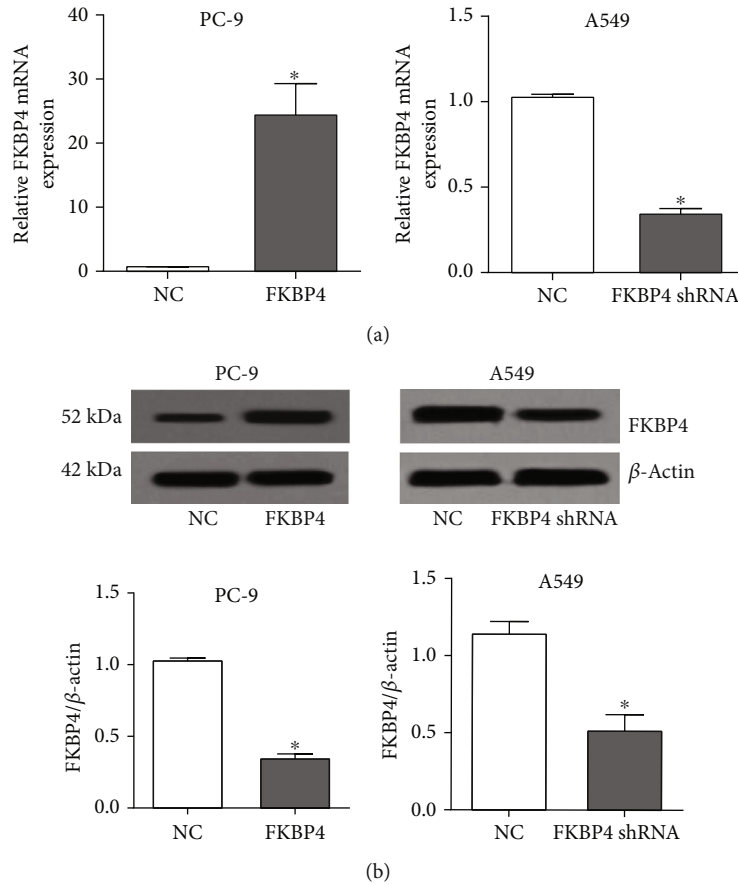


FIGURE 4: FKBP4 overexpression and silencing verification: (a) FKBP4 mRNA expression changes detected by qRT-PCR; (b) FKBP4 protein expression changes detected by western blot;  $N = 3$ ,  $*P < 0.05$ .

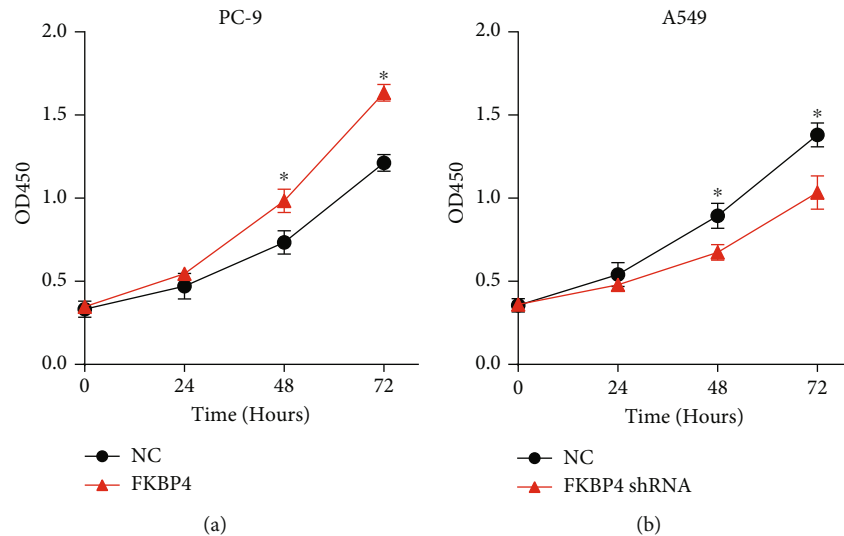


FIGURE 5: FKBP4 promotes the proliferation of NSCLC cells: cell proliferation after FKBP4 was overexpressed in PC-9 cells (a) or FKBP4 was silenced in A549 cells (b);  $N = 3$ ,  $*P < 0.05$ .

performed after an appropriate period. FKBP4 shRNA was purchased from Santa Cruz Biotechnology; FKBP4 cDNA was amplified and inserted into the pCMV4 expression vector to obtain the overexpressed plasmid.

**2.5. CCK8 Experiment.** The CCK8 experiment was used to assess cell proliferation capacity. Cells were seeded in 96-well plates and cultured for 24 hours; plasmid or shRNA was transfected the next day. After 24, 48, and 72 hours

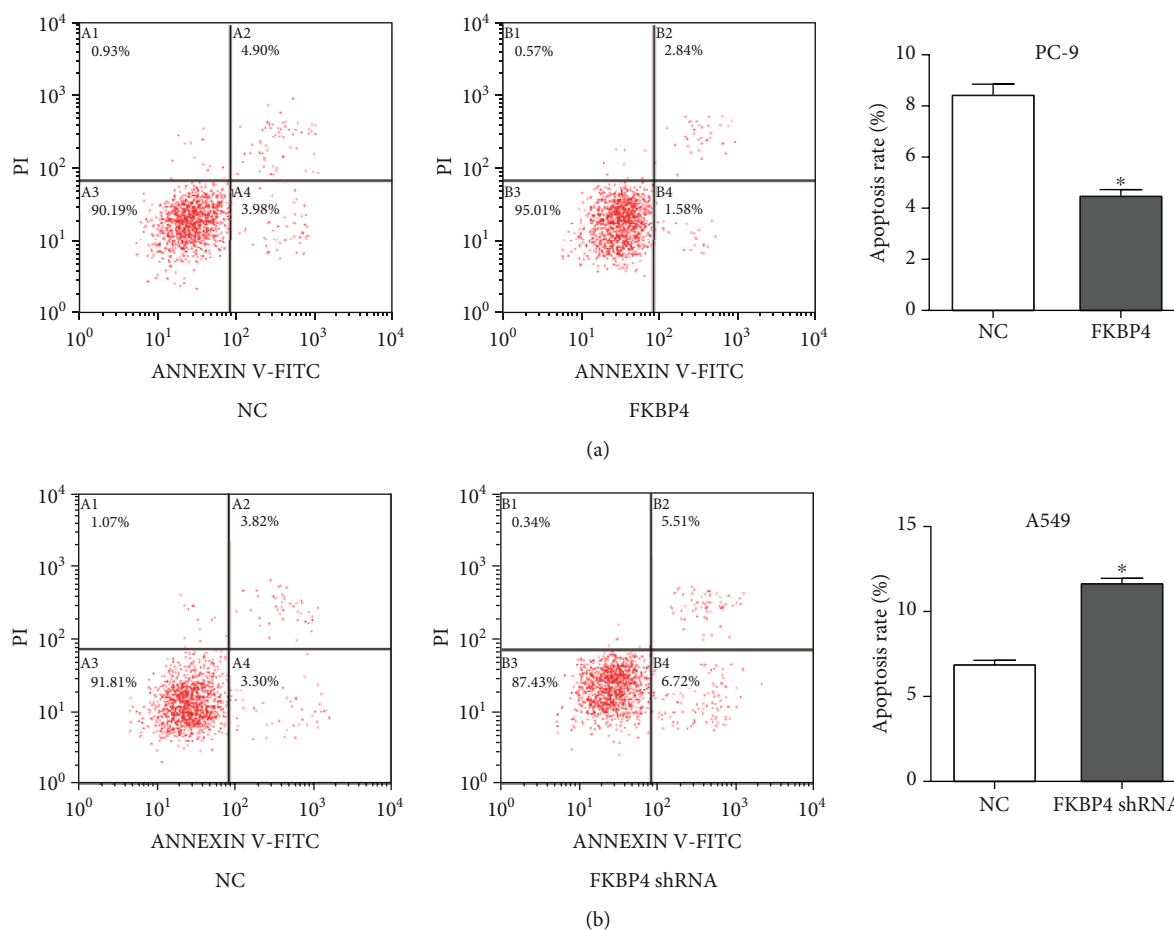


FIGURE 6: FKBP4 inhibits apoptosis of NSCLC cells: apoptosis of cells after overexpression of FKBP4 (a) in PC-9 cells and silencing of FKBP4 (b) in A549 cells;  $N = 3$ ,  $*P < 0.05$ .

of cell culture, the cell proliferation ability was measured using the CCK8 kit (GLP BIO, USA) and a spectrophotometer (450 nm).

**2.6. Flow Cytometry Detection.** Cells were seeded in 96-well plates and cultured for 24 hours; then, plasmid or shRNA was transfected the next day. 48 hours after the cells were transfected, the cells were collected, and cell apoptosis was detected using the Annexin V-FITC Apoptosis Kit (US Bio-Vision) and flow cytometry.

**2.7. Scratch Test.** Scratch tests were used to assess the migration ability of cells. First, cells were seeded in 96-well plates and cultured for 24 hours; then, plasmid or shRNA was transfected the next day. 48 hours after the cells were transfected, a straight scratch was made on the monolayer of cells with the tip of a  $10\ \mu\text{l}$  sterile pipette tip and washed three times with PBS. After the cells were cultured in serum-free DMEM for 24 hours, the migration of the cells was photographed using a microscope, and statistical comparison was performed.

**2.8. Transwell Experiment.** The Transwell assay was used to assess the invasion ability of cells. Cells were seeded in 96-well plates and cultured for 24 hours, and plasmid or shRNA

was transfected the next day. 48 hours after cell transfection, cells were collected and counted. Invasion experiments were performed using a matrix gel-coated Transwell cell. First,  $8 \times 10^4$  cells were seeded with  $100\ \mu\text{l}$  of serum-free DMEM in the upper chamber of the Transwell coated with matrix gel, and the lower chamber was filled with  $500\ \mu\text{l}$  of complete medium containing 10% FBS. After that, the cells were cultured in an incubator for 24 hours. Finally, the cell was fixed with methanol and stained with crystal violet, and the number of cells passing through the membrane was counted.

**2.9. Subcutaneous Tumor Formation in Nude Mice.** The animal experiments in this study were approved by our ethics committee. BALB/c nude mice (male, 5-6 weeks,  $18.0 \pm 0.5$  g) were obtained from Changzhou Cavins Experimental Animal Co., Ltd. First, the lentiviral-infected A549 cells ( $1 \times 10^7$ ) with stably knocked out FKBP4 were injected subcutaneously in nude mice. Then, the tumor volume was measured every 5 days, and statistical analysis was performed. After the experiment, the mice were sacrificed by cervical dislocation.

**2.10. Real-Time Quantitative PCR (qRT-PCR).** Total RNA was extracted from tissues and cells using Trizol reagent (Life

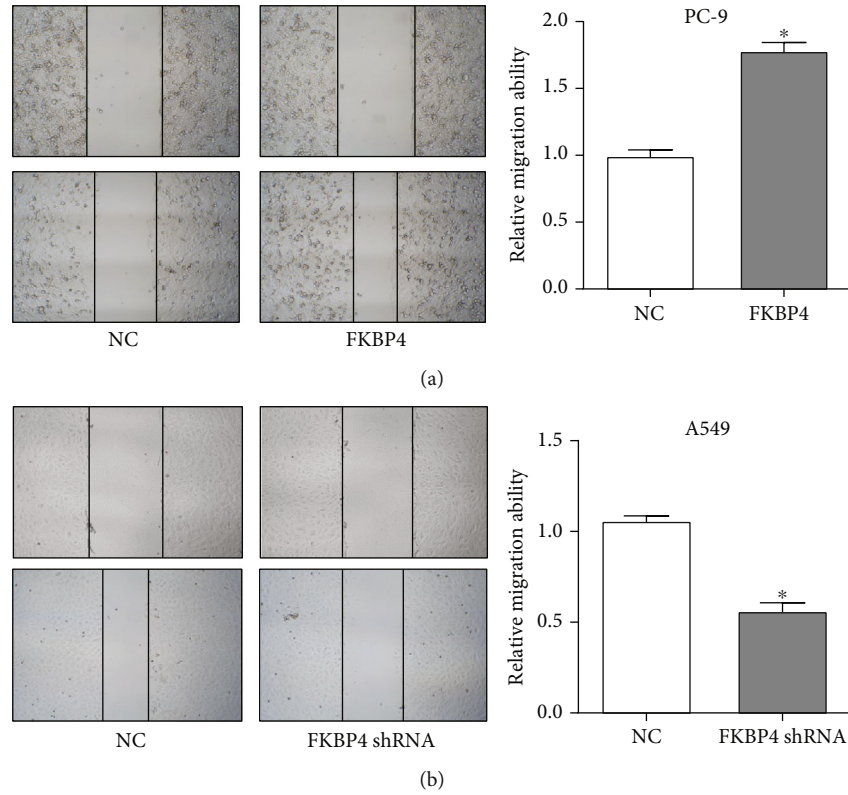


FIGURE 7: FKBP4 promotes NSCLC cell migration: cell migration after overexpression of FKBP4 (a) in PC-9 cells and silencing of FKBP4 (b) in A549 cells;  $N = 3$ ,  $*P < 0.05$ .

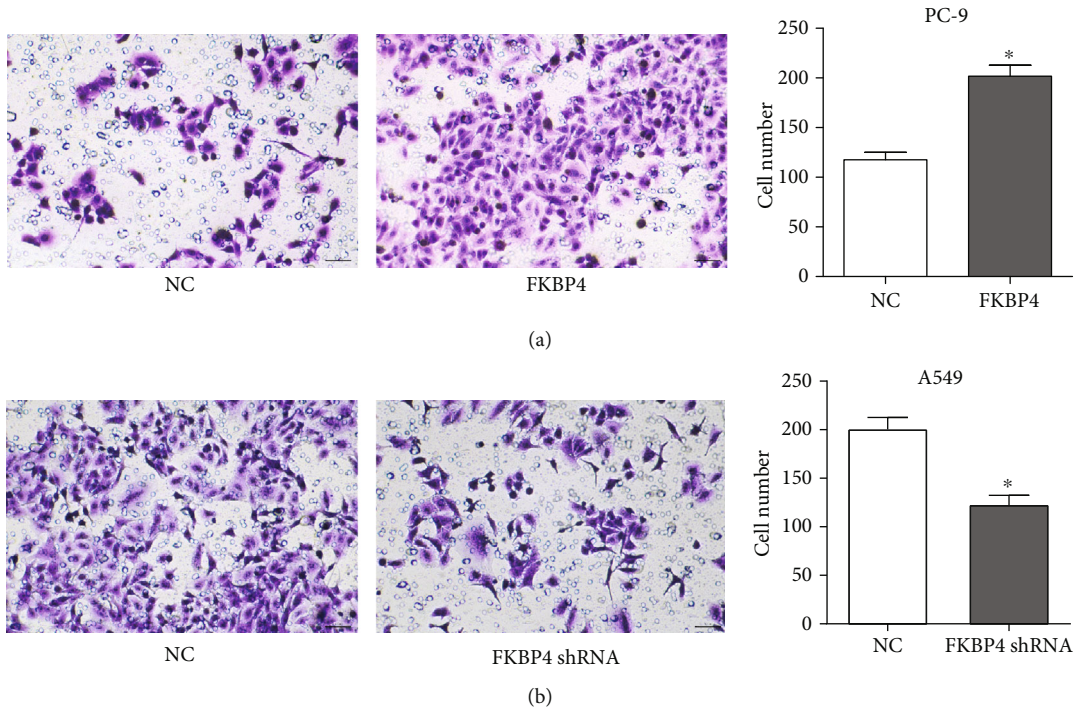


FIGURE 8: FKBP4 promotes NSCLC cell invasion: cell invasion after overexpression of FKBP4 (a) in PC-9 cells and silence of FKBP4 (b) in A549 cells;  $N = 3$ ,  $*P < 0.05$ .

Technologies), and 1.0  $\mu\text{g}$  of total RNA was reverse transcribed into cDNA with a total volume of 20  $\mu\text{l}$  using the PrimeScript RT Master Mix reverse transcription kit (Takara, Japan). Subsequently, PCR reactions were performed using the ABI 7900 system (Applied Biosystems, USA) with the SYBR Select Master Mix kit (Applied Biosystems) and 0.5  $\mu\text{l}$  cDNA.  $\beta$ -Actin was used as an internal reference, and the relative expression of FKBP4 was calculated using the  $2^{-\Delta\Delta\text{Ct}}$  method. The primer sequences are FKBP4-F: GAAGCGGTGCTGAAGGTCAT, FKBP4-R: TGCCATCTAATAGCCAGCCAG Anti-pan-AKT antibody (ab8805, 1:1000, Abcam), anti-AKT (phospho T308) antibody (ab38449, 1:1000, Abcam), anti-AKT1 (phospho S473) antibody (ab81283, 1:5000, Abcam), anti-mTOR antibody (ab32028, 1:1000, Abcam), anti-mTOR (phospho S2448) antibody (ab109268, 1:1000, Abcam), anti-mTOR (phospho S2481) antibody (ab137133, 1:1000, Abcam), anti-S6K1 (phospho S424) antibody (ab131436, 1:1000, Abcam), anti-S6K1 antibody (ab32359, 1:1000, Abcam), anti-eIF4EBP1 (phospho T37) antibody (ab75767, 1:1000, Abcam), anti-eIF4EBP1 antibody (Y329) (ab32024, 1:1000, Abcam), and anti-beta-actin antibody-loading control (ab8226, 1:2000, Abcam).

**2.11. Statistical Analysis.** The results were analyzed using SPSS 19.0 software. Data was expressed as mean  $\pm$  standard deviation. Statistical significance was compared between groups by the *t*-test and one-way analysis of variance. The chi-square test was used for clinical correlation analysis. All experiments were repeated at least three times; the difference is statistically significant when  $P < 0.05$ .

### 3. Results

**3.1. FKBP4 Is Upregulated in NSCLC through Bioinformatics Analysis.** First, the Oncomine database was used to analyze the expression of FKBP4, and it was found that the expression of FKBP4 was upregulated both in large cell lung cancer (Figure 1(a)) and in squamous cell lung cancer (Figure 1(b)) compared with that in normal tissue. At the same time, the FKBP4 expression was also analyzed using TCGA Lung Cancer database and discovered that the expression of the FKBP4 gene was upregulated in lung adenocarcinoma (Figure 1(c)) compared to that in normal tissue. Through these bioinformatics analyses, we believe that FKBP4 is upregulated in NSCLC, and subsequent verification was performed.

**3.2. FKBP4 Is Highly Expressed in NSCLC Tissues and Cells.** 40 pairs of NSCLC tissues and corresponding normal lung tissues were collected, and the expression of FKBP4 mRNA was detected by qRT-PCR. It was found that the expression of FKBP4 in tumor tissues was significantly higher than that in normal lung tissues (Figure 2(a)). Furthermore, it is discovered that the expression of FKBP4 was also higher in NSCLC cell lines than that in human normal bronchial epithelial cells (Figure 2(b)). These results indicate that FKBP4 is upregulated in NSCLC.

**3.3. Clinical Significance of FKBP4 Expression.** Subsequently, the clinical data of 40 corresponding patients were collected, and the correlation between the clinical data and FKBP4

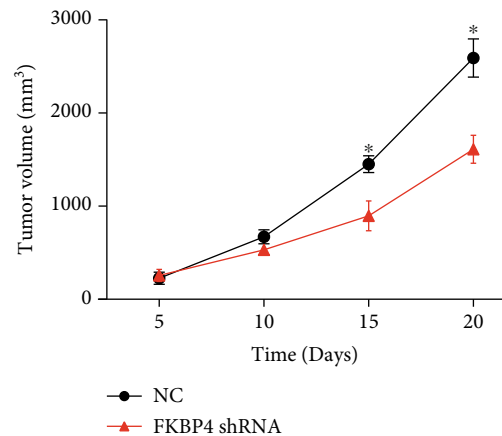


FIGURE 9: FKBP4 promotes NSCLC growth in vivo;  $N = 3$ , \* $P < 0.05$ .

expression was analyzed. As shown in Table 1, FKBP4 expression is closely related to tumor size and lymph node metastasis. Moreover, through survival analysis, it was found that patients with high expression of FKBP4 had significantly shorter overall survival (Figure 3).

**3.4. FKBP4 Overexpression and Silence Verification.** Since among all NSCLC cell lines, the expression of FKBP4 in PC-9 cells is the lowest and the expression of FKBP4 is the highest in A549 cells, we transfected the FKBP4 expression plasmid in PC-9 and FKBP4 shRNA in A549 cells. qRT-PCR experiments and western blot experiments demonstrated the effectiveness of FKBP4 overexpression and silencing (Figures 4(a) and 4(b)).

**3.5. FKBP4 Promotes Proliferation of NSCLC Cells.** After FKBP4 was overexpressed in PC-9 cells, it is found that the cell's proliferative capacity was significantly increased (Figure 5(a)) in the CCK8 experiment. However, after FKBP4 was silenced in A549 cells, the cell's proliferative capacity was significantly reduced (Figure 5(b)). These results indicate that FKBP4 can promote the proliferation of NSCLC cells.

**3.6. FKBP4 Inhibits Apoptosis of NSCLC Cells.** After FKBP4 was overexpressed in PC-9 cells, it is discovered that the apoptosis rate of the cells was significantly reduced in a flow cytometry experiment (Figure 6(a)), and after FKBP4 was silenced in A549 cells, the apoptosis rate was significantly increased (Figure 6(b)). These results indicate that FKBP4 can inhibit the apoptosis of NSCLC cells.

**3.7. FKBP4 Promotes NSCLC Cell Migration.** After FKBP4 was overexpressed in PC-9 cells, it is shown that the cell's ability to migrate was significantly enhanced (Figure 7(a)) in the scratch test; while after FKBP4 was silenced in A549 cells, the cell's ability to migrate was significantly reduced (Figure 7(b)). These results indicate that FKBP4 can promote the migration of NSCLC cells.

**3.8. FKBP4 Promotes NSCLC Cell Invasion.** After FKBP4 was overexpressed in PC-9 cells, the invasion ability of the cells was significantly enhanced (Figure 8(a)); whereas after FKBP4 was silenced in A549 cells, the cells' invasion ability



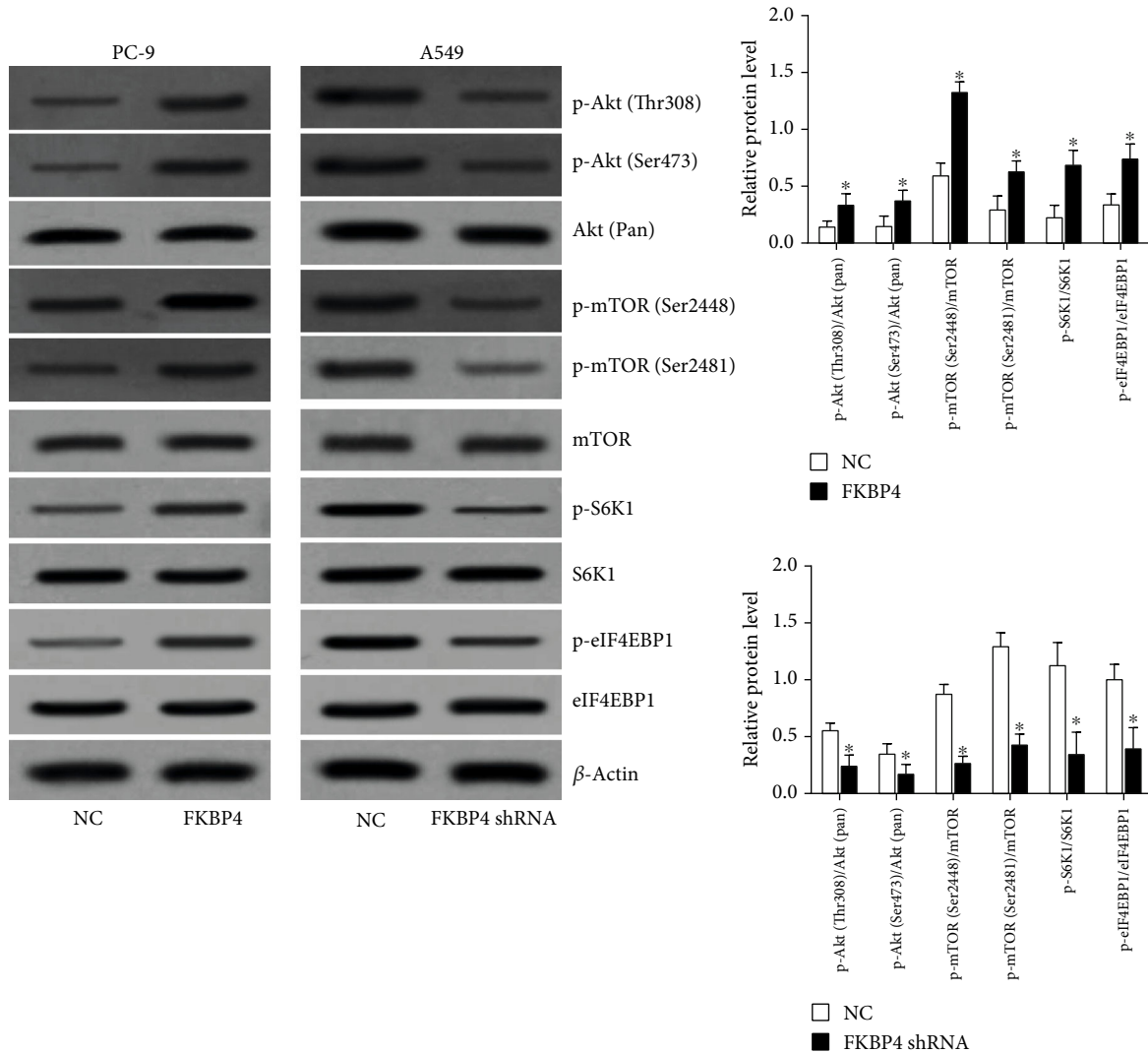


FIGURE 10: FKBP4 activates the Akt/mTOR signaling pathway in NSCLC cells;  $N = 3$ ,  $*P < 0.05$ .

was significantly reduced (Figure 8(b)). These results indicate that FKBP4 can promote the invasion of NSCLC cells.

**3.9. FKBP4 Promotes NSCLC Growth In Vivo.** The results of subcutaneous tumor formation experiments in nude mice demonstrated that after silencing the FKBP4 gene, the tumor growth rate was significantly lower than that of the control group (Figure 9), indicating that tumor growth was inhibited. This result shows that FKBP4 promotes NSCLC growth in vivo.

**3.10. FKBP4 Activates the Akt/mTOR Signaling Pathway in NSCLC Cells.** After FKBP4 was overexpressed in PC-9 cells, it is demonstrated that Akt and mTOR phosphorylation levels were significantly increased, while after FKBP4 was silenced in A549 cells, Akt and mTOR phosphorylation levels were significantly reduced (Figure 10). Moreover, the phosphorylation levels of mTOR downstream proteins including S6K1 and eIF4EBP1 were significantly raised by FKBP4 overexpression and reduced by FKBP4 silencing (Figure 10).

These results indicate that FKBP4 activates the Akt/mTOR signaling pathway in NSCLC cells.

**3.11. mTOR Inhibitor Neutralizes the Functions of FKBP4 in NSCLC Cells.** The PC-9 cells transfected with FKBP4 overexpression plasmids were treated with mTOR inhibitor rapamycin (200 nmol/l). It was observed that mTOR inhibitor neutralizes the effects of FKBP4 in promoting proliferation (Figure 11(a)), inhibiting apoptosis (Figure 11(b)), enhancing migration (Figure 11(c)), and invasion of PC-9 cells (Figure 11(d)). These results indicate that the mTOR inhibitor neutralized the functions of FKBP4 in NSCLC cells.

## 4. Discussion

With the continuous improvement of tumor-related databases and the development of bioinformatics analysis technology, more and more oncogenes and tumor suppressor genes are abnormally expressed in a variety of malignant tumors and have been confirmed as biological markers and

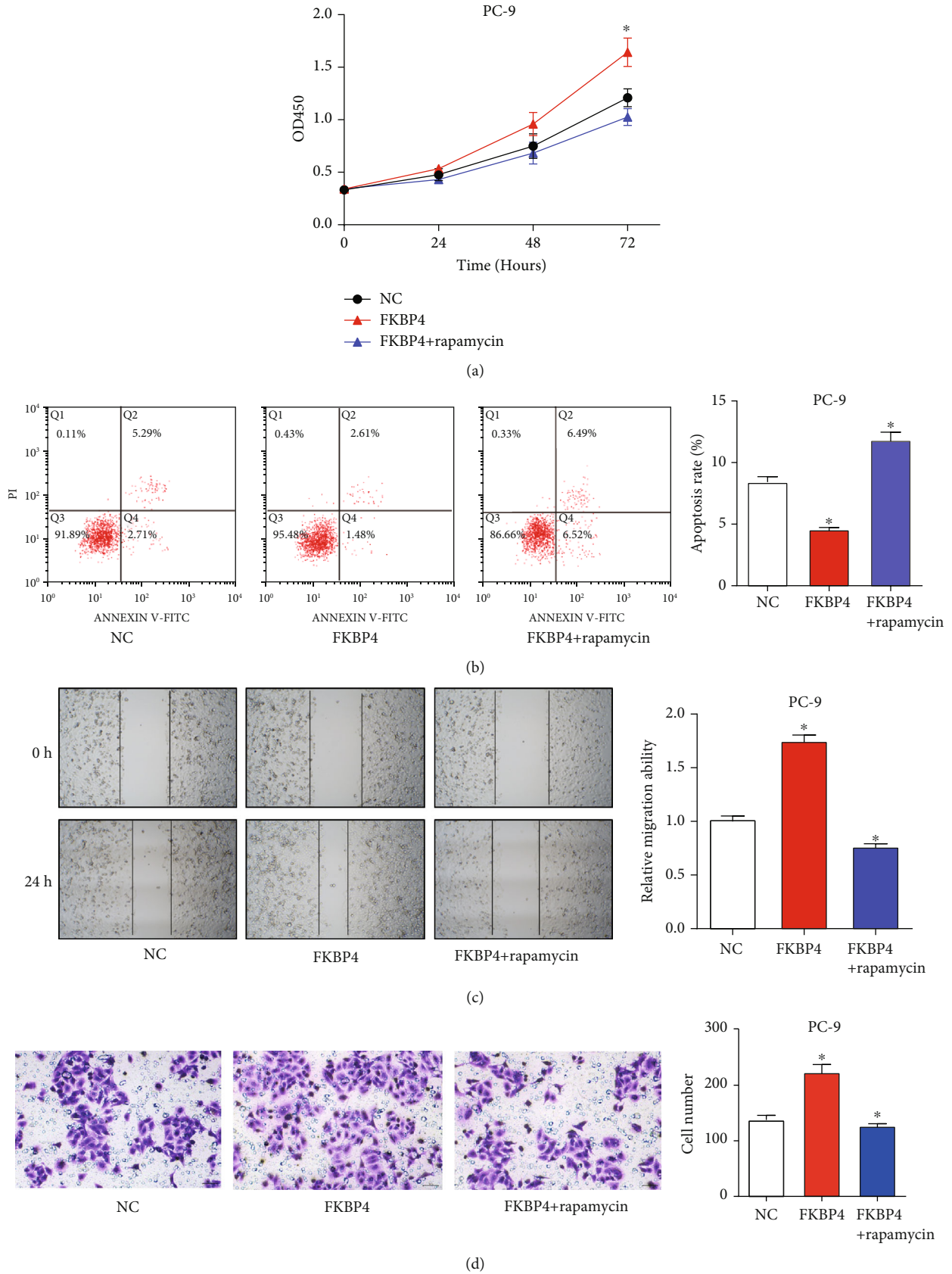


FIGURE 11: mTOR inhibitor neutralizes the functions of FKBP4 in NSCLC cells. The PC-9 cells transfected with FKBP4 overexpression plasmids were treated with mTOR inhibitor rapamycin (200 nmol/l). Cell proliferation, apoptosis, migration, and invasion were analyzed by the CCK8 assay (a), flow cytometry (b), scratch test (c), and Transwell experiment (d), respectively;  $N = 3$ ,  $*P < 0.05$ .

potential therapeutic targets for tumors [15, 16]. In this study, through bioinformatics analysis, it is found that FKBP4 expression was significantly upregulated in NSCLC and verified by qRT-PCR in NSCLC tissues and cell lines. So far, the expression level of FKBP4 in NSCLC has not been reported, and its clinical significance is not clear. In this study, it is also found that the expression of FKBP4 is closely related to the tumor size and lymph node metastasis of NSCLC, and its high expression suggests a poor prognosis for patients. Therefore, we believe that FKBP4 can be used as a biomarker of NSCLC to indicate the malignant progression of tumors and prognosis and has certain clinical significance.

Since the biological function of FKBP4 in NSCLC is not clear, the effect of FKBP4 on the malignant progression of NSCLC was further explored in NSCLC cells and animal models. The results showed that FKBP4 can promote the proliferation, migration, and invasion of NSCLC cells and inhibit the apoptosis of NSCLC cells in vitro. Also, FKBP4 can promote the growth of NSCLC tumors in vivo. Therefore, we believe that FKBP4 is an oncogene in NSCLC, can promote the malignant process of NSCLC, and may become a therapeutic target for NSCLC.

It is reported that FKBP4 is involved in the pathophysiological process of various diseases. For instance, FKBP4 can increase the current and calcium flux mediated by TRPC3 and activate the calcineurin and T-cell nuclear factor in the transient receptor potential, thereby causing pathological hypertrophy of cardiomyocytes in chronic heart disease [17]. FKBP4 may also be involved in the progesterone resistance process of endometriosis [18]. Patients with Alzheimer's disease have abnormally reduced levels of FKBP4 in the brain and can cause the formation of nerve fiber tangles [19]. In tumors, it has been demonstrated that FKBP4 plays a role in triple-negative breast cancer and castration-resistant prostate cancer [13, 14]; however, the role of FKBP4 in other tumors has not been reported. Therefore, the role of FKBP4 in tumors is largely unknown, and it has a very innovative significance for the research around FKBP4.

The mechanism by which FKBP4 promotes the malignant process of NSCLC was further explored in this study. Our research illustrated that FKBP4 can activate the Akt/mTOR signaling pathway. Previous studies have found that FKBP4 can interact with PI3K in breast cancer and activate Akt through PDK1 and mTORC2, thereby activating the Akt/mTOR signaling pathway [13]. Akt is a protooncogene that regulates various cell functions in tumors, including metabolism, proliferation, survival, migration, and invasion [20]. The activation of Akt depends on the phosphorylation of threonine (Thr) 308 and serine (Ser) 473 [21]. mTOR is an atypical serine/threonine kinase which can promote tumor development by regulating cell biological processes such as metabolism, autophagy, and cellular stress [22]. mTOR involves 2 structurally and functionally distinct signaling complexes mTORC1 and mTORC2. mTORC1 is a growth regulator, which can enhance anabolism or repress catabolism by phosphorylation of substrates, thus promoting cell growth. mTORC2 can phosphorylate the Ser473 site of Akt and activate Akt signaling, thus promoting cell survival

[23]. Activated mTORC1 upregulates protein synthesis by phosphorylating key regulators including S6K1 and eIF4EBP1. Our data showed that FKBP4 could promote the phosphorylation of S6K1 and eIF4EBP1 which indicated that FKBP4 might mainly regulate mTORC1 signaling. In summary, we believe that FKBP4 may regulate the biological functions of proliferation, apoptosis, migration, and invasion by activating the Akt/mTOR signaling pathway in NSCLC.

## 5. Conclusion

The results of this study indicate that the expression of FKBP4 is significantly increased in NSCLC and is closely related to the malignant progression of tumors and poor prognosis. FKBP4 can promote the proliferation, migration, and invasion of NSCLC cells by activating the Akt/mTOR signaling pathway, inhibiting NSCLC cell apoptosis, and promoting the growth of NSCLC tumors in vivo. This study suggests that FKBP4 has potential as a biomarker and therapeutic target for clinical application in NSCLC.

## Data Availability

The data used to support the findings of this study are included within the article.

## Conflicts of Interest

The authors declare that there is no conflict of interest regarding the publication of this paper.

## Authors' Contributions

Wen Meng and Jingfei Meng contributed equally to this work.

## Acknowledgments

This research was supported by the Zhejiang Provincial Natural Science Foundation of China under Grant No. LY15H160009, the Zhejiang Provincial Science and Technology Program under Grant No. 2014C33116, the Medical Health Science and Technology Project of Zhejiang Provincial Health Commission (No. 2014KYA173), and the Zhejiang Provincial Science and Technology Plan of Traditional Chinese Medicine (2012ZB125).

## References

- [1] R. L. Siegel, K. D. Miller, and A. Jemal, "Cancer statistics, 2017," *CA: a Cancer Journal for Clinicians*, vol. 67, no. 1, pp. 7–30, 2017.
- [2] W. Chen, R. Zheng, P. D. Baade et al., "Cancer statistics in China, 2015," *CA: a Cancer Journal for Clinicians*, vol. 66, no. 2, pp. 115–132, 2016.
- [3] B. Meador Catherine and N. Hata Aaron, "Acquired resistance to targeted therapies in NSCLC: updates and evolving insights," *Pharmacology & Therapeutics*, vol. 210, p. 107522, 2020.

- [4] S. Song and Y. Tan, "Expression of FKBP52 in the ovaries of PCOS rats," *International Journal of Molecular Medicine*, vol. 43, no. 2, pp. 868–878, 2019.
- [5] J. Solassol, A. Mange, and T. Maudelonde, "FKBP family proteins as promising new biomarkers for cancer," *Current opinion in pharmacology*, vol. 11, no. 4, pp. 320–325, 2011.
- [6] D. A. Peattie, M. W. Harding, M. A. Fleming et al., "Expression and characterization of human FKBP52, an immunophilin that associates with the 90-kDa heat shock protein and is a component of steroid receptor complexes," *Proceedings of the National Academy of Sciences of the United States of America*, vol. 89, no. 22, pp. 10974–10978, 1992.
- [7] B. K. Ward, P. J. Mark, D. M. Ingram, R. F. Minchin, and T. Ratajczak, "Expression of the estrogen receptor-associated immunophilins, cyclophilin 40 and FKBP52, in breast cancer," *Breast Cancer Research and Treatment*, vol. 58, no. 3, pp. 267–280, 1999.
- [8] P. Kumar, P. J. Mark, B. K. Ward, R. F. Minchin, and T. Ratajczak, "Estradiol-regulated expression of the immunophilins cyclophilin 40 and FKBP52 in MCF-7 breast cancer cells," *Biochemical and Biophysical Research Communications*, vol. 284, no. 1, pp. 219–225, 2001.
- [9] S. Periyasamy, M. Warriar, M. P. M. Tillekeratne, W. Shou, and E. R. Sanchez, "The immunophilin ligands cyclosporin A and FK506 suppress prostate cancer cell growth by androgen receptor-dependent and -independent mechanisms," *Endocrinology*, vol. 148, no. 10, pp. 4716–4726, 2007.
- [10] C. Desmetz, C. Bascoul-Molleivi, P. Rochaix et al., "Identification of a new panel of serum autoantibodies associated with the presence of in situ carcinoma of the breast in younger women," *Clinical Cancer Research*, vol. 15, pp. 4733–4741, 2009.
- [11] J. F. Lin, J. Xu, H. Y. Tian et al., "Identification of candidate prostate cancer biomarkers in prostate needle biopsy specimens using proteomic analysis," *International Journal of Cancer*, vol. 121, no. 12, pp. 2596–2605, 2007.
- [12] Y. Liu, C. Li, Z. Xing et al., "Proteomic mining in the dysplastic liver of WHV/c-myc mice—insights and indicators for early hepatocarcinogenesis," *The FEBS Journal*, vol. 277, no. 19, pp. 4039–4053, 2010.
- [13] A. Mangé, E. Coyaud, C. Desmetz et al., "FKBP4 connects mTORC2 and PI3K to activate the PDK1/Akt-dependent cell proliferation signaling in breast cancer," *Theranostics*, vol. 9, no. 23, pp. 7003–7015, 2019.
- [14] J. R. Federer-Gsponer, C. Quintavalle, D. C. Müller et al., "Delineation of human prostate cancer evolution identifies chromothripsis as a polyclonal event and FKBP4 as a potential driver of castration resistance," *The Journal of Pathology*, vol. 245, no. 1, pp. 74–84, 2018.
- [15] J. Liu, Y. Wan, S. Li et al., "Identification of aberrantly methylated differentially expressed genes and associated pathways in endometrial cancer using integrated bioinformatic analysis," *Cancer Medicine*, vol. 9, no. 10, pp. 3522–3536, 2020.
- [16] Z. Zhang, J. Huang, G. Wang et al., "Serum miRNAs, a potential prognosis marker of loco-regionally advanced nasopharyngeal carcinoma patients treated with CCRT," *BMC Cancer*, vol. 20, no. 1, p. 183, 2020.
- [17] S. Bandleon, P. P. Strunz, S. Pickel et al., "FKBP52 regulates TRPC3-dependent Ca signals and the hypertrophic growth of cardiomyocyte cultures," *Journal of Cell Science*, vol. 132, 2019.
- [18] N. R. Joshi, E. H. Miyadahira, Y. Afshar et al., "Progesterone resistance in endometriosis is modulated by the altered expression of microRNA-29c and FKBP4," *The Journal of Clinical Endocrinology and Metabolism*, vol. 102, no. 1, pp. 141–149, 2017.
- [19] G. Meduri, K. Guillemeau, O. Dounane et al., "Caspase-cleaved tau-D(421) is colocalized with the immunophilin FKBP52 in the autophagy-endolysosomal system of Alzheimer's disease neurons," *Neurobiology of Aging*, vol. 46, pp. 124–137, 2016.
- [20] M. Mirza-Aghazadeh-Attari, E. M. Ekrami, S. A. M. Aghdas et al., "Targeting PI3K/Akt/mTOR signaling pathway by polyphenols: implication for cancer therapy," *Life Sciences*, vol. 255, p. 117481, 2020.
- [21] I. Yudushkin, "Control of Akt activity and substrate phosphorylation in cells," *IUBMB Life*, vol. 72, no. 6, pp. 1115–1125, 2020.
- [22] Z. Zou, T. Tao, H. Li, and X. Zhu, "mTOR signaling pathway and mTOR inhibitors in cancer: progress and challenges," *Cell & Bioscience*, vol. 10, no. 1, 2020.
- [23] G. Ferrín, M. Guerrero, V. Amado, M. Rodríguez-Perálvarez, and M. de la Mata, "Activation of mTOR signaling pathway in hepatocellular carcinoma," *International Journal of Molecular Sciences*, vol. 21, no. 4, p. 1266, 2020.



## Research Article

# PKM2 Promotes Breast Cancer Progression by Regulating Epithelial Mesenchymal Transition

Hui Xiao,<sup>1</sup> Longxiao Zhang,<sup>2</sup> Yuan Chen,<sup>1</sup> Chengjun Zhou,<sup>1</sup> Xiao Wang,<sup>1</sup> Dehai Wang <sup>1</sup>,  
and Zhenzhong Liu <sup>1</sup>

<sup>1</sup>The Second Hospital, Cheeloo College of Medicine, Shandong University, Jinan, Shandong 250033, China

<sup>2</sup>The Affiliated Hospital of Qingdao University, Qingdao, Shandong 266003, China

Correspondence should be addressed to Dehai Wang; [w\\_yuanjing@126.com](mailto:w_yuanjing@126.com) and Zhenzhong Liu; [zhenzhongl@163.com](mailto:zhenzhongl@163.com)

Received 17 June 2020; Revised 27 October 2020; Accepted 6 November 2020; Published 27 November 2020

Academic Editor: Victor H. Villar

Copyright © 2020 Hui Xiao et al. This is an open access article distributed under the Creative Commons Attribution License, which permits unrestricted use, distribution, and reproduction in any medium, provided the original work is properly cited.

Breast cancer is the leading cause of females characterized by high invasive potential. It is necessary to explore the underlying mechanism of breast cancer metastases and to find specific therapeutic targets. PKM2 is considered a new biomarker of cancer with upregulated expression in tumor tissue. PKM2 participates in the cancer-specific Warburg effect to regulate fast glucose intake consumption. Besides, PKM2 also contributes to cancer progression, especially tumor metastasis. In this study, we showed that PKM2 is upregulated in breast cancer tissues and the upregulating of PKM2 in breast cancer correlates with poor prognosis. PKM2 can regulate tumor progression by promoting tumor cell viability and mobility. Furthermore, overexpression of PKM2 can promote EMT to encourage tumor metastasis. These findings indicate PKM2 is a potentially useful diagnostic biomarker and therapeutic target in breast cancer.

## 1. Introduction

Breast cancer is the most frequently diagnosed cancer and the leading cause of cancer death among females [1]. It is stratified into three major subtypes: luminal, HER-2 positive, and TNBC (triple-negative breast cancer, estrogen receptor-negative, progesterone receptor-negative, and HER2-negative). Breast cancer, especially TNBC is characterized by high invasive potential. Approximately 30% of patients with early-stage breast cancer will develop metastases, with 5-year relative survival of 25% [2]. However, the molecular mechanisms underlying breast cancer development of different subtype are not clear, and the specific targetable biomarkers which can lead to the overall poor prognosis of the patients need to be further explored.

Activating invasion and metastasis is an important hallmark of cancer [3]. The metastasis of tumors is closely associated with epithelial-mesenchymal transition (EMT), which is an important step in carcinoma progression with the increasing ability to invade, to resist apoptosis, and to disseminate [4, 5]. In EMT, the typical epithelial histologic features are replaced by mesenchymal phenotypes including loss of cell-

cell adhesion and cell polarity, downregulation of epithelial protein markers, and upregulation of mesenchymal markers [6]. Several signal pathways, including PI3K/AKT/mTOR, Wnt, and transforming growth factor  $\beta$  (TGF- $\beta$ ), participate in EMT. The complex interactions among cells, microenvironment, and multiple signaling pathways enable the transition from tumor in situ to aggressive and invasive carcinoma.

The roles of Pyruvate kinase M2 (PKM2) involving in cancer development have attracted considerable attention since Christofk et al. found that the PKM2 expression is necessary for cancer-specific aerobic glycolysis which is known as the Warburg effect [7]. Besides the tumor metabolic function, PKM2 also contributes to tumor metastasis, oncogenic cytokinesis, or tumor growth [8–11]. PKM2 also works as a protein kinase to regulate gene transcription by phosphorylating its substrates [12]. Previous studies have reported the significance of PKM2 in cancer cell growth and survival [11]. Therefore, understanding the biochemical functions of PKM2 in tumor progress will become crucial to find potential therapeutic targets and to develop novel therapies in both primary and metastatic TNBC.



In the present study, we found that PKM2 was upregulated in clinical breast cancer samples and correlated with poor prognosis. Our results suggested that the viability and mobility of breast cancer cells (MDA-MB-231 and MCF-7 cells) were regulated by PKM2. Moreover, we also showed that PKM2 mediates EMT to promote the migration and invasion of breast cancer cells by analyzing the EMT marker protein level and EMT transcription factor (EMT-TF) mRNA expression. Our findings have implications for the development of specific biomarkers and therapeutic drugs targeting PKM2.

## 2. Materials and Methods

**2.1. Clinical Samples and Immunohistochemical Staining.** This study was approved by the Ethics Committee of the Second Hospital of Shandong University, Jinan, China. The certificate number is KYLL-2018(LW)030. All of the patients or their guardians provided written consent. 66 breast cancer tissues (35 triple-negative, 15 luminal, and 16 HER-2-positive) and adjacent normal tissues derived from patients undergoing surgical procedures were fixed in ethanol and embedded in paraffin. Slides were incubated with anti-PKM2 primary antibody and then incubated with a secondary antibody. Antibody binding was visualized by incubating with the DAB kit (Solarbio, China). Immunohistochemical results of PKM2 in the tissue were evaluated independently by two pathologists blinded to the clinical data according to the semiquantitative immunoreactivity score (IRS). The IRS is calculated by the percentage of positive cells (4, >80%; 3, 51–80%; 2, 10–50%; 1, <10%; 0, 0%) and the intensity of the staining (3, strong; 2, moderate; 1, mild; and 0, no staining).

**2.2. Cell Culture.** The human breast cancer cell line MDA-MB-231 cells and MCF-7 cells were obtained from the American Type Culture Collection (ATCC). Cells were cultured in DMEM high glucose (Hyclone, USA) with 10% FBS (Gibco, USA) and 1% 100 U/mL penicillin-streptomycin (Gibco, USA) and maintained at 37°C in a humidified incubator containing 5% CO<sub>2</sub>.

**2.3. RNA Interference.** The small interfering RNA (siRNA) of PKM2 and negative control (NC) siRNA were synthesized in RiboBio Company (China). PKM2 and NC siRNA were transfected into MDA-MB-231 and MCF-7 cells by Lipofectamine™ RNAiMAX Transfection Reagent (Thermo, USA) according to the manufacturer's protocol.

**2.4. EMT Induction.** Cells were induced EMT as described before [8]. In brief, cells were seeded in a standard medium with 10% FBS for 48 h and then treated with 2.5 ng/mL TGF-β1 (Sigma-Aldrich). Next, they were incubated with 10 ng/mL EGF (Sigma-Aldrich, USA), 100× insulin-transferring selenium (ITS; Gibco, USA), and 50 nmol/L hydrocortisone (Sigma-Aldrich, USA) in FBS-free media for 48 h.

**2.5. Cell Proliferation.** The Cell Counting Kit (CCK-8) and colony formation assays were performed to evaluate the viability and proliferative capacity of MDA-MB-231 and MCF-7 cells in the absence or presence of siRNA to PKM2. In brief, 2 × 10<sup>3</sup> cells were seeded in 96-well plates and incubated for 48 hours, and then, CCK-8 (Beyotime, China) solutions

were added to each well. After 30 minutes of incubation, the optical density of each well was measured at 450 nm using the Victor spectrophotometer (Thermo Fisher Scientific, USA).

**2.6. Colony Formation Assay.** 1 × 10<sup>3</sup> MDA-MB-231 and MCF-7 cells were seeded in a 6-well plate and cultured in complete medium in 5% CO<sub>2</sub> at 37°C for 2 weeks. The cell colonies were stained by the crystal violet and then counted.

**2.7. Cell Migration and Invasion.** 5 × 10<sup>5</sup> cells in serum-free medium were seeded into the upper chamber of the transwell of 8 μm pore size (Millipore, USA) while 10% FBS was added to the bottom chamber. After 12 h incubation, the cells were fixed with 4% paraformaldehyde and stained with 0.1% crystal violet. The cells on the upper surface of the filter were removed using a moistened cotton swab, and then, the cells of the lower surface of the filter were counted under a microscope (Nikon, Japan) at ×100 magnification. In invasion assay, the upper chamber was coated with 50 μl of a matrigel solution before cell seeding.

**2.8. Western Blot.** Western blotting was performed in accordance with the standard protocols. In brief, cellular proteins were extracted using the RIPA lysis buffer, separated on SDS-PAGE gels, and transferred onto NC membranes (Millipore, Billerica, USA). After incubated in primary and second antibodies separately, proteins were detected by ECL reagent (Millipore, USA) and imaged with FluorChem Q (Protein simple, USA). The following antibodies were used for western blotting: PKM2 antibody (Proteintech, China, 1:1000, 15822-1-AP), vimentin antibody (Proteintech, China, 1:1000, 10366-1-AP), E-cadherin antibody (Proteintech, China, 1:1000, 20874-1-AP), N-cadherin antibody (Proteintech, China, 1:1000, 22018-1-AP), and GAPDH antibody (ZSGB-bio, China, 1:1000, TA-8).

**2.9. Quantitative Real-Time PCR.** The primers were synthesized by BGI (China), and the sequences are listed in Table 1. Total RNA was isolated from MDA-MB-231 using the RNA simple kit (Tiangen, China) following the manufacturer's instructions. cDNA was synthesized using the HiScript II Q RT SuperMix for qPCR (Vazyme, China), and quantitative real-time PCR (Q-RT PCR) was performed using Fastking One Step RT-PCR kit (Tiangen, China). GAPDH was used as the reference gene. The ΔΔCt method was used to analyze the real-time PCR data.

**2.10. Genomics Data Analyze.** We used the analysis tool UALCAN to study the TCGA (<http://cancergenome.nih.gov/>) database of the expression level of PKM2 in breast cancer. Then, we used the Kaplan Meier plotter database (<https://kmplot.com/analysis/>) to analyze the correlations between PKM2 and prognosis.

**2.11. Statistical Analysis.** Three or more independent experiments were performed for each result, and the results were presented as mean ± S.D. Data analysis was performed with GraphPad Prism 5. Statistical analyses were performed using a two-tailed Student's *t*-test. *P* < 0.05 was considered to be significant.

TABLE 1: Primer sequences for quantitative real-time PCR.

Gene name	Forward	Reverse
Zeb-1	GCTGGGAGGATGACACAGG	GTCCTCTTCAGGTGCCTCAG
Snail2	GAACTGGACACACATACAGTGAT	ACTCACTCGCCCCAAAGATG
Twist1	GCCGGAGACCTAGATGTCATT	TTTTAAAAGTGCGCCCCACG
Slug	CTGTGACAAGGAATATGTGAGCC	CAAATGCTCTGTTGCAGTGAG
N-cadherin	CCCTGCTTCAGGCGTCTGTA	TGCTTGCATAATGCGATTTCACC
Vimentin	CCACCAGGTCCGTGTCCTCGT	CGCTGCCCAGGCTGTAGGTG
E-cadherin	TTGCACCGGTGCGACAAAGGAC	TGGAGTCCCAGGCGTAGACCAA
GAPDH	GCACCGTCAAGGCTGAGAAC	TGGTGAAGACGCCAGTGGA

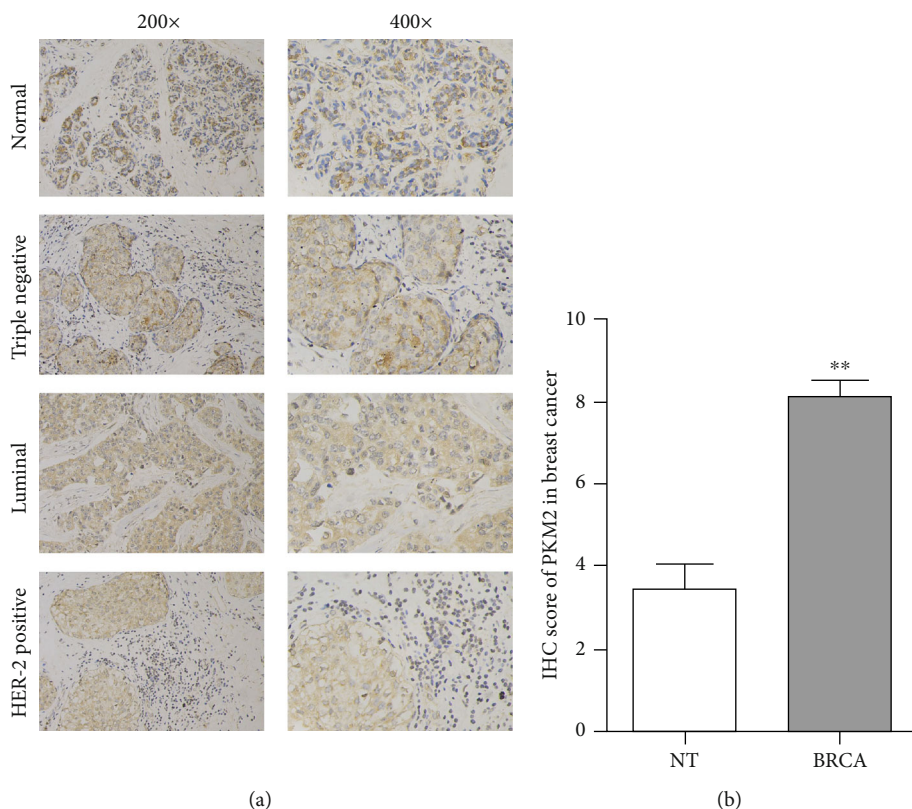


FIGURE 1: PKM2 is upregulated in breast cancer tissues. (a) Representative images of IHC staining of PKM2 in normal breast tissues and breast cancer tissue samples (TNBC, luminal, and HER-2 positive;  $\times 200$  and  $\times 400$  magnification). (b) IHC score of PKM2 in normal tissues (NT) and breast cancer (BRCA) (\*\* $P < 0.01$ ).

### 3. Results

3.1. *PKM2 Is Upregulated in Breast Cancer Tissues.* To investigate the expression level of PKM2 in breast cancer, we analyzed breast cancer samples by immunohistochemistry (IHC) and then assessed the staining. We found that PKM2 was significantly upregulated homogeneously in breast cancer tissues compared with normal adjacent noncancerous tissues, and the upregulation of PKM2 was in all 3 major subtypes (Figure 1(a) and 1(b)).

3.2. *PKM2 Expression Associates with the Prognosis of Breast Cancer Patients.* To further understand the clinical significance of PKM2 in breast cancer, we analyzed the PKM2

expression using UALCAN and patient prognosis using the Kaplan Meier plotter database. It revealed that PKM2 is upregulated in primary tumor tissues compared with adjacent noncancerous tissues (Figure 2(a)). PKM2 is overexpressed in different subclasses (luminal, HER-2 positive, and triple-negative) of breast cancer. Furthermore, we found that the expression of PKM2 shows no difference between HER2-positive and TNBC. However, there is a significant difference between luminal and HER-2 positive, or luminal and TNBC, according to the gene expression level analysis of the TCGA database (Figure 2(b)). The Kaplan–Meier survival analysis showed that breast cancer patients with high PKM2 expression had a poorer prognosis (Figure 2(c)).

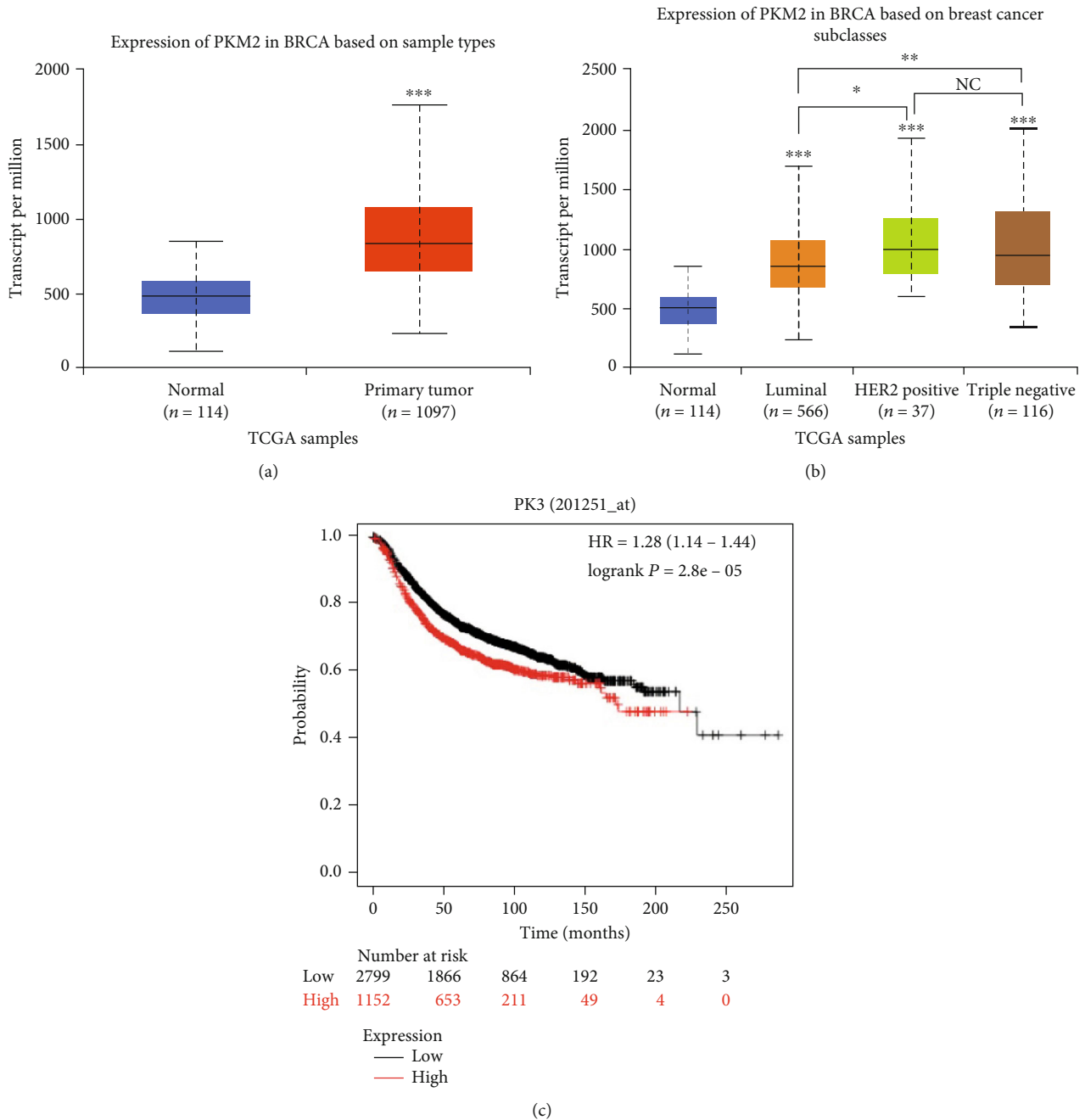


FIGURE 2: PKM2 expression associates with the prognosis of breast cancer patients. (a) Expression level of PKM2 in normal tissue and primary breast cancer tissues. (b) Expression level of PKM2 in different subclasses (TNBC, luminal, and HER-2) of breast cancer. (c) Kaplan–Meier curves showed that the patients with higher PKM2 expression had poorer overall survival ( $P < 0.005$ ). Abbreviations: BRCA: breast invasive carcinoma (\*\* $P < 0.001$ ; \* $P < 0.01$ ; \* $P < 0.05$ ; NC :  $P > 0.01$ ).

These results indicated that the upregulation of PKM2 in breast cancer tissues correlates with poor prognosis of patients, suggesting that PKM2 may play important roles during carcinoma progression.

**3.3. PKM2 Is Required for Breast Cancer Cell Viability.** To determine the effect of PKM2 on cell viability, we knocked down the PKM2 expression by siRNA. The decreased protein levels of PKM2 in MDA-MB-231 cells were confirmed by western blot and Q-RT-PCR analysis compared with NC siRNA

(Figure 3(a) and 3(b)). Then, CCK-8 and colony formation assays were performed to evaluate the viability and proliferative capacity of MDA-MB-231 and MCF-7 cells. Firstly, CCK-8 results showed that in the PKM2-knockdown (PKM2-KD) group, the cell viability was significantly decreased (Figures 3(c) and 3(d)). Colony formation assay is an in vitro cell survival assay based on the ability of a single cell to grow into a colony. The results showed that knockdown PKM2 significantly inhibited the number and size of all cell colonies of breast cancer cells compared to the control group (Figure 3(e) and 3(f)).

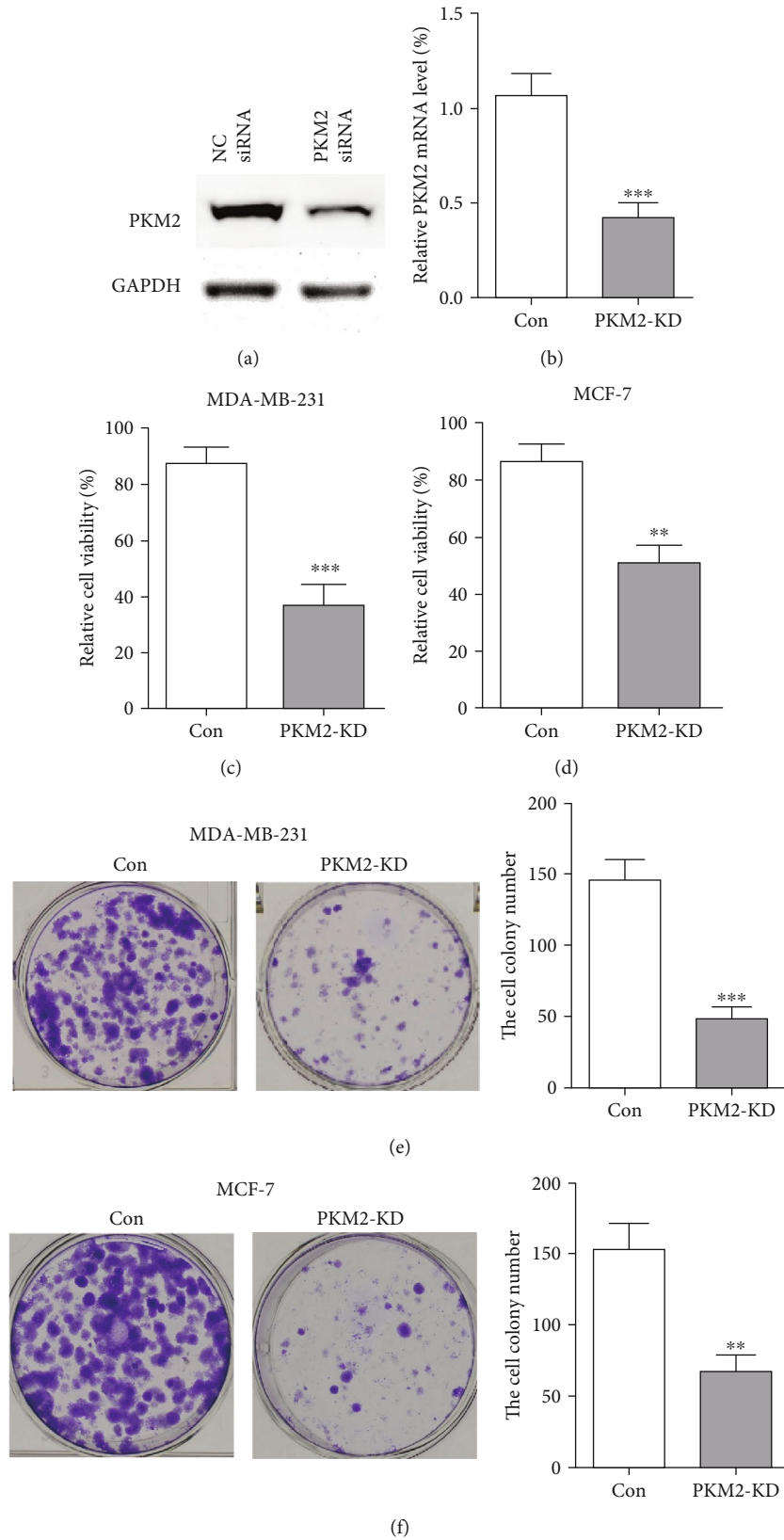


FIGURE 3: PKM2 is required for breast cancer cell viability. (a) PKM2 protein level was reduced by PKM2 siRNA, and GAPDH was used as a loading control. (b) Q-RT PCR analysis of PKM2 mRNA levels normalized to GAPDH in the control group and PKM2-KD cells. (c), (d) Cell viability was measured by CCK-8 assay in MDA-MB-231 and MCF-7 cells following PKM2 silencing by siRNA. (e), (f) Colony formation of PKM2-knockdown MDA-MB-231 and MCF-7 cells was reduced (\*\* $P < 0.01$ ; \*\*\* $P < 0.001$ ).



**3.4. PKM2 Is Required for Breast Cancer Cell Migration and Invasion.** To evaluate the role of PKM2 on breast cancer mobility, the migrating and invasive ability of MDA-MB-231 and MCF-7 were measured after PKM2 knockdown using transwell. PKM2-KD cells migrated significantly slowly than the cells of the control group (Figure 4(a)). Furthermore, the invasive capacity of MDA-MB-231 cells was reduced in PKM2-KD cells (Figure 4(b)). The knockdown of PKM2 also inhibits the migration and invasion of the MCF-7 cells (Figures 4(c) and 4(d)). These results indicate that PKM2 has a vital role in promoting breast cancer cell migration and invasion.

**3.5. Silencing PKM2 Suppresses Breast Cancer Cell EMT.** To determine how PKM2 controls the migratory and invasive phenotypes and whether PKM2 is responsible for the EMT of MDA-MB-231 cells, we evaluated the expression levels of the EMT biomarkers (vimentin, N-cadherin, and E-cadherin) by western blot after activating or knockdown of PKM2. These results showed that the activation of PKM2 by the specific activator, Mitapivat, resulted in increased mesenchymal markers (N-cadherin and vimentin) and decreased epithelial protein markers E-cadherin expression, while the knockdown of PKM2 blocked the E-cadherin loss and mesenchymal marker gain, which suggested that the EMT is inhibited (Figure 5(a)). Furthermore, we found that in MDA-MB-231 cells, PKM2 knockdown increased the expression of the key EMT-related genes (Snail, Slug, Zeb1, and Twist1) (Figure 5(b)). In a TGF- $\beta$ 1-induced EMT experiment, the results show that after the PKM2 knockdown, the MDA-MB-231 cells were less sensitive to TGF- $\beta$ 1, showing no significant alteration of the mRNA expression level of the key EMT markers to EMT induction (Figure 5(c)). This result suggested that PKM2 plays a vital role in EMT. Therefore, tumor cells gain mesenchymal morphology, and the promoted EMT increases cancer cell invasion and metastasis (Figure 5(d)). In brief, PKM2 promotes breast cancer cell EMT to regulate the migration and invasion in tumor progression.

## 4. Discussion

Our results showed that the TCGA database analysis indicated that the high PKM2 expression in breast cancer samples was correlated with reduced patient survival. PKM2 is upregulated in breast cancer tissues and proved that PKM2 can promote breast cancer progression by regulating tumor cell viability and motility. Furthermore, our results suggested that PKM2 is a key regulator of cell migration and invasion during breast cancer progression by promoting EMT.

Four isozymes of pyruvate kinase (M1, M2, R, and L) are differentially expressed in human tissue. PKM2 is expressed during embryonic development, while the PKM1 isoform is expressed in most adult tissues. However, reports showed that tumor tissues exclusively express PKM2 [13–15]. PKM2 locates both in the cytoplasm and nucleus, which illustrates its multiple functions in cancer cells. The allosteric switch between tetrameric form (high-activity state) and dimeric form (low-activity state) of PKM2 may lead to the variable functions of PKM2 as a pyruvate kinase and a pro-

tein kinase in cell metabolism [12, 15]. It was identified that PKM2 is regulated by several signals including EGF and hypoxia and then leading to downstream effects such as metabolic reprogramming and oncogene activation. PKM2 has an essential role in the Warburg effect, a cancer-specific glycolytic system that allows tumor cells to obtain energy rapidly to proliferate, migrate, and invade by converting glucose to lactate even when oxygen is abundant, meeting the biosynthetic demands for tumor development. Knocking down PKM2 and replacing it with PKM1 lead to reduced lactate production, increased oxygen consumption, and reduced tumor cell growth [7]. The allosteric switch between tetrameric form (high-activity state) and dimeric form (low-activity state) of PKM2 may lead to the variable functions of PKM2 in cell metabolism [15]. However, the nonmetabolic functions of PKM2 have remained controversial. Recent studies have revealed the new mechanisms of PKM2 in tumorigenesis, cell growth, survival, apoptosis, cancer stem-like properties, and EMT [8, 16–19]. Moreover, it has been proved as a useful diagnostic biomarker and therapeutic target in malignancies [20–22].

EMT is a biologic process during embryogenesis, organ development, and tissue regeneration [5]. Moreover, EMT is an important driver of cancer progression which has been shown to link closely to carcinoma metastasis [4]. Activating invasion and metastasis is an important hallmark of cancer [3]. A lot of literature showed that the metastasis of tumor is closely associated with EMT, which is an important step in the carcinoma progression with the increasing ability to invade, to resist apoptosis, and to disseminate [4, 5]. In EMT, the typical epithelial histologic features are replaced by mesenchymal phenotype including loss of cell-cell adhesion and cell polarity, downregulation of epithelial protein markers, and upregulation of mesenchymal markers [6]. Several signal pathways, including PI3K/AKT/mTOR, Wnt, and transforming growth factor  $\beta$  (TGF- $\beta$ ), participate in EMT. The complex interactions among cells, microenvironment, and multiple signaling pathways enable the transition from tumor in situ to aggressive and invasive carcinoma. Series molecular processes are engaged in EMT. As an early step, the loss of E-cadherin expression is the biochemical feature of EMT, inducing the activation of EMT-TFs including Snail, Slug, Twist1, and Zeb1. EMT-TFs which drive mesenchymal protein expression to permit subsequent invasion and metastasis by creating a protumorigenic environment [23, 24]. The mesenchymal protein markers, including N-cadherin, vimentin, fibronectin, and matrix metalloproteinases (MMPs), are upregulated, while the epithelial markers E-cadherin, desmoglein, and cytokeratin-18 are downregulated. Cancer cells that undergo EMT acquire epigenetic and genetic changes in expression of specific protein markers, morphology (from epithelial to fibroblastic-like and spindle-shaped), and function to enable invasion and metastasis (Figure 5(d)). Therefore, to find some small molecule inhibitors which specifically targeted EMT offers a novel approach to regulating tumor progression.

There is an increasing concern on the role of PKM2 in EMT. PKM2 expression and activity contribute to EMT in multiple cancers such as colon cancer, oral squamous cell



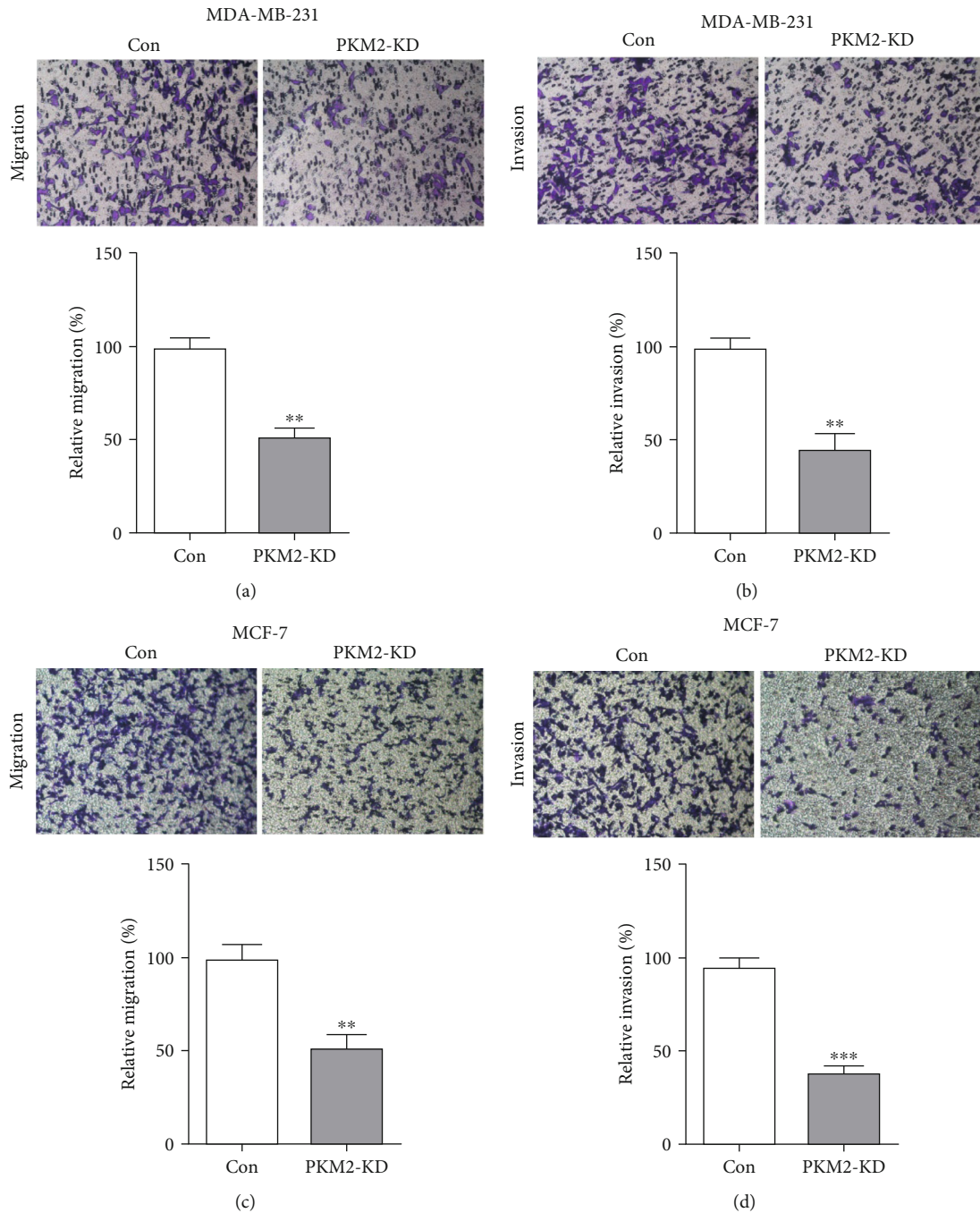


FIGURE 4: PKM2 is required for breast cancer cell migration and invasion. Cell migration (a) and invasion (b) of MDA-MB-231 cells after PKM2 knockdown was determined by transwell assay. Cell migration (c) and invasion (d) of MCF-7 cells after PKM2 knockdown was determined by transwell assay. Representative images from the migration and invasion of control and PKM2-KD cells of MDA-MB-231 and MCF-7 cells (top panel). Cell migration and invasion are expressed as a percentage of control (bottom panel). Cells were counted for at least five random microscope fields. Results are shown as mean  $\pm$  SD from three independent experiments. (\*\* $P < 0.01$ ). (\*\*\*) $P < 0.001$ ).

carcinoma, esophageal squamous cell carcinoma, and so on [8, 25, 26]. The translocation from cytoplasm to the nucleus of PKM2 may promote EMT by regulating gene transcriptional activity. Therefore, we tested the contributions of PKM2 in EMT of breast cancer by analyzing the EMT marker protein expression. Our results indicated that PKM2 plays a vital role in tumor cell migration and invasion. After the knockdown of PKM2 by siRNA in MDA-MB-231

and MCF-7 cells, the ability to migrate and invade is inhibited. However, the underlying mechanism needs to be further explored.

Therefore, a specific drug targeting PKM2 is with great potential, for it can not only inhibit the Warburg effect to cut the energy source of the biosynthetic demands of cancer cells but also abolish the proliferation and metastasis of cancer cells to block the tumor progress.

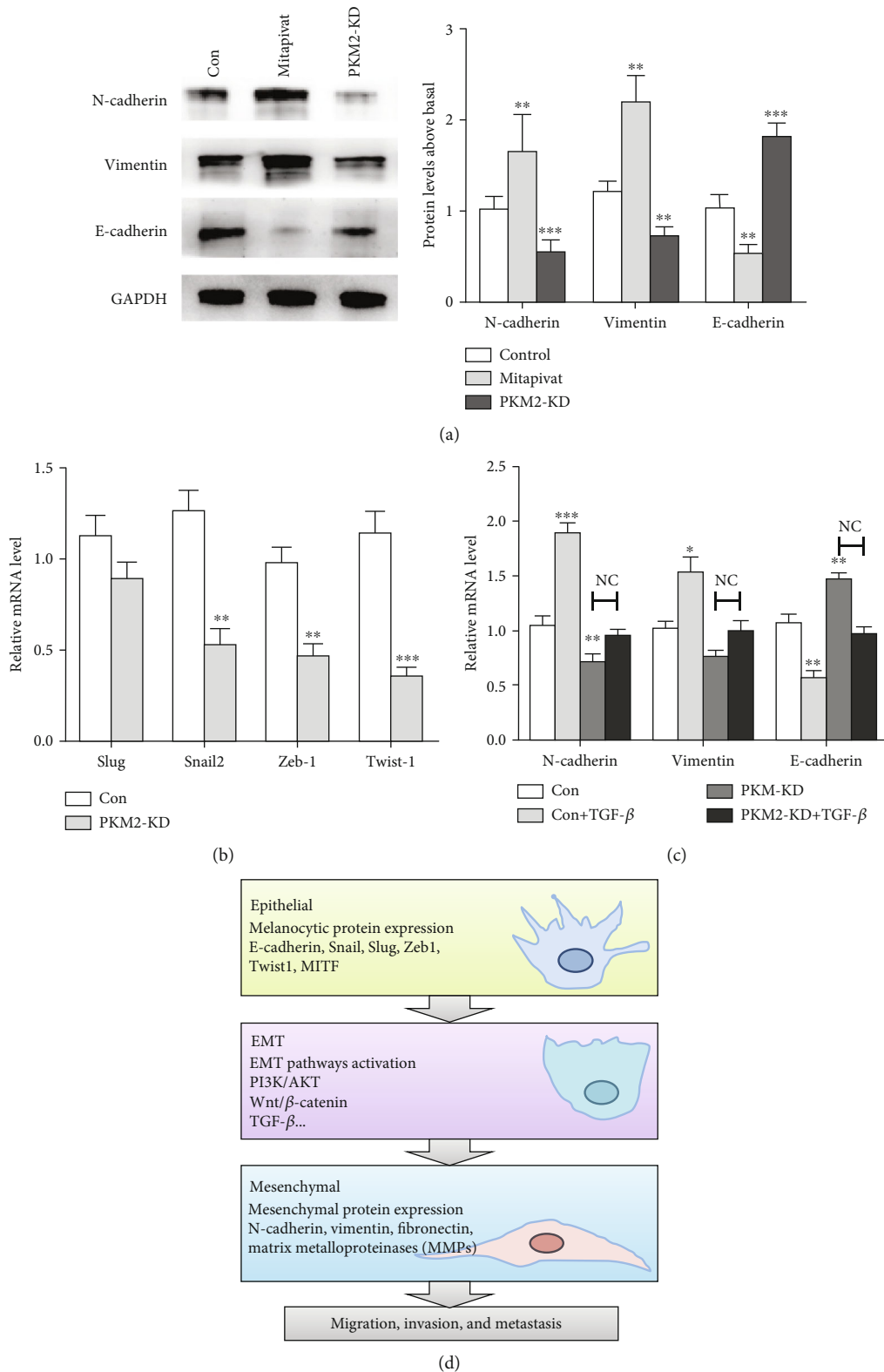


FIGURE 5: Silencing PKM2 suppresses MDA-MB-231 cell EMT. (a) Western blot analysis of protein levels of EMT marker proteins in control, Mitapivat, and PKM2-KD groups. GAPDH was used to normalize protein expression (left panel). The protein levels of EMT markers were quantified and compared (right panel). (b) Q-RT PCR analysis of mRNA levels of key EMT-related genes (Snail, Slug, Zeb1, and Twist1) in control and PKM2-KD cells normalized to GAPDH. (c) Relative mRNA levels of vimentin, N-cadherin, and E-cadherin after EMT induction in MDA-MB-231 cells in control and PKM2-KD cells for 48 h. (d) Changes involved in EMT (\*\*\*)  $P < 0.001$ , \*\*  $P < 0.01$ , NC :  $P > 0.01$ ).

As the most commonly diagnosed cancer and the leading cause of cancer death in women, breast cancer is recognized as a serious, worldwide health concern which is widely explored over the past decades, and great improvements have been made. Breast cancer, especially TNBC, exhibited a highly invasive behavior and enhanced the proliferating and migrating capacity of tumor cells. The application of multiple treatments partly decreases the overall mortality of breast cancer. Besides the systemic cytotoxic chemotherapy, targeted therapies make contributions in improving patient outcomes. However, owing to the highly aggressive behavior and metastatic rate of breast cancer, efforts to investigate the underlying mechanism and improve the outcome are still underway.

## 5. Conclusions

In our study, we focused on the bioactive role of PKM2 in EMT. The results proved that the upregulation of PKM2 in breast cancer samples is correlated with a poor prognosis of patients. The knockdown of PKM2 inhibits the proliferation, migration, and invasive capacities of breast cancer cells. Furthermore, our findings indicate that PKM2 contributes to EMT that activates the metastasis. The high-specific and low-toxic compounds targeting PKM2 are good candidates in cancer therapy. The results of our study have proved the role of PKM2 in EMT, which can have important clinical implications, providing a very promising biomarker in cancer diagnosis and targeted therapy.

## Abbreviations

ATCC:	American Type Culture Collection
BRCA:	Breast invasive carcinoma
EMT:	Epithelial-mesenchymal transition
EMT-TFs:	EMT transcription factors
IHC:	Immunohistochemistry
IRS:	Immunoreactivity score
KD:	Knockdown
NC:	Negative control
PKM2:	Pyruvate kinase M2
Q-RT PCR:	Quantitative real-time PCR
siRNA:	Small interfering RNA
TGF- $\beta$ :	Transforming growth factor $\beta$
TNBC:	Triple-negative breast cancer.

## Data Availability

The data used to support the findings of this study are included within the article.

## Ethical Approval

We received the informed consent of patients and ethical approval of the Ethics Committee of the Second Hospital of Shandong University. The ethics certificate was issued on 1st Jan 2018 and the certificate number is KYLL-2018(LW)030.

## Consent

All of the patients or their guardians provided written consent.

## Conflicts of Interest

The authors declare that there is no conflict of interest regarding the publication of this paper.

## Authors' Contributions

Dehai Wang and Zhenzhong Liu contributed equally to this work.

## Acknowledgments

We thank the members of the central laboratory of The Second Hospital of Shandong University. This work was supported by the Natural Science Foundation of Shandong Province (grant NO. ZR2019PH106).

## References

- [1] F. Bray, J. Ferlay, I. Soerjomataram, R. L. Siegel, L. A. Torre, and A. Jemal, "Global cancer statistics 2018: GLOBOCAN estimates of incidence and mortality worldwide for 36 cancers in 185 countries," *CA: a Cancer Journal for Clinicians*, vol. 68, no. 6, pp. 394–424, 2018.
- [2] G. Bianchini, J. M. Balko, I. A. Mayer, M. E. Sanders, and L. Gianni, "Triple-negative breast cancer: challenges and opportunities of a heterogeneous disease," *Nature Reviews. Clinical Oncology*, vol. 13, no. 11, pp. 674–690, 2016.
- [3] D. Hanahan and R. A. Weinberg, "Hallmarks of cancer: the next generation," *Cell*, vol. 144, no. 5, pp. 646–674, 2011.
- [4] M. A. Nieto, R. Y. Huang, R. A. Jackson, and J. P. Thiery, "EMT: 2016," *Cell*, vol. 166, no. 1, pp. 21–45, 2016.
- [5] R. Kalluri and R. A. Weinberg, "The basics of epithelial-mesenchymal transition," *The Journal of Clinical Investigation*, vol. 119, no. 6, pp. 1420–1428, 2009.
- [6] J. P. Thiery, H. Acloque, R. Y. Huang, and M. A. Nieto, "Epithelial-mesenchymal transitions in development and disease," *Cell*, vol. 139, no. 5, pp. 871–890, 2009.
- [7] H. R. Christofk, M. G. Vander Heiden, M. H. Harris et al., "The M2 splice isoform of pyruvate kinase is important for cancer metabolism and tumour growth," *Nature*, vol. 452, no. 7184, pp. 230–233, 2008.
- [8] A. Hamabe, M. Konno, N. Tanuma et al., "Role of pyruvate kinase M2 in transcriptional regulation leading to epithelial-mesenchymal transition," *Proceedings of the National Academy of Sciences of the United States of America*, vol. 111, no. 43, pp. 15526–15531, 2014.
- [9] N. Wong, D. Ojo, J. Yan, and D. Tang, "PKM2 contributes to cancer metabolism," *Cancer Letters*, vol. 356, no. 2, pp. 184–191, 2015.
- [10] Y. Jiang, Y. Wang, T. Wang et al., "PKM2 phosphorylates MLC2 and regulates cytokinesis of tumour cells," *Nature Communications*, vol. 5, no. 1, 2014.
- [11] I. Harris, S. Mccracken, and T. W. Mak, "PKM2: a gatekeeper between growth and survival," *Cell Research*, vol. 22, no. 3, pp. 447–449, 2012.

- [12] X. Gao, H. Wang, J. J. Yang, X. Liu, and Z. R. Liu, "Pyruvate kinase M2 regulates gene transcription by acting as a protein kinase," *Molecular Cell*, vol. 45, no. 5, pp. 598–609, 2012.
- [13] M. S. Jurica, A. Mesecar, P. J. Heath, W. Shi, T. Nowak, and B. L. Stoddard, "The allosteric regulation of pyruvate kinase by fructose-1,6-bisphosphate," *Structure*, vol. 6, no. 2, pp. 195–210, 1998.
- [14] S. Mazurek, C. B. Boschek, F. Hugo, and E. Eigenbrodt, "Pyruvate kinase type M2 and its role in tumor growth and spreading," *Seminars in Cancer Biology*, vol. 15, no. 4, pp. 300–308, 2005.
- [15] J. D. Dombrackas, B. D. Santarsiero, and A. D. Mesecar, "Structural basis for tumor pyruvate kinase M2 allosteric regulation and catalysis," *Biochemistry*, vol. 44, no. 27, pp. 9417–9429, 2005.
- [16] H. R. Christofk, M. G. Vander Heiden, N. Wu, J. M. Asara, and L. C. Cantley, "Pyruvate kinase M2 is a phosphotyrosine-binding protein," *Nature*, vol. 452, no. 7184, pp. 181–186, 2008.
- [17] L. Wei, K. Li, X. Pang et al., "Leptin promotes epithelial-mesenchymal transition of breast cancer via the upregulation of pyruvate kinase M2," *Journal of Experimental & Clinical Cancer Research*, vol. 35, no. 1, 2016.
- [18] W. Yang, Y. Xia, H. Ji et al., "Nuclear PKM2 regulates  $\beta$ -catenin transactivation upon EGFR activation," *Nature*, vol. 480, no. 7375, pp. 118–122, 2011.
- [19] Y. Shi, N. Liu, W. Lai et al., "Nuclear EGFR-PKM2 axis induces cancer stem cell-like characteristics in irradiation-resistant cells," *Cancer Letters*, vol. 422, pp. 81–93, 2018.
- [20] J. Schneider, K. Neu, H. G. Velcovsky, H. Morr, and E. Eigenbrodt, "Tumor M2-pyruvate kinase in the follow-up of inoperable lung cancer patients: a pilot study," *Cancer Letters*, vol. 193, no. 1, pp. 91–98, 2003.
- [21] T. K. Chao, T. S. Huang, Y. P. Liao et al., "Pyruvate kinase M2 is a poor prognostic marker of and a therapeutic target in ovarian cancer," *PLoS one*, vol. 12, no. 7, article e0182166, 2017.
- [22] W. Hu, S. X. Lu, M. Li et al., "Pyruvate kinase M2 prevents apoptosis via modulating Bim stability and associates with poor outcome in hepatocellular carcinoma," *Oncotarget*, vol. 6, no. 9, pp. 6570–6583, 2015.
- [23] T. T. Onder, P. B. Gupta, S. A. Mani, J. Yang, E. S. Lander, and R. A. Weinberg, "Loss of E-cadherin promotes metastasis via multiple downstream transcriptional pathways," *Cancer Research*, vol. 68, no. 10, pp. 3645–3654, 2008.
- [24] A. Puisieux, T. Brabletz, and J. Caramel, "Oncogenic roles of EMT-inducing transcription factors," *Nature Cell Biology*, vol. 16, no. 6, pp. 488–494, 2014.
- [25] F. Tanaka, S. Yoshimoto, K. Okamura, T. Ikebe, and S. Hashimoto, "Nuclear PKM2 promotes the progression of oral squamous cell carcinoma by inducing EMT and post-translationally repressing TGIF2," *Oncotarget*, vol. 9, no. 73, pp. 33745–33761, 2018.
- [26] R. Ma, Q. Liu, S. Zheng, T. Liu, D. Tan, and X. Lu, "PKM2-regulated STAT3 promotes esophageal squamous cell carcinoma progression via TGF- $\beta$ 1-induced EMT," *Journal of cellular biochemistry*, vol. 120, no. 7, pp. 11539–11550, 2019.